Design, construction and testing of a lab-scale membrane distillation bioreactor for water purification

Kavisha Patel

A dissertation submitted to the Faculty of Engineering and the Built Environment, University of the Witwatersrand, in fulfilment of the requirements for the degree of Master of Science in Chemical Engineering.

Johannesburg, 2024

DECLARATION

I hereby declare that, unless otherwise acknowledged, this dissertation is my own unaided work and has not been submitted previously at this, or any other institution of learning for any degree or examination.

Kavisha Patel
1st of March 2024

SUMMARY

The pulp and paper industry produces a significant amount of wastewater that contains a variety of organic and inorganic contaminants. This makes it impossible to discharge untreated wastewater directly into a water source. As a result of the condition of the untreated mill effluent and strict environmental regulations, significant pressure has been placed to develop suitable technologies capable of treating and reusing this wastewater. In light of this, this study evaluated the potential of a membrane distillation bioreactor (MDBR), a technology which combines a conventional membrane bioreactor (MBR) with membrane distillation (MD) for the treatment and reuse of pulp and paper mill effluent. In this study, effluent from a paper mill was analyzed for its most significant components. The analysis identified sulphate, sodium, chloride and calcium as the main components of the feed wastewater with concentrations of 391 mg/L, 300 mg/L, 160 mg/L and 157 mg/L respectively. A high TDS of 1 394-1 566 mg/L, TSS of 496-876 mg/L and COD of 397-496 mg/L were found for the feed wastewater, typical of pulp and paper mill effluent.

MDBR performance characteristics including permeate water quality, permeate flux as well as membrane fouling and membrane wetting were investigated systematically. The performance of the MDBR was also evaluated at three different operating temperatures of 45ºC, 55ºC and 65ºC. Experimental results showed that the MDBR achieved 99.4% removal of all compounds and a high salt rejection rate of 86.3%, regardless of the operation temperature. However, the MDBR was only able to achieve an organic rejection rate of 78.0%. It was found that the effects of bioreactor temperatures had strong impacts on both the permeation performance and fouling behaviour. The permeate flux dropped by 88.1% over the duration of the experimental program at the relatively low operational temperatures due to membrane fouling. SEM analysis showed a compact fouling layer on the membrane surface from the bioreactors operated at the temperatures of 55ºC and 65ºC while only a few depositions were found on the membrane from the 45ºC bioreactor. EDS results indicated that the deposits formed on the membrane surface mainly consisted of calcium. A loss in membrane hydrophobicity of 66.0% at increased temperatures was detected with contact angle measurement due to the partial wetting of the membrane. In the present study, the optimal MDBR temperature was found to be 65ºC as it showed better process performance and treatment efficiency. Overall, the MDBR in this study was effective in remediating pulp and paper mill effluent.

DEDICATION

This dissertation is dedicated to the people who serve as my inspiration – *my parents*.
For their unconditional love, support and encouragement and,
without whom none of my success would have been possible.
I am forever thankful.

ACKNOWLEDGEMENTS

I would sincerely like to thank the following people and organizations for their support and help to complete this degree:

My research supervisor, Prof. Craig Sheridan, for affording me the opportunity to pursue this degree under his supervision and guidance.

My managers, Mr. Frans Matfield and Mrs. Maryna Driescher, for always being willing to assist and offer advice where possible. Your understanding and cooperation towards the completion of this degree is greatly appreciated.

Sappi Southern Africa, through the Paper Manufacturer's Association of South Africa (PAMSA), for funding this project.

The Chemical Sciences staff at Sappi Technology Centre for lending a hand with the water quality analysis.

My colleague, Mr. Ronnie Bothma, for taking time out to assist me with contact angle measurement.

Miss Zaynab Cader for her help with SEM analysis of the membrane samples.

The gentlemen, Mr. Rodney Gurney and Mr. Hopewell Gumede, at Richard Ward, School of Chemical and Metallurgical Engineering's Workshop for their help with the construction of my laboratory setup.

Lastly, and most importantly, my wholehearted thanks to my sister, family and friends for their motivation and unfailing support.

OUTPUTS FROM THIS RESEARCH

Patel, K., & Sheridan, C. (2018). Design, construction and testing of a laboratory-scale membrane distillation bioreactor for water purification. *World Water Congress and Exhibition*. Tokyo, Japan: World Water Congress.

Patel, K., & Sheridan, C. (2021). Design, construction and testing of a laboratory-scale membrane distillation bioreactor (MDBR) for water purification. *South African Chemical Engineering Congress (SACEC)*, pp. 167-176. Johannesburg, South Africa.

CONTENTS

LIST OF FIGURES

LIST OF TABLES

LIST OF ABBREVIATIONS

AGMD	Air Gap Membrane Distillation
BOD	Biochemical Oxygen Demand
COD	Chemical Oxygen Demand
CCD	Charge-Coupled Device
DCMD	Direct Contact Membrane Distillation
DO	Dissolved Oxygen
EC	Electrical Conductivity
EDS	Energy-Dispersive X-Ray Spectroscopy
HRT	Hydraulic Retention Time
ICP	Inductively Coupled Plasma
ICP-OES	Inductively Coupled Plasma-Optical Emission Spectroscopy
ICS	Ion Chromatography System
ID	Inner Diameter
LEP	Liquid Entry Pressure
MBR	Membrane Bioreactor
MD	Membrane Distillation
MDBR	Membrane Distillation Bioreactor
MF	Microfiltration
N	Nitrogen
NDIR	Non-Dispersive Infrared
NF	Nanofiltration
ORT	Organic Retention Time
P	Phosphate
PFD	Process Flow Diagram
PP	Polypropylene
PTFE	Polytetrafluoroethylene
PVC	Polyvinyl Chloride
PVDF	Polyvinylidene Fluoride
RO	Reverse Osmosis
SE	Secondary Electron
SEM	Scanning Electron Microscopy

SGMD	Sweeping Gas Membrane Distillation
SRT	Sludge Retention Time
SS	Suspended Solids
TDS	Total Dissolved Solids
TN	Total Nitrogen
TOC	Total Organic Carbon
TrOC	Trace Organic Contaminants
TSS	Total Suspended Solids
UF	Ultrafiltration
VMD	Vacuum Membrane Distillation

1 INTRODUCTION

Over recent years, South Africa has been faced with a growing scarcity of its fresh water resources (Brink, Sheridan, & Harding, 2018). This decline in available water sources can be attributed to irregular climate patterns, little to no rainfall, a growing population, rapid industrialization and increasing domestic, agricultural and industrial demands. The lack of adequate wastewater management and water pollution control has also intensified this growing issue. The generation of harmful industrial effluents and the way in which it is disposed of is considered as one of the main contributing factors to fresh water pollution (Gebreyohannes, Mazzei, & Giorno, 2016; Luo et al., 2016).

The pulp and paper industry consumes large quantities of fresh water to produce paper; the associated discharge of used water from the processes results in it being ranked sixth in the world amongst the most polluting industries (Singh & Chandra, 2019). Wastewater produced from the paper manufacturing process contains a variety of organic and inorganic contaminants, making it high in chemical oxygen demand (COD), biochemical oxygen demand (BOD), suspended solids (SS), toxicity and colour (Eskelinen, Särkkä, Kurniawan, & Sillanpää, 2010). It is not possible to discharge the untreated effluent directly into a water source as it can cause slime growth, scum formation, oxygen depletion and loss of aesthetic quality of the environment. It may also harm aquatic organisms (Kamali & Khodaparast, 2015; Pokhrel & Viraraghavan, 2004).

As a result of the condition of the untreated mill effluent, growing water costs and strict environmental regulations, significant resources have been placed to develop cost effective, environmentally friendly and suitable technologies capable of treating this wastewater for reuse. The reuse of treated industrial wastewater is a potential way forward to bridge the gap between water supply and demand, encourage water conservation by reducing fresh water consumption, assist with water circuit closure within the pulp and paper industry and achieve nutrient recovery (Mannina, Gulhan, & Ni, 2022).

Wastewater treatment in the pulp and paper industry is usually divided into primary, secondary and tertiary treatment. Primary treatment is used to remove the majority of the SS with common systems like flotation units or clarifiers (Ashrafi, Yerushalmi, & Haghighat, 2015). Secondary treatment involves the usage of biological processes for the elimination of organic contaminants in the mill effluent. Tertiary treatment is only incorporated when treated effluent from the previous stages do not meet acceptable standards for reuse or disposal (Brink et al., 2018). Separation technologies such as membrane bioreactors (MBRs) are used in the pulp and paper industry for secondary treatment of wastewater such that they can meet reuse standards (Pokhrel & Viraraghavan, 2004). However, the MBR is not always able to retain slowly biodegradable organic substances before they can be degraded. As a result, the treated MBR effluent may contain an elevated amount of organics which can impact on downstream processes and can result in adverse effects on the environment and human health (Nguyen et al., 2016).

Currently, research is being conducted on the integration of the MBR system with a high retention process known as membrane distillation (MD). The resulting combined process, the membrane distillation bioreactor (MDBR), is a membrane separation process that is driven by the temperature difference induced across a hydrophobic membrane, allowing only volatile components such as water vapour to pass through. This advanced system has the potential to produce high quality water for reuse purposes whilst effectively retaining non-volatile organics and salts which are biodegraded by thermophilic microorganisms (Khaing, Li, Li, Wai, & Wong, 2010). The MDBR is therefore potentially able to provide significant advantages over conventional membrane separation processes and can be used for the purpose of improving water quality in South Africa.

Although a limited number of studies on this system exist, this study aims to experimentally determine the potential of the MDBR system to treat and reuse pulp and paper mill effluent. The laboratory-scale MDBR was evaluated in terms of produced water quality and its potential to meet reuse requirements, membrane flux performance, the rejection of non-volatiles, and the membrane fouling phenomenon.

1.1 Research objectives

The objectives of this research study are:

1. To determine the composition and chemical properties of the pulp and paper mill effluent.
2. To design, construct and test the laboratory-scale MDBR.
3. To study the use of the MDBR in the treatment of pulp and paper mill effluent at different operating conditions and determine its viability to produce water of reuse standards according to the National Water Act No.36 of 1998.

1.2 Outline of the dissertation

This dissertation has been divided into 5 Chapters:

Chapter 1 provides a background and a motivation for this work. The objectives for this study are also listed.

Chapter 2 contains a review of the literature related to this study.

Chapter 3 provides the design and development of the MDBR. It also describes the experimental method along with the analytical techniques used for water quality analysis and membrane fouling determination.

Chapter 4 investigates the performance of the MDBR in treating pulp and paper mill effluent. The results obtained from experimental work are presented and discussed. Additional data can be found in the appendices.

The final chapter, Chapter 5, provides final deductions and recommendations for future work.

2 LITERATURE REVIEW

2.1 Membrane bioreactor (MBR)

The MBR has been identified as a promising technology that can help municipalities and industries to manage their water resources effectively. MBRs have been successfully implemented at several municipal and industrial wastewater treatment plants and are becoming increasingly popular due to tightening environmental regulations, improved performance and the development of cost-effective membranes (Liang, Zhao, Liu, & Song, 2008; Wang & Menon, 2011). This technology, which is a combination of a biological treatment process and membrane filtration, also has the potential to treat wastewater so that it can meet reuse standards (Sert et al., 2017). The MBRs biological process is based on the activated sludge process, whereby biological microorganisms are utilized to degrade organic matter in the wastewater. The membrane process makes use of low-pressure membrane filtration such as ultrafiltration (UF) and microfiltration (MF) membranes which allow effective solid-liquid separation between the treated water and the mixed liquor (Fraga et al., 2017; Kharraz et al., 2022; Melin et al., 2006). These pressure-driven filtration membranes are used to retain larger molecules; the MF membrane is used for the separation of SS with a particle size range of 0.08-10 µm while the UF membrane separates macromolecular solids with a particle size range of 0.01-0.1 µm (Wang & Menon, 2011).

2.1.1 MBR configurations and types

MBRs can be classified based on the position of the membrane unit; where the membrane is either immersed in the bioreactor (submerged MBR) or where the membrane is placed on the outside of the bioreactor (side-stream MBR) (Kharraz et al., 2022).

Figure 2.1 a) displays the configuration of a submerged MBR. This configuration operates in a similar manner as the activated sludge process however, aeration, secondary clarification and filtration all take place within the bioreactor. Treated effluent is extracted from the membrane unit using a permeate pump that creates a vacuum, leaving the solids behind in the bioreactor. The arrangement of a side-stream or an external circulation MBR is shown in Figure 2.1 b). In this process, the feed is screened prior to entering the bioreactor where it is broken down by biological microorganisms. The mixed liquor from the bioreactor is pumped through the external crossflow membrane filtration module using a high transmembrane pressure. Treated effluent is removed from the system while the retentate stream consisting of concentrated biosolids is sent back to the bioreactor. Excess biosolids are usually removed with the waste stream (Kharraz et al., 2022; Wang & Menon, 2011).

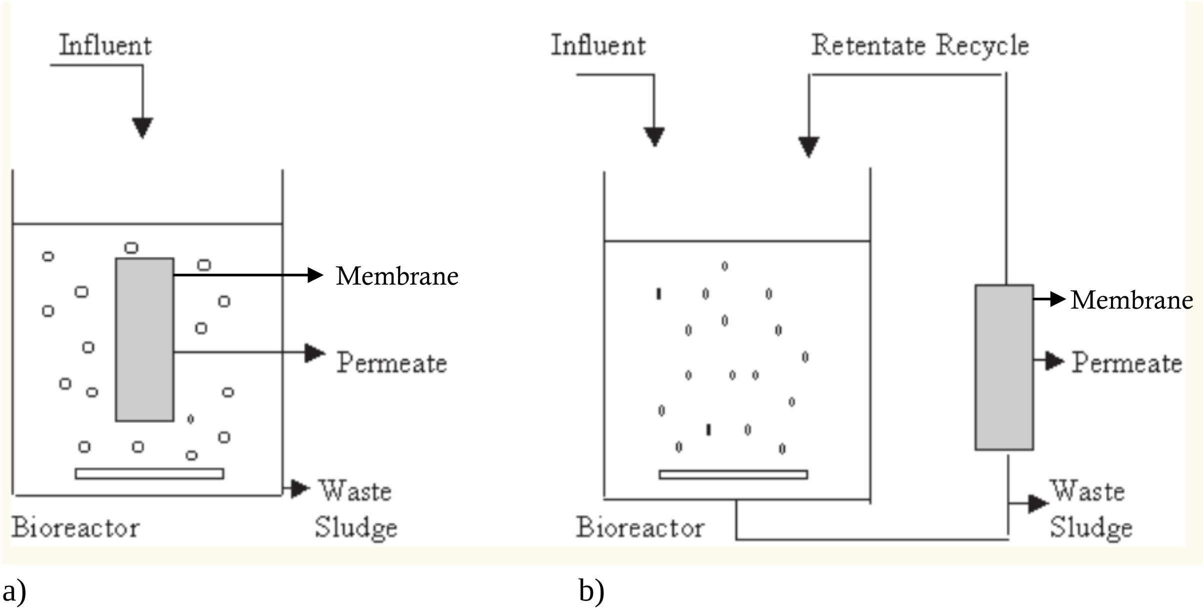

Figure 2.1. Configuration of MBR systems: a) Submerged MBR and b) Side-stream MBR (Melin et al., 2006)

The MBRs bio-treatment process can also be classified according to its oxygen dependence. There are three types namely aerobic, anoxic and anaerobic. In an aerobic process, dissolved oxygen is used for the biochemical conversion of organic carbon. In an anoxic process, conversion occurs in the absence of dissolved oxygen but in the presence of another form of oxygen. An anaerobic process is able to biochemically convert organic carbon without the need for dissolved oxygen or any other oxygen source (Kharraz et al., 2022).

2.1.2 Advantages, disadvantages and limitations of the MBR

The effective solid-liquid separation that is accomplished by the MBR provides a series of advantages which include a smaller footprint due to minimal space required when compared with conventional wastewater treatment systems, a longer sludge retention time (SRT) and reduced sludge production owing to a high biomass concentration in the bioreactor (Huang, Xiao, & Shen, 2010; Kaya et al., 2013; Nguyen et al., 2016). The MBR also produces a more stable and better quality effluent than most typical treatment systems, as a result of membrane filtration (Melin et al., 2006).

Although the MBR produces treated effluent of a better quality, the MF and UF membranes used in this application are not efficiently able to retain slowly biodegradable organic substances, dissolved salts and some bacteria. This is due to the substances having a smaller size than the typical pore size of membranes. The treated MBR effluent can potentially contain these organics, salts and bacteria and therefore it is not necessarily possible to use this water directly for non-potable reuse applications such as irrigation and process water. Tertiary treatment processes such as nanofiltration (NF) and reverse osmosis (RO) are still required to improve the quality of the effluent (Kharraz et al., 2022; Sert et al., 2017). Apart from this, the MBR is also associated with other disadvantages or limitations such as high capital and operational costs, temperature, pressure and pH restrictions because of membrane tolerances, and a high tendency for membrane fouling (Melin et al., 2006). In addition, the occurrence of membrane fouling results in several operational issues which include low permeate flux, frequent membrane cleaning and shortened membrane lifespan. The MBR is also regarded as an energy intensive technology because of its use of aeration as an oxygen source during the aerobic process (Yao et al., 2019).

2.2 Membrane distillation (MD)

MD is a membrane separation process that uses the vapour pressure difference, that is created by the temperature difference across the membrane, as the driving force for solid-liquid separation (Damtie, Kim, Woo, & Choi, 2018; Meng, Hsu, Ye, & Chen, 2015). The MD process is operated at low temperatures (within the range of 30˚C to 80˚C) and at atmospheric pressure (Mokhtar, Lau, Ismail, & Veerasamy, 2015; Phattaranawik, Fane, Pasquier, & Bing, 2008). The operational principle of this process is based on separation by means of phase equilibria and this is shown in Figure 2.2. This occurs as follows:

1) During the MD process, the microporous hydrophobic membrane comes into contact with the heated feed on one side.
2) The hydrophobic nature of the membrane creates a vapour-liquid interface at the membrane entrance and thus, only volatile components in vapour form are transported across the membrane. Liquid, macromolecules and non-volatile compounds are rejected (Kharraz et al., 2022).
3) The vapour is then condensed on the opposite side of the membrane by the permeate or the cooling stream (Curcio & Drioli, 2005; Goh, Zhang, & Fane, 2013).

In this manner, the system can retain recalcitrant compounds, non-volatile solutes and low-molecular weight organics and is therefore able to produce treated water of high quality (Goh et al., 2013).

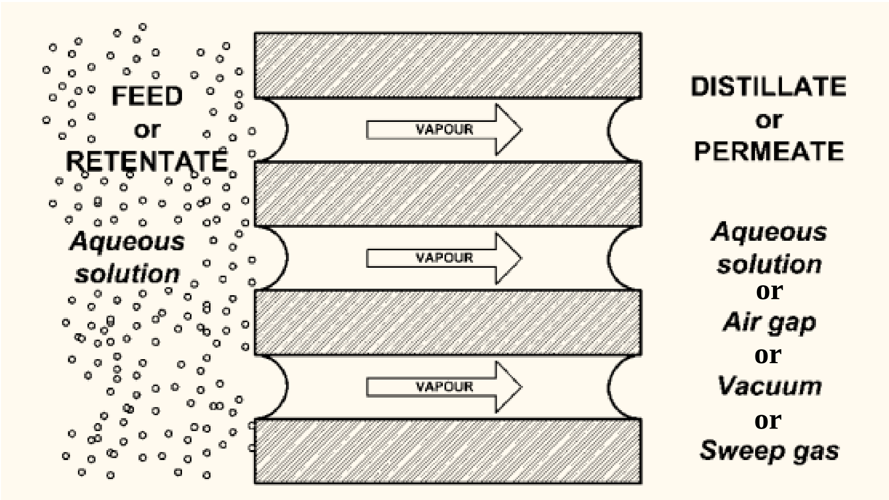

Figure 2.2. Operational principle of the MD process (Curcio & Drioli, 2005)

The use of MD as a separation process has many benefits, some of which include the possibility to achieve 100% rejection of non-volatile compounds and dissolved salts because of its operational principle, its ability to easily combine with other treatment processes such as UF and RO, its production of good quality effluent and it is operated at moderate conditions that is lower operating temperatures and pressures than those used in the conventional pressure-driven membrane separation processes, i.e. the process operates at atmospheric pressure and relies on the temperature gradient across the membrane (Choudhury, Anwar, Jassby, & Rahaman, 2019; Li, Wu, Sun, Cheng, & Liu, 2016; Liu & Wang, 2013). Due to the use of lower temperatures, the process is able to utilize alternative energy sources such as solar power, geothermal energy or waste heat for its energy production. In addition, the moderate operating conditions of the MD process also places less requirements on the mechanical properties of the membrane being used and results in less fouling (Naidu, Tijing, Johir, Shon, & Vigneswaran, 2020; Yang, Fane, & Wang, 2014). Based on these distinct advantages, the MD process has been applied for seawater desalination, wastewater treatment and solute recovery (Wu et al., 2018).

The first MD patent was granted in 1963 (P. Wang & Chung, 2015). However, slow progress related to the development of the MD process was observed. This was mainly due to the unavailability of suitable membranes for the application, insufficient knowledge regarding module design, the membrane wetting phenomenon, low flux performance and the high energy consumption of the process (Chamani, Woloszyn, Matsuura, Rana, & Lan, 2021; Drioli, Ali, & Macedonio, 2015; Wang & Chung, 2015). Since then, MD has become more attractive due to the growing research activities in this field. It has been applied at a laboratory scale for the treatment of industrial wastewaters which include olive mill wastewater, radioactive wastewater as well as textile dying wastewater (Fortunato, Elcik, Blankert, Ghaffour, & Vrouwenvelder, 2021; Liu & Wang, 2013). In these studies, MD has achieved good permeate water quality and has also demonstrated less fouling on the membrane (Li et al., 2016). The MD process has also been used in the food industry for milk and juice concentration and in pharmaceutical and biomedical industries processing (Jiao, Cassano, & Drioli, 2004; Kim, Lee, & Cho, 2016). MD has been investigated for decades and despite the numerous amount of studies conducted in the scientific community, it is yet to be commercialized in industry. Although, a few pilot plants are in operation (Tijing et al., 2015; Yang et al., 2014).

Since MD can operate at higher concentrations, has a high retentive ability and is merely used to concentrate waste and not treat it, it should be integrated with other treatment technologies in order to maximize its overall performance (Goh et al., 2013; Kesieme & Aral, 2015).

2.2.1 MD configurations

MD can be classified into four basic configurations depending on the way in which the vapours leaving the system are condensed and collected. The four basic MD configurations are direct contact membrane distillation (DCMD), air gap membrane distillation (AGMD), sweeping gas membrane distillation (SGMD) and vacuum membrane distillation (VMD) (González, Amigo, & Suárez, 2017). Figure 2.3 illustrates the mechanisms of each of the four basic configurations.

a) DCMD

In DCMD, both the hot feed and the cool permeate come into direct contact with the hydrophobic membrane surface on either side, as seen in Figure 2.3 a). Condensation of the vapours leaving the membrane occurs inside the membrane module and therefore DCMD requires the least amount of pieces of equipment when compared to other configurations. Its high treatment efficiency and simple design makes it the most investigated configuration with 48% of studies focusing on it (González et al., 2017; Kharraz et al., 2022). It has been used for desalination, wastewater treatment and the concentration of aqueous solutions in the food and acid production industry. However, this configuration experiences the highest heat loss through conduction due to direct contact of the solutions with the membrane, resulting in increased energy requirements for evaporation (González et al., 2017; Kharraz et al., 2022).

b) AGMD

In AGMD, as the schematic diagram in Figure 2.3 b) shows, a stagnant air gap is introduced on the permeate side between the membrane and the condensation surface. Vapours pass through the air gap before condensing on the cold surface inside the membrane module. The addition of the air gap reduces heat losses through conduction however, a drawback is that it creates a mass transfer resistance which affects flux performance (Kharraz et al., 2022; Onsekizoglu, 2012). This configuration is not as well received as DCMD with only a 15% research interest. AGMD has been employed for desalination and the removal of volatile compounds from aqueous solutions (Alkhudhiri, Darwish, & Hilal, 2012; González et al., 2017).

c) SGMD

SGMD makes use of an inert gas that sweeps the vapours on the permeate side of the membrane as depicted in Figure 2.3 c). The collected vapours are transported outside the membrane module, where they are condensed (El-Bourawi, Ding, Ma, & Khayet, 2006). The presence of the inert gas reduces heat loss and enhances mass transfer as the gas is not stationary as in AGMD. The main disadvantage of this configuration is the high costs associated with the large amounts of gas that are required thus, making it the least used configuration. SGMD is useful for volatile compound removal from aqueous solutions (Alkhudhiri et al., 2012; Kharraz et al., 2022).

d) VMD

VMD uses a vacuum pump on the permeate side to suck the vapours out of the membrane module and transport them to an external condenser, as shown in Figure 2.3 d). The operation of the system under vacuum allows it to operate at lower temperatures and pressures, placing less strain on the mechanical strength of the membrane. VMD also results in other benefits such as a higher flux, a lower heat loss through conduction and a reduced resistance to mass transfer. However, it is more prone to membrane fouling when compared to the other configurations. Despite this drawback, VMD has gained a substantial increase in attention in the scientific community and is frequently used for the separation of volatile compounds from aqueous solutions (González et al., 2017; Kharraz et al., 2022).

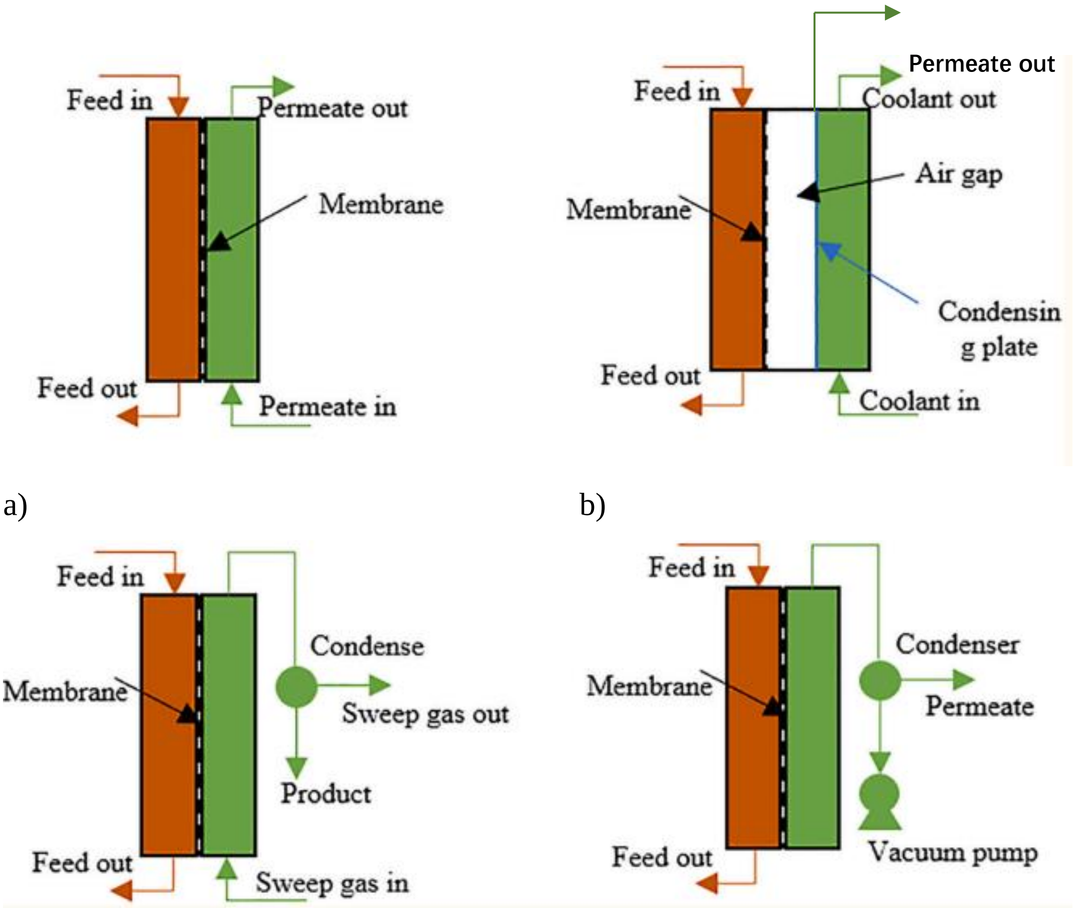

a) b)

c) d)

Figure 2.3. Basic MD configurations: a) DCMD, b) AGMD, c) SGMD and d) VMD (Kharraz et al., 2022)

2.2.2 MD membranes

In MD, the selection of a membrane has a great influence on separation performance. A membrane that is hydrophobic or non-wetting, and porous is generally used in the MD process (Drioli et al., 2015).

2.2.2.1 Membrane properties

Membranes employed in the MD process are usually fabricated from polymers due to their hydrophobic nature, ability to easily be modified, low thermal conductivity and low cost (Chamani et al., 2021). Polytetrafluoroethylene (PTFE), polyvinylidene fluoride (PVDF) and polypropylene (PP) are the most used polymeric materials, with PTFE being the most favourable as it exhibits the best hydrophobic characteristics and has excellent chemical and thermal stability. PVDF membranes also possess good chemical resistance and thermal stability while PP membranes display high crystallinity and exceptional solvent resistant properties (González et al., 2017; Onsekizoglu, 2012; Thomas, Mavukkandy, Loutatidou, & Arafat, 2017).

The performance of MD is also affected by the membrane structure in terms of pore size, porosity, thickness, pore distribution and geometry. MD membranes should have a pore size in the range of 0.1 µm to 1 µm and a porosity between 38% and 90%, for effective MD to take place. The membrane should also have an optimum thickness that ranges between 30 µm and 60 µm in order to ensure that the resistance to mass transfer remains low for vapour transport (Abu-Zeid et al., 2015). Another important property that a MD membrane should possess is a low thermal conductivity to reduce heat losses. Other characteristics that the membrane should display are a good thermal stability to withstand high temperatures, a uniform or narrow pore size distribution and a high resistance to chemicals (González et al., 2017). Table 2.1 provides an overview of the membrane properties desired for MD.

Table 2.1. Overview of the membrane properties desired for MD (Eykens, De Sitter, Dotremont, Pinoy, & Van der Bruggen, 2017)

Parameter	**Affects**	**Range used in literature**	**Recommendation**
Contact angle (θ)	Wetting resistance	80-160˚	>90˚, as high as possible
Liquid entry pressure (LEP)	Wetting resistance	0.5-4.6	> 2.5 bar
Pore diameter (d_{av})	Wetting resistance, flux and energy efficiency (for d_{av} < 0.3µm)	0.012-1.2 µm	0.1-1 µm 0.3 µm
Porosity (ε)	Flux, energy efficiency, strength	38-90%	80%
Thickness (δ)	Flux, energy efficiency, strength	10-200 µm	Low salinity: 30-60 µm High salinity: 2-700 µm
Tortuosity (τ)	Flux, energy efficiency	1.1–3.9	As low as possible
Thermal conductivity of the material (κ_m)	Flux, energy efficiency	0.031–0.057 W/mk 2–5 W/mk	As low as possible

Tensile strength	Strength	3.4–57.9 MPa	As high as possible
Compaction	Flux and energy efficiency at full scale, strength	PTFE: 22% at 0.6 bar	Not compressible

2.2.2.2 Membrane modules

A membrane module is usually chosen based on both economic considerations and MD operating conditions (Curcio & Drioli, 2005). There are three types of membrane modules currently being used in MD; these are the plate and frame, hollow fiber and spiral wound.

The plate and frame module makes use of a flat sheet membrane that is placed between two plates, as shown in Figure 2.4 a). This type of module is commonly used at a laboratory scale as it is easy to design, assemble and operate. It is also easy to clean and allows for easy replacement of the membranes (Qasim, Samad, Darwish, & Hilal, 2021). However, this module has a low packing density, which is the ratio of membrane area to packing volume, resulting in slow permeation (Alkhudhiri et al., 2012).

The hollow fiber module consists of many fibers that are bundled and stored within a shell, as seen in Figure 2.4 b). This module offers a higher packing density than the plate and frame module, making it suitable for industrial applications (González et al., 2017; Qasim et al., 2021). It is also energy efficient. On the other hand, it exhibits a low flux, is difficult to clean and has a high tendency to fouling (Alkhudhiri et al., 2012).

A spiral wound module contains numerous flat sheet membrane envelopes that are wrapped around a central collection pipe in a tubular vessel. Figure 2.4 c) provides a schematic of this module. The spiral wound module has a good packing density, an allowable energy consumption and minimal pressure drop (Alkhudhiri et al., 2012; González et al., 2017). These advantages make it popular for industrial use. However, the module is difficult to clean and is prone to fouling (Qasim et al., 2021).

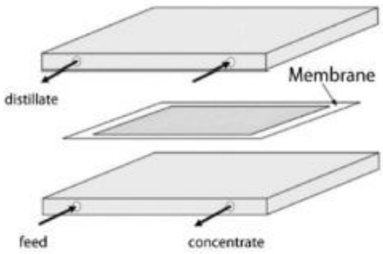

a)

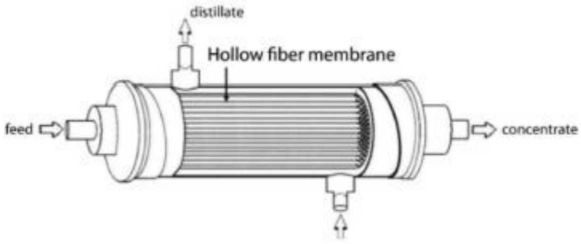

b)

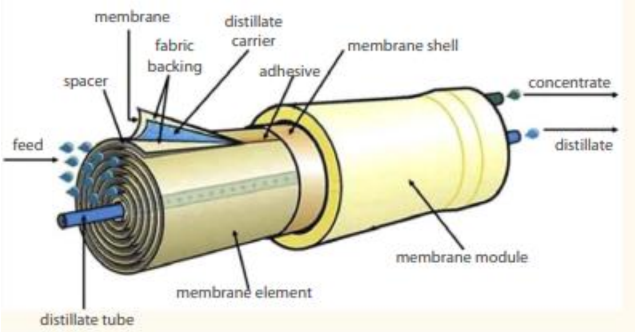

c)

Figure 2.4. Typical MD membrane modules: a) Plate and frame, b) Hollow fiber and c) Spiral wound (González et al., 2017)

2.2.2.3 Membrane fouling and wetting

Although MD is associated with many benefits, there are two potential problems that may lead to system failure. These potential problems are membrane fouling and membrane wetting.

Membrane fouling is the accumulation of undesirable materials on the surface of the membrane or inside the pores of the membrane that reduce its permeate flux and the process efficiency (Abdel-Karim et al., 2021; Tijing et al., 2015; Warsinger, Swaminathan, Guillen-Burrieza, Arafat, & Lienhard V, 2015). The foulant characteristics, membrane properties, operational conditions and the feed solution quality all influence the degree of membrane fouling (Choudhury et al., 2019).

Fouling can be classified into three groups according to the fouling material which may be organic, inorganic or biological in nature. Organic fouling involves the adsorption of dissolved and colloidal organic matter on the membrane surface which usually has to be cleaned with the use of chemicals. Inorganic fouling or scaling occurs when precipitated hard minerals deposit on the membrane surface as crystals (Tijing et al., 2015). Biological fouling or biofouling takes place when biological microorganisms such as bacteria, algae and fungi attach themselves to the membrane surface (González et al., 2017).

In order to reduce the effects of fouling and improve MD performance, it is important to understand the factors that aid in fouling, find effective mitigation methods and better MD design.

Membrane wetting is a phenomenon that takes place as a result of the penetration of feed solution through the pores of the membrane. This occurrence results in the membranes hydrophobic properties being lost (Choudhury et al., 2019). It happens due to two reasons; membrane wetting can be stimulated by membrane fouling or it can occur if the hydraulic pressure on the membrane surface exceeds the liquid entry pressure (LEP) or the pressure at which the solution starts to penetrate the membrane pores. Membrane wetting leads to the decrease in permeate flux as well as the decline in permeate quality (Rezaei et al., 2018).

The wettability of membranes has been classified into four degrees which include non-wetted, surface-wetted, partially wetted and fully wetted membranes (Rezaei et al., 2018). MD membranes that are non-wetted maintain their full functionality while membranes that are surface-wetted still retain non-volatile solutes present in the feed solution and are responsible for a reduction in permeate flux. In the case of a partially or fully wetted membrane, the feed solution flows through the membrane pores either partially or completely, leading to a permeate of low quality (Choudhury et al., 2019; González et al., 2017).

The contact angle is a measurement that is used to determine the hydrophobicity of a membrane. This is done by depositing a droplet of water on the membrane surface and calculating the angle between the wetted surface and a tangential line to the curved surface of the water droplet. A contact angle that is greater than 90˚ is considered as hydrophobic (Curcio & Drioli, 2005; Onsekizoglu, 2012).

2.3 Membrane distillation bioreactor (MDBR)

The MDBR is a hybrid system that combines the MD process with the conventional MBR. The process is based on the same operational principle as MD whereby a vapour-liquid interface created from a temperature gradient allows only volatile substances to diffuse across a hydrophobic membrane to produce high quality water. The non-volatile solutes, dissolved salts and slowly biodegradable organics are retained by the membrane (Goh, Zhang, & Fane, 2015; Goh, Zhang, Zhang et al., 2013). However, the MDBR is operated at thermophilic conditions that is at a feed temperature range of 35˚C to 70˚C, which enhances the biodegradation of the retained compounds (Naidu et al., 2020; Wijekoon et al., 2014).

The MDBR is potentially able to resolve the problems associated with the MBR in the treatment of municipal and industrial wastewater. Dissolved salts, non-volatile solutes and slowly biodegradable organics are completely retained in the MDBR resulting in high quality effluent, as opposed to their passage through the membrane in the conventional MBR. The MDBR's SRT is also sufficiently longer than the hydraulic retention time (HRT), allowing the slowly biodegradable organics a longer amount of time to degrade (Kharraz et al., 2022; Phattaranawik et al., 2008). Table 2.2 summarizes the key differences between the MDBR and the conventional MF/UF-MBR.

Table 2.2. Key differences between the MF/UF-MBR and the MDBR (Phattaranawik et al., 2008)

Characteristic	**MF/UF-MBR**	**MDBR**
Driving force	Pressure (suction preferred)	Thermal (temperature difference), at atmospheric pressure
Membrane	UF or MF, hydrophilic preferred	Porous, hydrophobic MF such as polytetrafluoroethylene (PTFE) and polyvinylidene fluoride (PVDF) (preferred)
Phase in membrane pores	Liquid	Vapour, gas
Retention of target compounds and microorganisms by membranes	Incomplete: for MF less than 50% for small organic compounds, spores and small virus	100% for salts, non-volatile organic compounds, and microorganisms
Permeate quality	Dependent on biological activity; total organic carbon (TOC) of 3-10 ppm	Independent of biological activity, comparable to distillation product; TOC < 0.8 ppm
Inorganics	Salts not retained	Salts retained and discharged with waste sludge
Start-up time	Slow	Potentially faster
Organic retention time (ORT) and hydraulic retention time (HRT)	ORT ~ HRT	ORT~∞*, independent of HRT, *until organics become carbon dioxide (CO_2) or volatile
Flux	10-30 L/m^2h (typically)	2-15 L/m^2h (~RO fluxes) at 55°C
Membrane integrity monitoring	Particle counting techniques, laser-turbidity monitoring, intermittent pressure decay tests	Conductivity monitoring on a continuous basis

The MDBR is also potentially able to achieve wastewater reclamation in one stage as compared to a conventional system consisting of a MBR with RO as a post-treatment step (Phattaranawik et al., 2008). Table 2.3 shows a qualitative comparison of the costs associated with the MDBR and the dual MBR with RO process. The comparison indicates that the MDBR is able to operate and potentially able to produce treated water of high quality at reduced capital costs and operational requirements. This makes the MDBR a more cost effective process.

Table 2. 3. Qualitative economic comparison of the dual MBR-RO system and the MDBR (Phattaranawik et al., 2008)

Items	**Hybrid UF-MBR + RO**	**Novel MDBR**
I. Capital Costs		
Footprint	Larger than MDBR – expected because there are two processes: MBR and RO	Lower cost, but larger footprint than conventional MBR (MDBR has lower flux)
Membranes and modules	Higher cost because there are two processes: MBR and RO. Pressure vessels for RO	Single process at atmospheric pressure, but more than MBR due to materials and lower flux
Piping systems and valves and pumps	Higher cost, due to high pressure piping and pumps for RO	Low cost; operated at atmospheric pressure
Membrane integrity monitoring system	Higher cost; sophisticated instruments required	Lower cost; continuous monitoring by flow and conductivity
Heat exchangers	Not required	Requires good heat exchange and cooling systems
II. Energy and operating costs		
Energy sources for process operations	Electricity only	Low grade waste heat, solar energy Electrical power required is low
Labour cost	Potentially higher due to two processes	Potentially lower
Sludge disposal	Potentially higher	Potentially lower
III. Maintenance costs		
Various	Potentially higher, due to higher pressures, more equipment, etc.	Potentially lower

The MDBR has only been applied at a laboratory-scale for the treatment of synthetic wastewater and petrochemical wastewater (Shuwen Goh, Zhang, Liu, et al., 2013). Phattaranawik et al. conducted one of the first MDBR studies using synthetic wastewater and achieved a high quality permeate with a low total organic carbon (TOC) content. Khaing et al. demonstrated the feasibility of using the MDBR for petrochemical wastewater reclamation and obtained a permeate quality that consistently met the requirements of NEWater of Singapore except for a slightly higher TOC. Goh et al. achieved a TOC and total nitrogen (TN) removal efficiency of 88% and 68% respectively when using synthetic wastewater as the feed source. Yao et al. investigated the first anaerobic MDBR to treat synthetic wastewater and acquired an inorganic rejection rate of 99.99%. These results show the potential of the MDBR for water reuse applications. The MDBR is best suited to applications which require a high quality water product and a long residence time for the effective removal of problematic organics (Khaing et al., 2010). It also has the potential to recover nutrients and biogas, and may possibly facilitate the removal of trace organic contaminants (TrOCs) or small complex particles in wastewater (Kharraz et al., 2022).

2.3.1 MDBR configurations

MDBRs can be configured in two ways based on the position of its MD unit. The first configuration, also known as the submerged MDBR, directly immerses the MD unit inside the bioreactor, as displayed in Figure 2.5 a). In this configuration, the MD membrane replaces the MF or UF membranes that are typically used in MBRs and is directly involved in the treatment process. The submerged MDBR produces a permeate of high quality as well as effectively retaining and degrading slowly biodegradable organics within the bioreactor. The second configuration, referred to as the side-stream MDBR, connects the MD unit downstream of the bioreactor, as illustrated in Figure 2.5 b). In a side-stream MDBR, the MD unit does not actively get involved in the treatment or biodegradation process but acts as a post-treatment step for the bioreactor effluent (Kharraz et al., 2022; Naidu et al., 2020).

MDBR configurations can be operated in aerobic or anaerobic conditions. Under aerobic conditions, air is supplied to the system in order to provide oxygen to the thermophilic microorganisms and to decrease the effects of membrane fouling (Phattaranawik et al., 2008). In anaerobic conditions, the absence of air assists with the growth of anaerobic microorganisms and potentially recovers biogas (Yao et al., 2019).

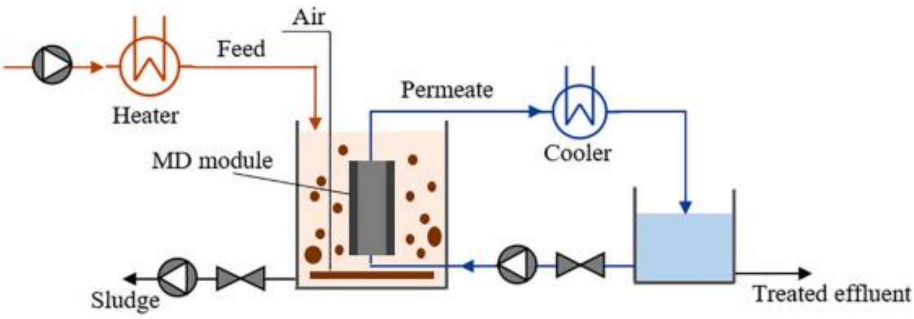

a)

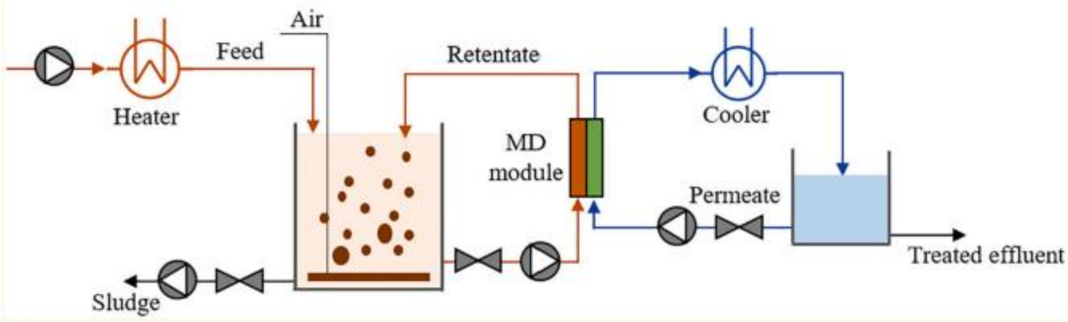

b)

Figure 2.5. MDBR configurations: a) Submerged MDBR and b) Side-stream MDBR (Kharraz et al., 2022)

2.3.2 Advantages of the MDBR

The MDBR offers several benefits when compared to the MBR, MD and other hybrid systems which include the complete retention of non-volatile organics, biomass and salts, lower energy requirements in contrast to pressure driven membrane processes, the potential usage of waste heat and alternative energy sources for its thermal energy requirements and it produces high quality water capable of meeting water reuse standards (Kharraz et al., 2022; Vijay, Ling, & Fane, 2013). The MDBRs permeate quality is also not influenced by the biological activity in the bioreactor as only vapours are transported across the hydrophobic membrane (Phattaranawik et al., 2008). In addition, the submerged MDBR configuration offers a smaller footprint as a single unit is used for water treatment instead of different units when compared with other hybrid treatment systems. The operation of the MDBR at thermophilic conditions and a longer residence time enhances the biodegradation of organics gradually and results in a low sludge yield (Kharraz et al., 2022).

2.3.3. Challenges associated with the MDBR

Despite the numerous advantages of the MDBR, the system has certain challenges. The main challenge faced by the MDBR system is that of low permeate flux. Fluxes in the range of 2-15 L/m^2h have been reported for the MDBR whereas the conventional MBR has permeate fluxes in the range of 10-30 L/m^2h, as outlined in Table 2.2 (Phattaranawik et al., 2008). This makes it difficult for wastewater treatment plants to realize the treatment of high volumes of wastewater using the MDBR (Kharraz et al., 2022; Naidu et al., 2020).

Another challenge experienced by the MDBR is the great energy requirement needed to create the separation mechanism of a temperature difference through feed heating and permeate cooling. At a large scale, the MDBR would only be viable if waste heat is available and low cost cooling options are used (Naidu et al., 2020; Phattaranawik et al., 2008).

The MDBR system is also associated with the problem of salinity build-up in the bioreactor due to the high rejection of inorganic salts. The increase in salinity affects the properties of the activated sludge being used, changes microbial dynamics as well as accelerates the potential of membrane fouling (Kharraz et al., 2022).

One of the other major difficulties related to the MDBR is that of membrane fouling. This occurs as a result of the deposition of various contaminants on the MD membrane due to its excellent rejection efficiency. Membrane fouling is yet to be overcome with proper mitigation methods and improved module design (Kharraz et al., 2022).

Another issue with the MDBR is that of fouling-induced membrane wetting which compromises the hydrophobicity of the membrane. The occurrence of membrane wetting leads to the deterioration in permeate quality which in turn affects process performance (Kharraz et al., 2022).

To date, there have only been a few studies applying the MDBR for wastewater treatment. The literature indicates that no work has been done on using the MDBR for the remediation of pulp and paper mill effluent. Therefore, for the work presented in this dissertation, effluent from a local pulp and paper mill was treated using a MDBR.

3 RESEARCH METHODOLOGY

3.1 Sampling protocol for feed wastewater

Effluent samples were obtained from a pulp and paper mill in Durban, South Africa, that utilizes recyclable materials as the feedstock to produce paper. The samples were taken from the overflow of a clarifier, which is the point where all the effluent streams from the mill combine, just before the effluent undergoes further treatment. This sampling point was chosen in order to ensure that the samples were representative of the entire papermaking process. Grab samples, comprising of 1 L plastic bottles, were taken for three days within the same week (from 10 May 2022 to 12 May 2022) at the same time each day. The effluent samples were stored in a refrigerator at 4˚C directly after sampling in order to prevent the biodegradation of the effluent due to microbial activity. Samples were sent off to an external laboratory to test for various water quality parameters and a brief description of each method is provided in Section 3.4.1. The ionic composition and other characteristics of the collected feed wastewater samples can be found in Section 4.1. This wastewater was used as feed in the MDBR treatment study.

3.2 Acclimatization of the microorganisms

Microorganisms that thrive at temperatures between 20℃ to 25℃ were collected from the aeration lagoon at the aforementioned pulp and paper mill. The microorganisms were adapted in order to stabilize to new environments at target temperatures of 45˚C, 55˚C and 65˚C, using Heldolph hot plates. The acclimation was conducted in batch mode for four weeks using 1 L glass cylinders each placed on hot plates, before the start of the MDBR experiments. Nutrients such as potassium nitrate (KNO_3) and potassium dihydrogen phosphate (KH_2PO_4) were added weekly in the wastewater order to maintain the chemical oxygen demand: nitrogen: phosphate (COD:N:P) ratio as 100:5:1 and to sustain the growth of the microorganisms (Sundararaman, 2016). A Regent 9500 aquarium air pump was used for aeration. Figure 3.1 shows the experimental setup for the microorganism acclimatization study at the target temperatures of 45˚C, 55˚C and 65˚C.

The total suspended solids (TSS) test was conducted every two days to monitor the growth of the microorganisms at each target temperature. Vacuum filtration apparatus was used to filter 50 mL of sample through a pre-weighed 1.2 μm glass fiber filter paper. The filter paper with collected solids was dried for an hour in an oven at 105˚C. Once dried, the filter paper was cooled in a desiccator and then weighed. The TSS for a sample was calculated using Equation 3.1 (Mazhar et al., 2019).

$$TSS\ (mg/L) = \frac{(Weight_{final}\ (g) - Weight_{initial}\ (g)) \times 1\ 000\ 000}{Sample\ Volume\ (mL)} \text{.............................Equation 3.1}$$

a) b)

Figure 3.1. Microorganism acclimatization setup: a) At 45˚C and b) At 65˚C (left) and at 55˚C (right)

3.3 Design of the MDBR system

The laboratory-scale MDBR system in this study was designed by carefully considering the properties of the pulp and paper mill effluent (feed wastewater), the characteristics of the membrane being used, the chosen type of bioreactor configuration and the system's layout and process operating conditions. The influence of varying operating temperatures on process performance was also investigated. These factors significantly influenced the treatment efficiency of the process.

3.3.1 Membranes

Hydrophobic flat sheet membranes fabricated from PTFE were chosen based on literature and were supplied by National Separations, South Africa (González et al., 2017). The membranes were used as received without any further modification and treatment. For the experiments, an unused (new) membrane was utilized each time for the different operating temperatures. Specifications of the membrane obtained are provided in Table 3.1.

Table 3.1. Specifications of the membrane

Item	**Unit**	**Specification**
Membrane pore size	µm	0.2
Membrane diameter	mm	100
Membrane thickness	µm	65
Membrane bubble point for Isopropanol	kPa	100

3.3.2 Bioreactor design

A laboratory-scale MDBR (schematic is shown in Figure 3.2) with a reactor volume of 3.6 L was used in this study. The MDBR was constructed from transparent glass in a cylindrical arrangement and comprised of two separate sections; the bottom half being the feed section and the top half consisting of the permeate section. The feed section was designed to handle a greater volume (300 mm high with a 100 mm inner diameter (ID)) than the permeate section (150 mm high with the identical ID) because of the phases that exist within each section. Three ports with an 8 mm ID were drilled into the sidewalls of the feed section; the feed inlet port located on the right side of the MDBR was at a height of 200 mm, the right air inlet port was at a height of 60 mm and the waste outlet port found on the left side of the MDBR was at a height of 60 mm. The permeate section consisted of one 8 mm ID outlet port, found on the left side of the MDBR, for the removal of the vapours. Five 15 mm ID probe ports (approximately at a height of 100 mm apart) were also drilled around the feed section for continuous monitoring of the mixed liquor within the MDBR. Both of the sections of the MDBR contained a sintered glass plate of porosity of two. This glass plate acted as a support for the membrane. The feed and the permeate sections were tightly fitted together, with the membrane placed in between, with ground glass flanges. Vacuum grease and bull dog clips were used to seal and secure the two sections together.

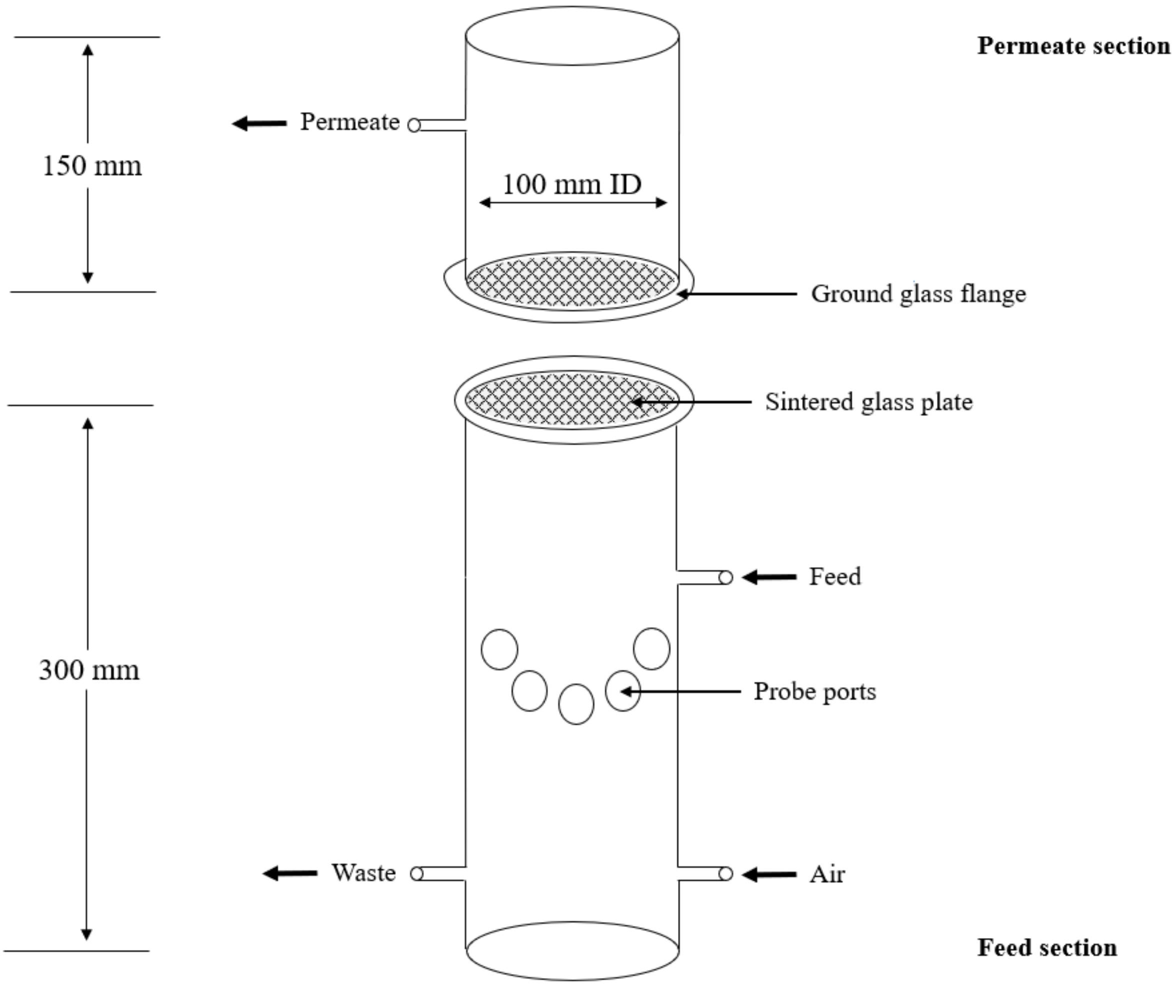

Figure 3.2. Design of the lab-scale MDBR

3.3.3 Experimental setup

3.3.3.1 Description of the laboratory-scale MDBR system

A process flow diagram (PFD) and an image of the experimental setup of the MDBR system are provided in Figure 3.3 and Figure 3.4 respectively. A VMD configuration was selected for the MDBR system because of its many advantages (as listed in Section 2.2.1). A membrane was placed in the bioreactor and sealed before the start of the experiments. Pulp and paper mill effluent (feed wastewater) was mixed with the acclimatized microorganisms in a ratio of 4:1, as recommended by Sundararaman, before continuously being fed to the bioreactor. The mixed feed from a 2.5 L polyvinyl chloride (PVC) feed tank was pumped at a rate of 150 mL/min using a Watson Marlow 520DU/R peristaltic pump to the bioreactor. The mixed liquor level in the bioreactor was monitored to ensure that the feed was in direct contact with the membrane. The MDBR was heated at varying temperatures of 45˚C, 55˚C and 65˚C using a Heldolph heater-stirrer plate. A digital temperature sensor was placed in the MDBR and used to verify that the correct temperature was maintained. Mixed liquor in the bioreactor was stirred with a magnetic stirrer at 110 rpm to maintain homogeneity within the bioreactor and air was supplied at a rate of 3 L/min with a Brooks microprocessor control and read out flow meter. The dissolved oxygen (DO) was maintained within a range of 2-4 mg/L and was monitored with an online DF Robot analog DO sensor. The pH and the electrical conductivity (EC) of the mixed liquor were also continuously observed using an online DF Robot analog pH and EC sensor respectively. All online monitors were connected to an Arduino program for 24-hour data collection. A vacuum pressure of 1 bar was applied through a KNF Neuberger Freiburg MW63/4 vacuum pump to draw out the vapours from the permeate section of the bioreactor. The vapours were transported and immediately condensed in a counter-current condenser setup run by a ViaAqua fish pond pump immersed in an ice bath. The condensate was collected by the adjoining 1 L conical flask, used as a permeate tank, that was placed on a Mettler Toledo electronic balance.

An experimental run at each temperature (45˚C, 55˚C and 65˚C) was performed for a period of three weeks (twenty-one days). The dates for each experimental run are listed:
Experimental run at 45˚C: 24 July 2022 – 14 August 2022
Experimental run at 55˚C: 05 September 2022– 26 September 2022
Experimental run at 65˚C: 27 September 2022– 18 October 2022

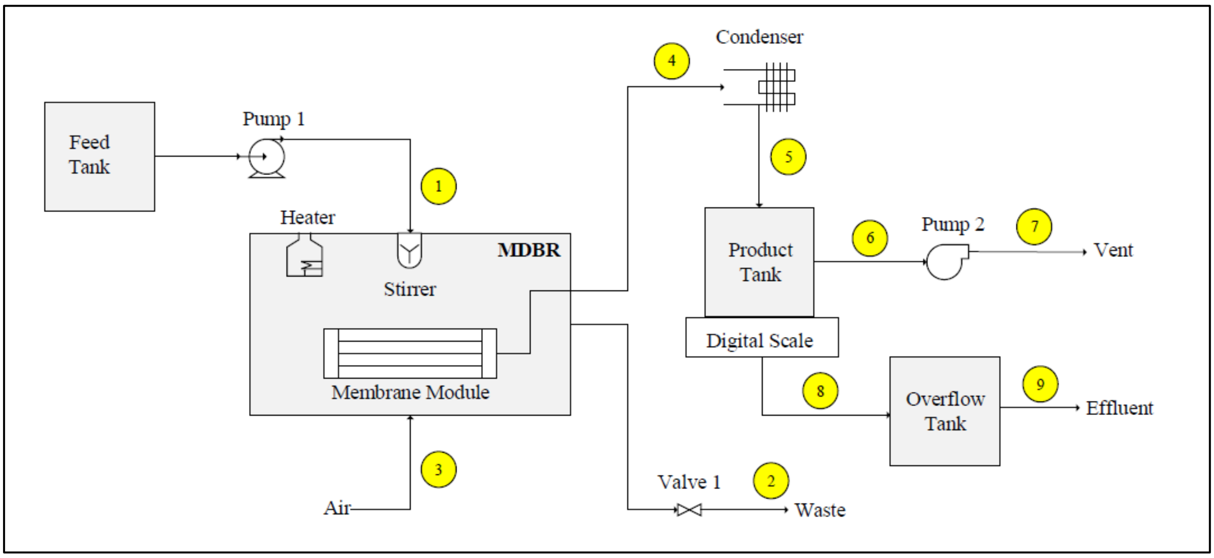

Figure 3.3. Process flow diagram of the designed and constructed MDBR system

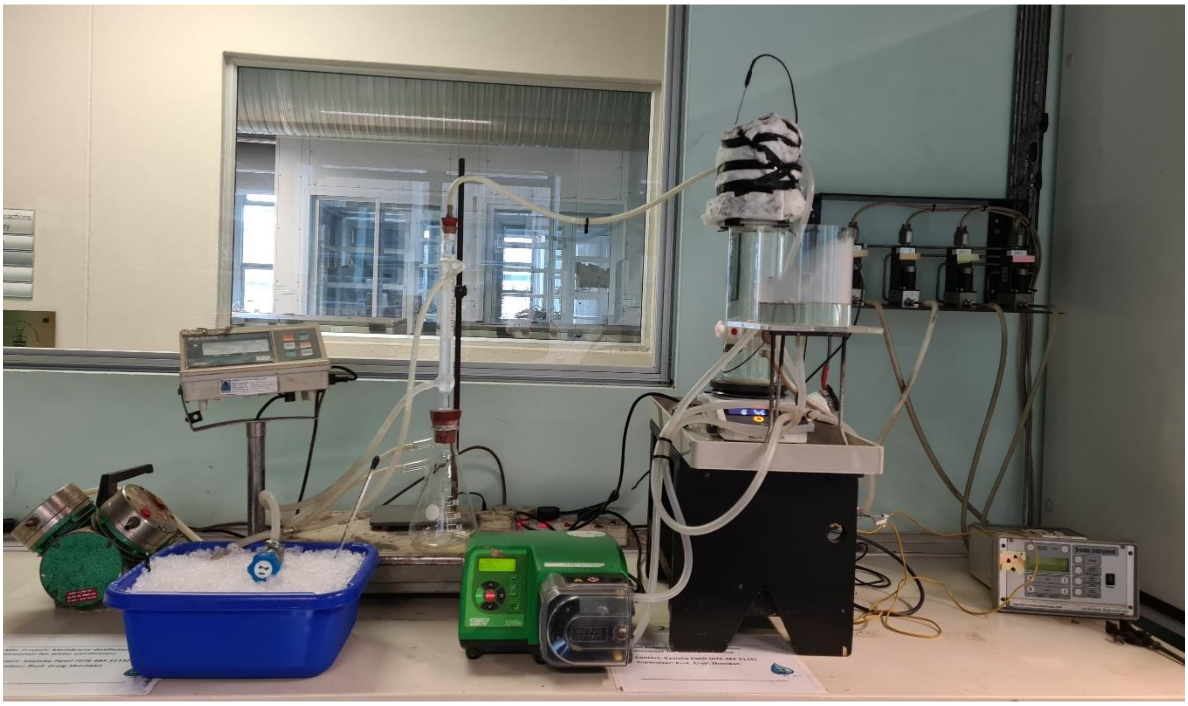

Figure 3.4. Experimental setup of the MDBR system

3.3.3.2 Sampling protocol for the MDBR system

Permeate samples of 500 mL aliquots were taken every two days at the same time by emptying the permeate tank, from the start to the completion of an experimental run. The sampling duration of two days was chosen because permeate production was relatively slow. Samples were sent to an external laboratory for the analysis of various water quality parameters, as described in Section 3.4.1.

A reactor sample of 50 mL was extracted every two days from the bioreactor and then topped up with wastewater. The samples were tested by an external laboratory for pH, EC, TSS and TDS. The detailed electronically logged data for the experiments are presented in Appendix F, Appendix G, Appendix H and Appendix I.

3.4 Analytical measurements

The MDBR's feasibility and performance in treating pulp and paper mill effluent was evaluated with basic water quality parameters. Analysis of the membranes was also carried out as an additional measure to determine the effect that membrane fouling and membrane wetting have on process performance.

3.4.1 Water quality parameters

Both the feed wastewater and the product samples at each target temperature (45˚C, 55˚C and 65˚C) were sent to an external lab for analysis. The external laboratory measured the following water quality parameters:

3.4.1.1 pH

The Mettler Toledo pH meter was calibrated using three prepared buffer solutions of pH 4.01, 7.00 and 10.01 respectively. In order to measure the acidity or alkalinity, both the feed and the permeate samples were preconditioned at 25˚C and tested for pH. The analysis of pH looked at the amount of hydrogen ions present in the sample.

3.4.1.2 Electrical conductivity (EC)

The EC of both the feed and the permeate samples was measured using a Mettler Toledo conductivity meter. Samples were preconditioned at 25˚C and tested for their ability to conduct electric current.

3.4.1.3 Total suspended solids (TSS)

TSS was conducted using vacuum filtration. A sample of 25 mL was filtered through a pre-weighed 1 μm glass fiber filter paper and the residual solids on the filter paper were dried at 105˚C in an oven overnight. Once dried, the filter paper was cooled and weighed.

3.4.1.4 Total dissolved solids (TDS)

Vacuum filtration was used to filter a sample of 25 mL through a 1 μm glass fiber filter paper. The remaining filtrate was poured into a pre-weighed beaker and evaporated at 105˚C overnight. Once the contents were evaporated, the beaker was placed in an oven at 180˚C for two hours. The sample was allowed to cool and was weighed thereafter.

3.4.1.5 Chemical oxygen demand (COD)

An open reflux method (titrimetric) using a Dosimat-Metrohm was used for the determination of COD. A 20 mL sample was oxidized in the presence of potassium dichromate ($K_2Cr_2O_7$) under acidic conditions, achieved by using sulphuric acid (H_2SO_4). The residual dichromate was back-titrated by making use of ferrous ammonium sulphate ($(NH_4)_2Fe(SO_4)_2 \cdot H_20$).

3.4.1.6 Total organic carbon (TOC)

The TOC of the feed and permeate samples was measured with catalytic combustion using the Teledyne Tekmar Torch Combustion TOC analyzer. The instrument was calibrated with standards of 5, 10, 25, 50 and 100 prior to the commencement of the sample run. Samples were injected with a syringe into a catalyst packed tube enclosed at high temperatures (680˚C-1 000˚C). The carbon present in the sample was oxidized into carbon dioxide (CO_2) and swept by the carrier gas to the non-dispersive infrared (NDIR) detector. The detector was sealed off when the gases inside the detector reached equilibrium. A single reading was used to determine the amount of CO_2 in the detector cell as it correlates directly to the concentration of the carbon contribution from the sample.

3.4.1.7 Ionic composition – cations

The ionic composition for various positively charged elements was tested using inductively coupled plasma optical emission spectroscopy (ICP-OES) with 5110 Agilent Technology. ICP-OES is the measurement of light intensity emitted by the elements in a sample after being introduced to an inductively coupled plasma (ICP) source. A sample in liquid form was placed into the instrument where it was converted into droplets (aerosol) by a nebulizer. The droplets were transported into the plasma torch and interacted with the radio frequency ICP at an approximate temperature of 4 726.85˚C. The elemental-specific emission spectra were produced and the intensities were measured with a vista chip II charge-coupled device (CCD) detector. The measured intensities were then compared to the intensities of the standards of known concentration to obtain an elemental concentration in the unknown sample.

3.4.1.8 Ionic composition – anions

An ion chromatography system (ICS) 2000 was used to determine the ionic composition of any negatively charged elements or anions found in the feed and permeate samples. A small volume of sample, approximately ± 5 mL, was introduced into the ion chromatograph. The anions of interest were separated and measured using a system consisting of a guard column, analytical column, suppressor and conductivity detector. Separation of the anions into the columns was based on their relative affinities for the low-capacity, strongly basic anion exchange resin of the columns. During suppression, the anions were converted to their highly conducive acidic forms and measured by conductivity. The peak area of the signal from the detector was compared to that from a standard solution.

3.4.2 Permeate flux

Permeate flux was measured by the change in water weight on the permeate side with an electronic balance. This was achieved by measuring the initial weight of the permeate tank before the start of each experiment at the temperatures of 45˚C, 55˚C and 65˚C. The permeate from the MDBR system was allowed to accumulate in the permeate tank and the quantity of permeate produced was measured every two days using the electronic balance. The permeate flux over a two day period was then calculated using Equation 3.2, where *J* is the permeate flux (L/m^{2}h), W_1 is the weight of the permeate tank at the start of the experiment (kg), W_2 is the weight of the permeate solution after a two day period (kg), ρ is the density of water (g/m^3), A is the membrane area (m^2) and Δt is the sampling interval (h) (Jacob, Phungsai, Fukushi, & Visvanathan, 2015; Jia, Li, Wang, & Sun, 2017).

$$J = \frac{(W_2 - w_{1)}}{\rho A \Delta t} \quad \text{Equation 3.2}$$

3.4.3 Membrane characterization

Membrane characterization was performed for the unused (virgin) membrane and for the membranes used at each of the target temperatures of 45˚C, 55˚C and 65˚C.

3.4.3.1 Scanning electron microscopy (SEM) & energy-dispersive x-ray spectroscopy (EDS)

Samples for both SEM and EDS were sputter-coated with palladium-gold (Pd-Au) prior to analysis. The surface morphology of the membrane samples was examined using a Sigma Zeiss scanning electron microscope in secondary electron (SE) mode. It was coupled with EDS in the SEM to obtain the elemental composition of the membrane surfaces. Compositional analysis of each membrane with EDS was performed on three different areas of the membrane surface and an average value was taken.

3.4.3.2 Contact angle measurement

The contact angle of both the virgin and fouled membranes at temperatures of 45˚C, 55˚C and 65˚C were measured with a sessile drop method using the KRUSS EasyDrop drop shape analyzer. A water droplet around 5 µL was released from a needle tip onto the membrane surface. The drop was illuminated on one side while a motion camera was mounted on the other side to capture the videos at a rate of twelve frames per second. The contact angle was automatically calculated using the drop shape analyzer software. Each set of membrane samples was measured three times and the average value was taken.

4 RESULTS AND DISCUSSION

This study investigated the potential of the MDBR system in treating pulp and paper mill effluent (feed wastewater) through experimental work using a laboratory-scale setup. The investigation further evaluated whether the quality of the treated water would meet industrial reuse requirements. Membrane analysis was conducted to determine the influence of fouling and wetting on the overall performance of the system. In light of this, the results determined experimentally are presented and discussed. Since no work has been done on the remediation of pulp and paper mill effluent using a MDBR, it was not possible to directly compare the results obtained in this study with those obtained from previous literature.

4.1 Feed wastewater composition

The composition of the feed wastewater was determined as an average of three separate representative samples, in order to identify the most significant components of pulp and paper mill effluent on the basis of concentration. Results are presented in Table 4.1. Sulphate (SO_4^{2-}) and chloride (Cl^-) were recognized as the main contributing non-metallic compounds in the feed with concentration ranges of 308–391 mg/L and 150-160 mg/L, while sodium (Na^+) and calcium (Ca^{2+}) were identified as the dominant metallic species with concentration ranges of 277-300 mg/L and 139-157 mg/L respectively. Silicon (Si^{2+}), potassium (K^+) and magnesium (Mg^{2+}) were also present in relatively high concentrations in the feed. The concentration of heavy metals such as barium (Ba^{2+}), cadmium (Cd^{2+}), cobalt (Co^{3+}), chromium (Cr^{3+}), copper (Cu^{2+}), iron (Fe^{2+}), manganese (Mn^{2+}), nickel (Ni^{2+}) and lead (Pb^{2+}) were found to be insignificant relative to the other components. Zinc (Zn^{2+}) was the only heavy metal found in abundance which can be ascribed to the loss of Zn^{2+} plating on galvanized plant equipment. These results are in agreement with data obtained from Singh & Chandra.

Additional characteristics of the feed wastewater were also investigated and have been summarized in Table 4.2. The data for each individual grab sample can be found in Appendix A. The pH of the feed wastewater was found to be acidic, with a range of 6.19-6.31, and is in accordance with data presented by Toczyłowska-Mamińska. A high COD range of 398-496 mg/L was obtained for the feed although it was found to be within the prescribed COD limits for pulp and paper mill effluent (Toczyłowska-Mamińska, 2017). TOC values acquired for the feed wastewater were in a low range (38.65–56.47 mg/L) and therefore it can be considered to be easily treatable by biological means. However, the TSS and TDS were beyond the normal limits for pulp and paper mill effluent as described by Singh & Chandra and this could be attributed to the presence of lignin fibers in the wastewater for the TSS. The high amount of TDS also explains the elevated conductivity in the feed.

Table 4.1. Ionic composition of the feed wastewater

Ions	**Unit**	**Concentration Range**
Nitrate	mg/L	0.16 – 0.70
Sulphate	mg/L	308 – 391
Chloride	mg/L	150 – 160
Calcium	mg/L	139 – 157
Potassium	mg/L	16.05 – 16.45
Magnesium	mg/L	12.84 – 13.88
Sodium	mg/L	277 – 300
Aluminium	mg/L	0.20 – 0.28
Barium	mg/L	~ 0.12
Beryllium	mg/L	< 0.05
Cadmium	mg/L	< 0.09
Cobalt	mg/L	< 0.21
Chromium	mg/L	0.01
Copper	mg/L	< 0.07
Iron	mg/L	0.15 – 0.75
Manganese	mg/L	0.38 – 0.40
Nickel	mg/L	< 0.15
Lead	mg/L	< 0.07
Silicon	mg/L	21.27 – 21.70
Strontium	mg/L	0.16 – 0.18
Zinc	mg/L	< 8.20

Table 4.2. Feed wastewater characteristics

Parameter	**Unit**	**Value**
pH	-	6.19 – 6.31
Conductivity	µS/cm	1 885 – 1 993
Total Suspended Solids (TSS)	mg/L	496 – 876
Total Dissolved Solids (TDS)	mg/L	1 394 – 1 566
Chemical Oxygen Demand (COD)	mg/L	398 – 496
Total Organic Carbon (TOC)	mg/L	38.65 – 56.47

4.2 Microorganism acclimatization

TSS tests were conducted every two days to determine if microorganism adaptation had occurred at each target temperature of 45°C, 55°C and 65°C. Figure 4.1 presents the results for this acclimatization study with experimental data available in Appendix B. It was found that microorganism growth and adaptation were achieved at each temperature. This can be deduced from the increase in TSS from day 0 until day 30. It is evident from the graph that microorganisms more readily adapted to a target temperature of 45°C starting from day 1. The biomass increased gradually and started to stabilize from day 24 onwards (at a TSS value of 1584 mg/L), with minimal disturbances occurring throughout the 30-day period. Microorganism acclimatization at the temperatures of 55°C and 65°C were observed to fluctuate substantially more and this could be attributed to non-ideal conditions (that is higher temperatures) and the variation of microorganisms in the wastewater. Nevertheless, the final TSS concentrations were similar in all cases.

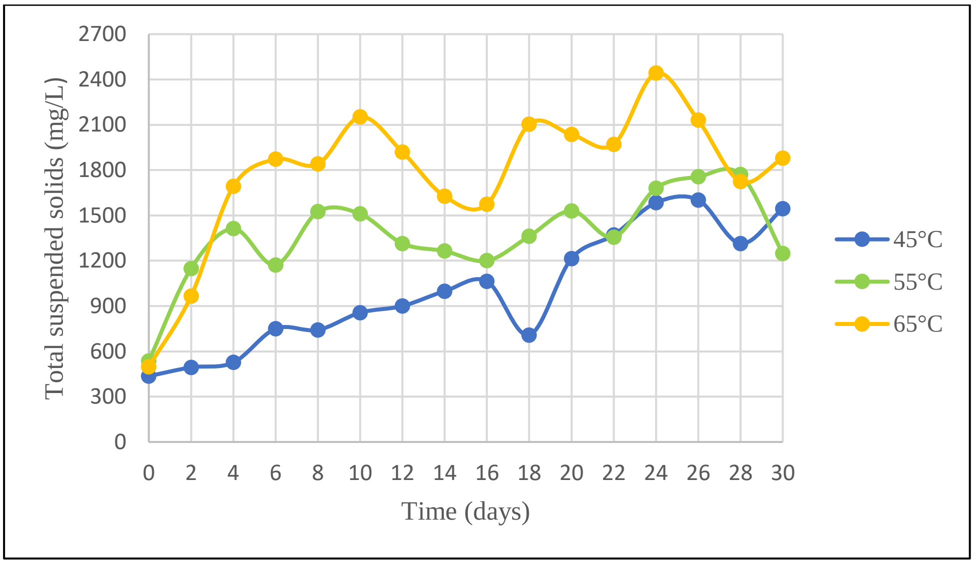

Figure 4.1. TSS as an indicator of microorganism growth

4.3 MDBR product quality

This section provides a comparison of the feed characteristics with the permeate water quality obtained from the MDBR at varying MDBR operating temperatures of 45°C, 55°C and 65°C. Experimental data for each experimental run can be accessed in Appendix C and Appendix D. Feed values for the graphs illustrated were determined by using the middle value of the feed concentration range as listed in Section 4.1.

4.3.1 Ionic composition

A comparison of the ionic composition between the feed and the permeate at varying MDBR operating temperatures (45°C, 55°C and 65°C) is presented in Table 4.3.

Table 4.3. Ionic composition between the feed and permeate at operating temperatures of 45°C, 55°C and 65°C

Ions	**Feed Concentration Range (mg/L)**	**Permeate Concentration Range (mg/L)**		
		MDBR at 45°C	**MDBR at 55°C**	**MDBR at 65°C**
Nitrate	0.16 – 0.70	0.41 – 1.13	0.05 – 2.80	0.11 – 1.60
Sulphate	308 – 391	6.83 – 36.41	1.09 – 6.27	1.02 – 8.40
Chloride	150 – 160	6.58 – 23.34	1.29 – 7.12	0.81 – 9.69
Calcium	139 – 157	0.52 – 10.78	0.43 – 14.88	0.85 – 4.13
Potassium	16.05 – 16.45	14.15 – 16.81	2.01 – 13.23	0.29 – 15.55
Magnesium	12.84 – 13.88	0.03 – 4.39	0.04 – 2.39	0.00 – 0.08
Sodium	277 – 300	3.33 – 21.51	1.02 – 7.41	0.00 – 12.60
Aluminium	0.20 – 0.28	0.00 – 0.18	0.00 – 0.01	0.00 – 0.13
Barium	~ 0.12	0.00 – 0.01	0.00	0.00 – 0.07
Beryllium	< 0.05	0.00	0.00	0.00
Cadmium	< 0.09	0.00 – 1.07	0.00 – 0.87	0.00 – 0.60
Cobalt	< 0.21	0.00 – 0.14	0.00	0.00 – 0.01
Chromium	0.01	0.00 – 0.01	0.00	0.00 – 0.01
Copper	< 0.07	0.00 – 0.03	0.00	0.00
Iron	0.15 – 0.75	0.00 – 0.73	0.00 – 0.38	0.00 – 0.06
Manganese	0.38 – 0.40	0.00 – 0.26	0.00 – 0.52	0.00 – 0.40
Nickel	< 0.15	0.00	0.00	0.00
Lead	< 0.07	0.00 – 0.06	0.00	0.00 – 0.08
Silicon	21.27 – 21.70	6.07 – 8.78	1.97 – 6.94	2.04 – 8.83
Strontium	0.16 – 0.18	0.00 – 0.02	0.00	0.00
Zinc	< 8.20	0.00 – 1.12	0.00 – 0.14	0.00 – 0.17

From the results, it can be seen that the MDBR achieved a good overall treatment efficiency in terms of ion concentration at each temperature. A high removal of compounds such as SO_4^{2-}, Cl^-, Ca^{2+}, Mg^{2+}, Na^+ and Zn^{2+} was attained by the MDBR in this study, with average removal rates of 99.2%, 98.1%, 99.6%, 99.8%, 99.5% and 100% for these substances respectively. Both K^+ and Si^{2+} were not as easily removed as the other compounds by the MDBR however, acceptable average removal efficiencies of 66.7% for K and 84.5% for Si^{2+}, were eventually realized. The nitrate (NO_3^-) permeate concentration range at each temperature was observed to overshoot the upper limit of the feed concentration range, however the concentrations in the permeate were still very low. This could be due to the formation of volatiles such as ammonia gas or nitrogen oxides that have passed through the membrane and dissolved in the permeate. The complete rejection of all heavy metals was accomplished by the MDBR, providing a good indication of the MDBRs performance in concentrating non-volatiles.

It is visible from Table 4.3 that an increase in temperature from 45°C to 65°C, resulted in the improvement in permeate water quality. At a temperature of 45°C, most compounds present in the feed wastewater were effectively retained by the MDBR with the exception of SO_4^{2-}, Cl^-, Ca^{2+}, K^+, Mg^{2+}, Na^+ and Si^{2+}, still present in significant concentrations. However, SO_4^{2-}, Cl^-, Ca^{2+}, K^+ and Si^{2+} existing in small concentrations, were the only compounds detected in the permeate for the operation of the MDBR at a temperature of 65°C. This decrease in ion concentration and in the quantity of compounds present in the permeate from a temperature of 45°C to 65°C indicates that the MDBR can be used to obtain high quality water at higher temperatures.

4.3.2 pH

Figure 4.2 displays the variation in pH at different MDBR operating temperatures. The pH at a MDBR temperature of 45°C was observed to constantly fluctuate between acidic and basic conditions at the start of the experimental run after which it increased beyond the feed pH set point of 6.25 to a pH of 6.85. It was noticed that the operation of the MDBR at a temperature of 55°C did not significantly affect the pH of the system as it remained in close range to the feed set point. At 65°C the system showed a gradual increase in pH from 6.25 to 7.26. The increasing trend in pH at higher operating temperatures was also observed by Tripathi & Allen who studied this phenomenon and deduced that it could be the result of the formation of basic chemical compounds or the treatment of the acids present in the feed wastewater by biological means (Tripathi & Allen, 1999).

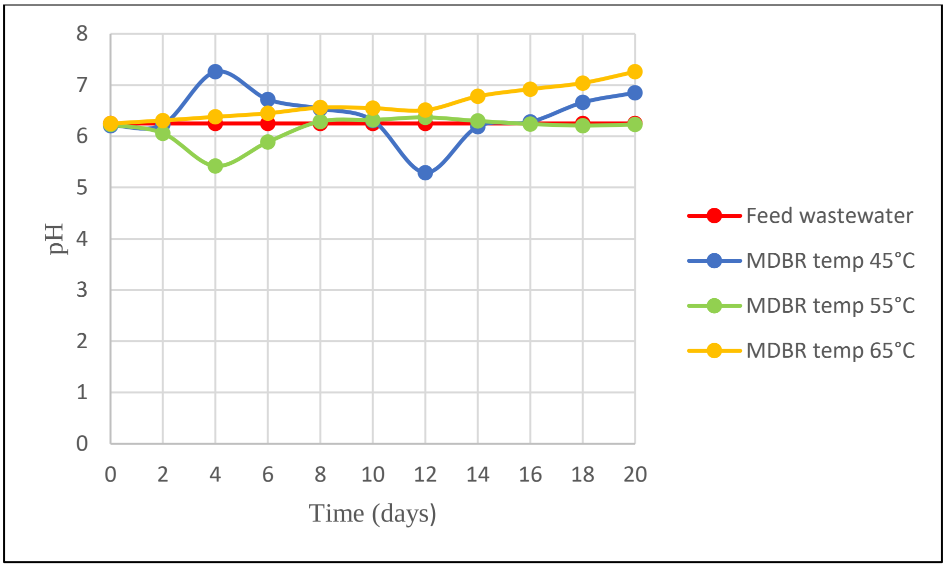

Figure 4.2. pH of the feed and MDBR product at temperatures of 45°C, 55°C and 65°C

4.3.3 TDS and EC

TDS and EC are both water quality parameters that are indicators of the salinity of a water sample. The TDS and the EC for the feed and the MDBR product throughout the study are illustrated in Figure 4.3 a) and b) respectively. It is evident from Figure 4.3 a) that from the onset the permeate TDS was found to be much lower than the feed TDS set point of 1480 mg/L. An exponential decrease in the permeate TDS was observed since day 1 of the treatment process, at each of the MDBR operating temperatures of 45°C, 55°C and 65°C. This trend in behaviour can be ascribed to the rejection of inorganic salts and organic matter by the MDBR. Final permeate TDS values of <150 mg/L were obtained from treatment using the MDBR in this study, which were well within industrial water reuse limits of 300-500 mg/L (Rusydi, 2018). It is also visible from the graph that the MDBR operation at 65°C accomplished the greatest reduction in permeate TDS (from 953 mg/L to 4.00 mg/L) among all the MDBR operating temperatures. This could be as a result of faster chemical reactions taking place due to the higher temperature.

It can be seen from Figure 4.3 b) that the EC of the system followed the same trend as the TDS data; permeate EC was also found to be much lower than the feed EC set point of 1 939 µS/cm and also followed the same exponential trend as the permeate TDS however, it remained relatively constant from day 6 onwards, at each of the MDBR operating temperatures. This decline in permeate EC is a direct result of the decrease in inorganic salts and organic matter

(TDS) in the permeate. A final permeate EC of <330 µS/cm was obtained for each of the operating temperatures, which met industrial discharge limits of 700-1 500 µS/cm (Department of Water Affairs and Forestry, 2004). It was noticed that the operation of the MDBR at a temperature of 55°C yielded the best salt rejection rate in terms of EC of 94.1%, while decent salt rejection rates of 70.8% and 93.9% were achieved for the temperatures of 45°C and 65°C respectively. The high salt rejection rates achieved at each operating temperature are essential to provide a good product quality for water reuse (Khaing et al., 2010).

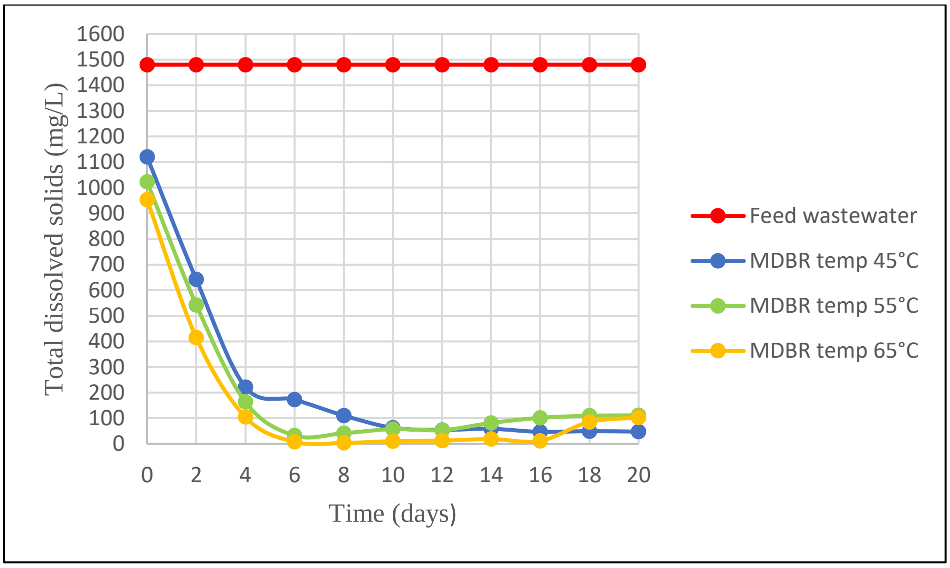

a)

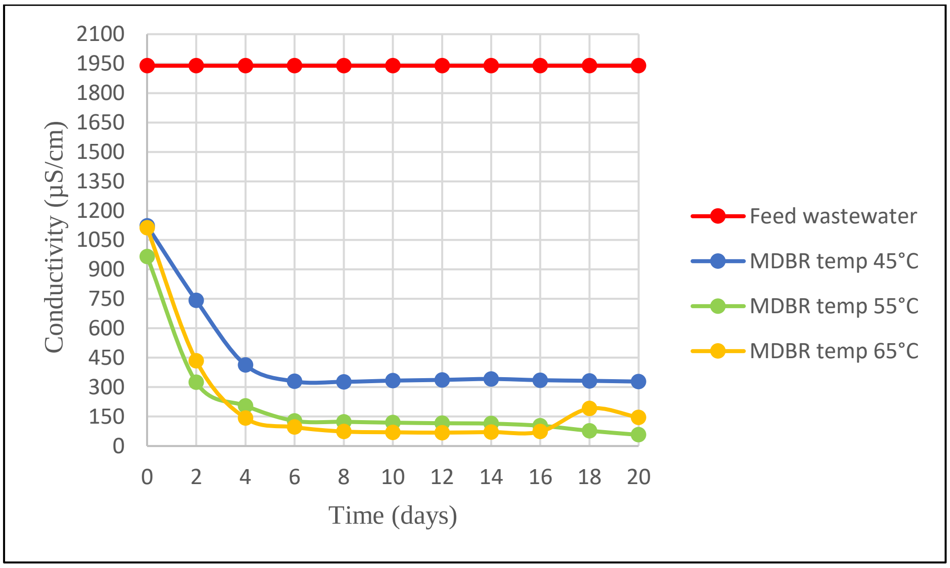

b)

Figure 4.3. Salinity indicators for the feed and MDBR product at temperatures of 45°C, 55°C and 65°C: a) TDS and b) EC

4.3.4 TSS

Figure 4.4 presents the TSS data over time at each of the MDBR operating temperatures.

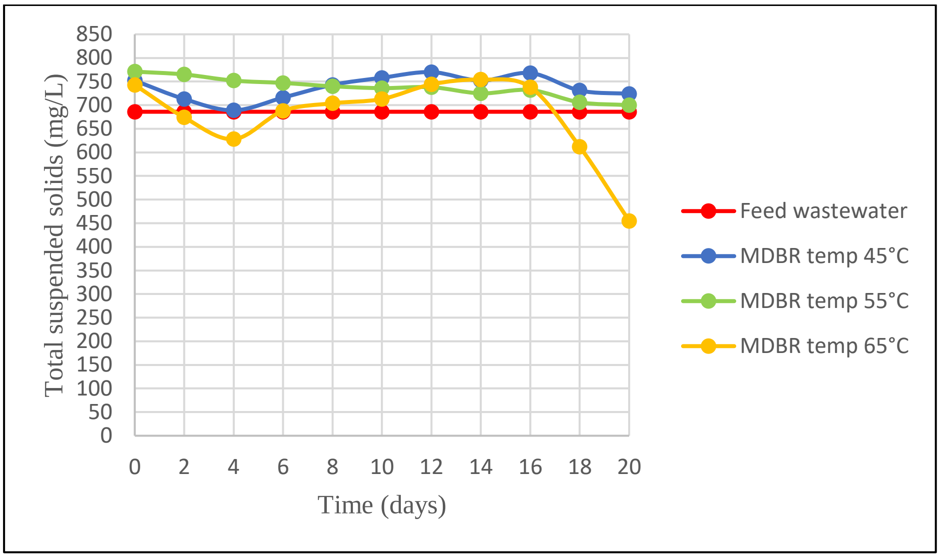

Figure 4.4. TSS of the feed and MDBR product at temperatures of 45°C, 55°C and 65°C

From the above results, it is noticeable that the TSS obtained at each MDBR operating temperature, for the most time, exceeded the feed TSS set point of 686 mg/L. It did however, not overshoot the higher limit of the feed TSS range (876 mg/L), as provided in Section 4.1. For the temperatures of 45°C and 55°C, the TSS was observed to constantly remain above the feed TSS set point. This higher TSS in the treated product could be due to the dispersed growth of the microorganisms or pinpoint flocs that have managed to pass through the pores of the hydrophobic membrane (Tripathi & Allen, 1999). The passage of microorganisms or small solids through the membrane could have taken place due to two reasons; the first reason being that the pinpoint flocs were smaller in size than the pore size of the membrane and the second reason could be due to the possibility that membrane wetting had occurred, thus affecting the quality of the permeate obtained. The same observation was made for the operation of the MDBR at a temperature of 65°C, although a significant decrease (from 738 mg/L to 455 mg/L) in TSS was detected from day 16. This sudden decline in permeate TSS at 65°C could be a result of uneven clogged pores at the membrane interface, a variation in microorganism population or that a greater amount of pinpoint flocs settled out from the wastewater. The temperature of 65°C was seen as favourable for TSS removal in comparison to the temperatures of 45°C and 55°C.

4.3.5 COD and TOC

Figure 4.5 a) and b) show the COD and TOC variations of the feed wastewater and the permeate throughout the entire study.

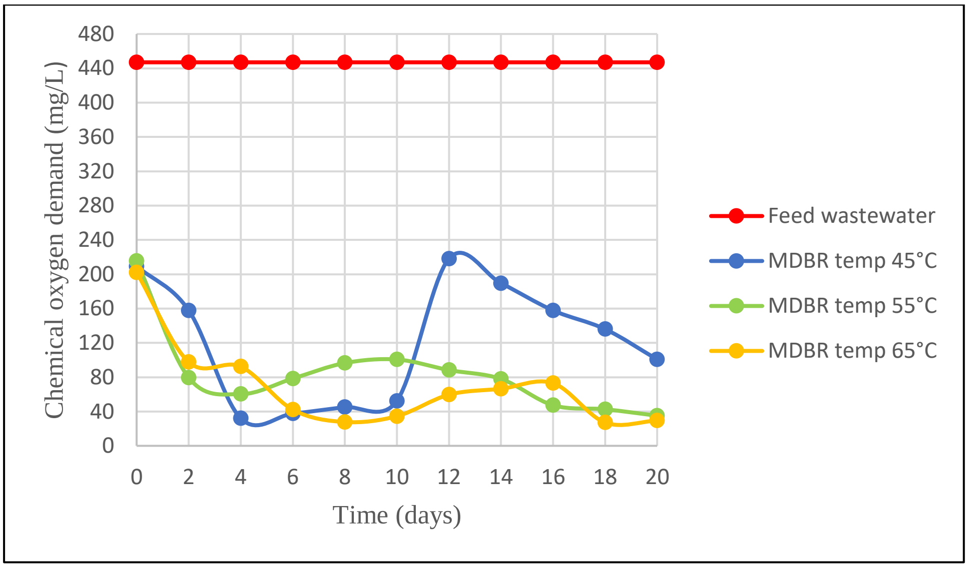

a)

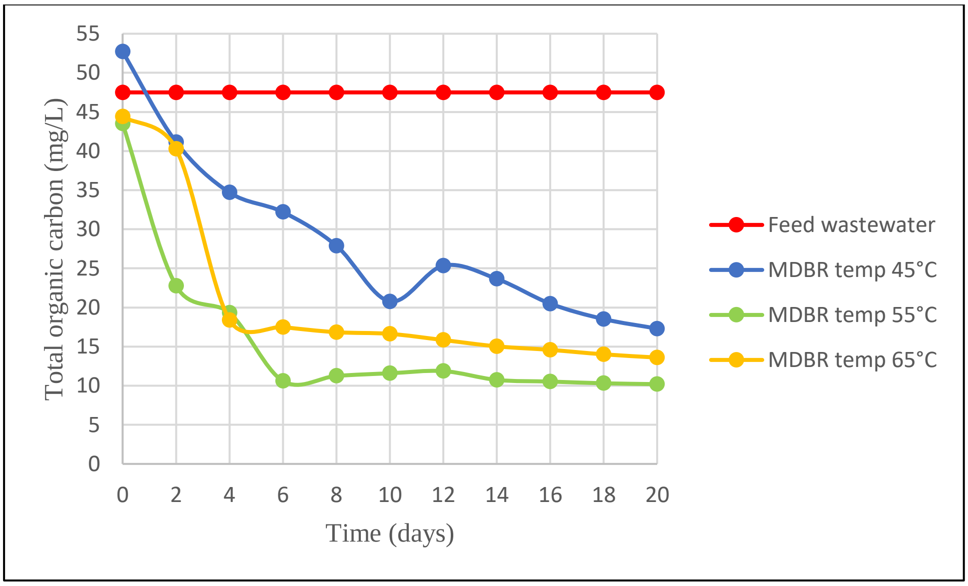

b)

Figure 4.5. Organic removal indicators of the feed and MDBR product at temperatures of 45°C, 55°C and 65°C: a) COD and b) TOC

It is visible from Figure 4.5 a) and b) that the MDBR was effective in treating COD and TOC, as observed from the overall decrease in both concentrations. In Figure 4.5 a), it can be seen that the permeate COD concentration at all operating temperatures was found to be well below the feed COD set point of 447 mg/L, indicative of good membrane function and organics removal via biodegradation. The system achieved good average COD removal rates of 84.7%, 83.7% and 86.6% at the operating temperatures of 45°C, 55°C and 65°C respectively, however, irregular fluctuations were observed throughout the study especially at a temperature of 45°C. The spike in permeate COD at a temperature of 45ºC from day 12 indicated that contaminants of the feed wastewater passed through the membrane. This occurrence could have possibly resulted due to the transfer of volatile compounds across the membrane or owing to the partial wetting of the membrane pores (Wu et al., 2018).

In Figure 4.5 b), the permeate TOC at the operating temperatures of 45ºC, 55ºC and 65ºC was also found to be lower than the feed TOC set point of 48 mg/L. An almost exponential decrease in permeate TOC was observed at each of the operating temperatures for the duration of the experiments, with less fluctuations experienced. This rapid decrease in permeate TOC is a direct result of the good functionality of the membrane as well as the break down (removal) of organics, specifically organic carbon, by microorganisms. Acceptable TOC removal rates of 67.2%, 76.6% and 69.4% at the temperatures of 45ºC, 55ºC and 65ºC respectively were obtained, with the operation of the MDBR at 55ºC yielding the best TOC result.

4.4 Permeate flux

The permeate flux was measured every two days at each of the target temperatures of 45ºC, 55ºC and 65ºC using an electronic balance. Figure 4.6 illustrates the permeate flux results for this study with experimental data and flux calculations available in Appendix E. It is important to note that the fluxes obtained for this study at each operating temperature are much lower than the typical flux range achieved in literature (2–15 L/m^2h) (Phattaranawik et al., 2008). This deviation could be attributed to the systems specifications used in this study that is a smaller bioreactor volume and a smaller effective membrane area (0.00785 m^2) were utilized.

From the results obtained, it can be seen that the flux performance at all MDBR operating temperatures decreased over time. At a MDBR temperature of 45ºC, the permeate flux was noticed to decrease by 48.1% over the first two days after which it decreased gradually from day 2 until day 20, obtaining an overall flux decline of 88.5%. It was observed that the operation of the MDBR at a temperature of 55ºC started off with a higher initial permeate flux than those obtained at the temperatures of 45ºC and 65ºC and yet, the MDBR operation at 55ºC experienced a sharp overall flux decline of 89.0%. The system operated at 65ºC showed a gradual decrease in flux, with an overall flux decline of 80.8%. This smaller drop in flux indicates that the MDBR at a temperature of 65ºC was much more acceptable for practical long-term MDBR treatment. The decline in permeate flux may be caused by membrane fouling and biofouling (unwanted build-up of microorganisms on a surface) which would lead to the decrease in effective membrane area (Goh et al., 2013). An SEM study was done to confirm this.

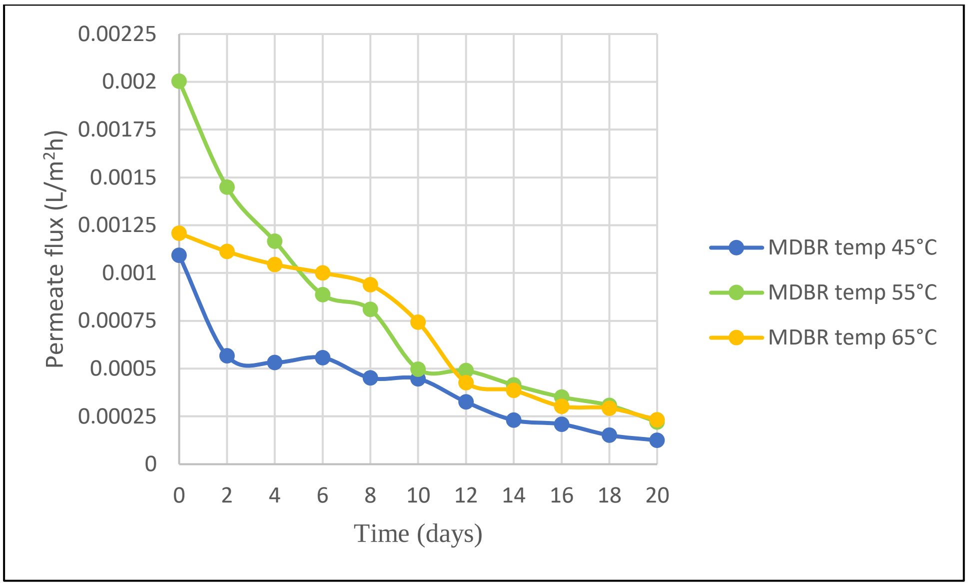

Figure 4.6. Profile of permeate flux at MDBR temperatures of 45°C, 55°C and 65°C

4.5 Membrane characterization

4.5.1 SEM and EDS

The respective SEM images of the virgin membrane and the used membranes at each of the MDBR operating temperatures of 45ºC, 55ºC and 65ºC are provided in Figure 4.7. As can be seen in Figure 4.7 a), the virgin membrane consisted of a relatively uniform surface structure with a large number of open pores. The used membrane at an operating temperature of 45ºC, as illustrated in Figure 4.7 b), showed an uneven deposition of some foulants on the membrane surface which led to a noticeable reduction in the effective membrane area. In the cases of the used membranes at the operating temperatures of 55ºC and 65ºC, as depicted in Figures 4.7 c) and d), the membrane pores were covered in a dense fouling layer each exhibiting different properties. The membrane used at a temperature of 55ºC (Figure 4.7 c)) displayed a rough, almost cement-like layer whereas the membrane used at a temperature of 65ºC (Figure 4.7 d)) seemed to have a rock-like structure. The difference in the appearance of the fouling layers could be the result of a combined effect of salt deposition (inorganic fouling), organic adsorption and increased microbial products concentration (biofouling) (Wu et al., 2018; Yao et al., 2019). It is evident from the SEM imaging that the degree of fouling increased with an increase in MDBR operating temperature.

The composition of the membrane foulants was analyzed with EDS and is summarized in Table 4.4. The EDS results showed that the virgin membrane comprised of both carbon (C) and fluorine (F), which are typical of the PTFE molecular chain ($(C_2F_4)_n$) (Wang & Chung, 2015). However, for the fouled membrane at a temperature of 45ºC, small amounts of other elements such as Si (1.19 Wt.%), Na (0.96 Wt.%), K (0.88 Wt.%) and Ca (0.27 Wt.%) were also detected. The results revealed that a significant concentration of the compound oxygen (O) was found (38.83 Wt.% and 28.42 Wt.%) at the temperatures of 55ºC and 65ºC respectively. The presence of O in larger quantities was likely due to the air being fed into the bioreactor for microorganism sustenance. Additionally, the analysis also identified Ca as a major component of the fouling layers of the membranes used at the temperatures of 55ºC and 65ºC, with a weight percentage of 26.73 Wt.% and 10.27 Wt.% respectively. The study by Khaing et al., (2010) reported the same findings with regards to Ca. Elements such as Na, Si, K, Cl, Mg, Fe and Al were also present in small quantities at the temperatures of 55ºC and 65ºC. From the results obtained, it was noticed that an increase in temperature resulted in the increase in the number of foulants on the membrane surface. These results confirm the observations made from the SEM imaging. The SEM and EDS results therefore support the data obtained in Section 4.4 in terms of permeate flux.

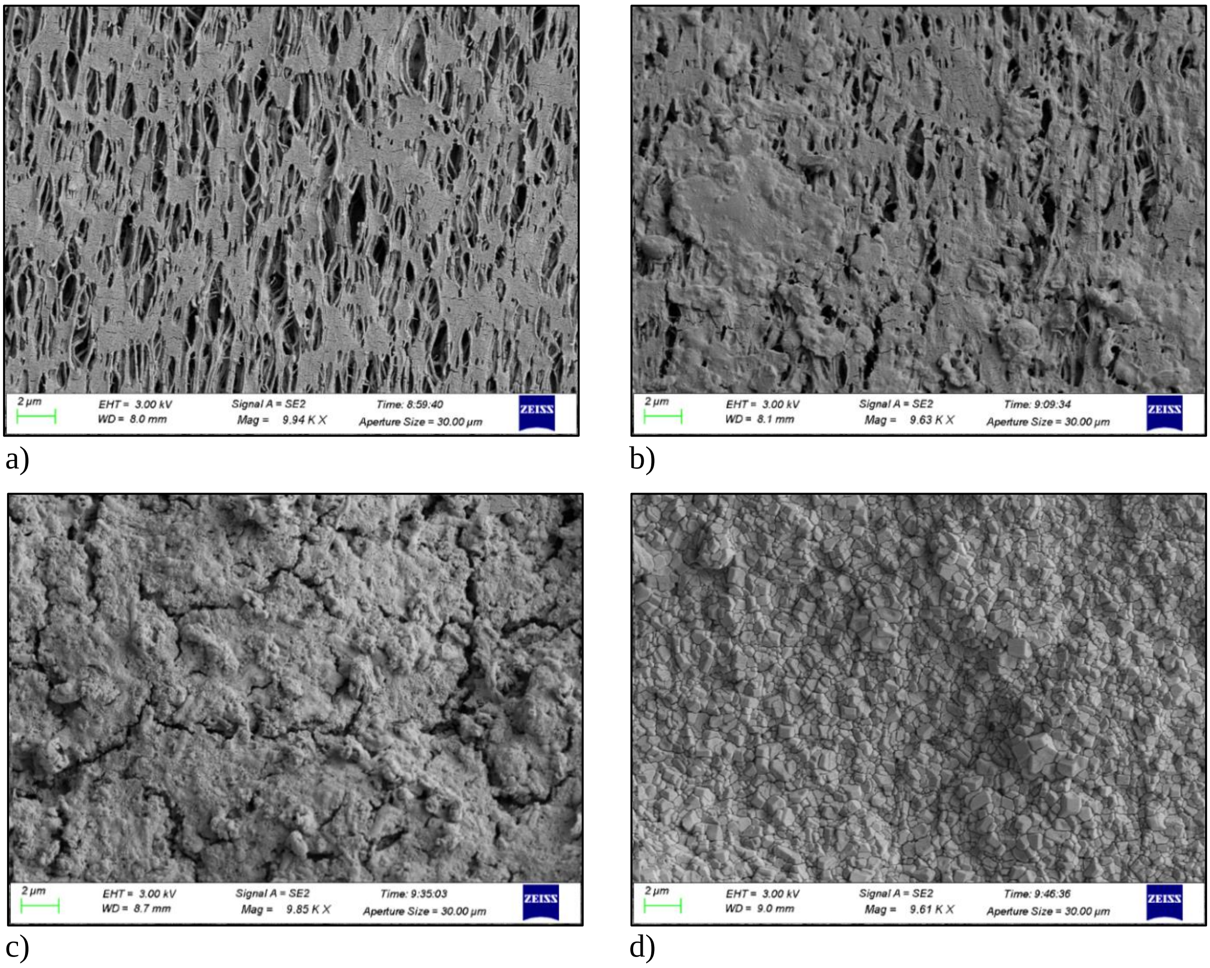

Figure 4.7. SEM imaging of the virgin and fouled membranes: a) Virgin membrane, b) Fouled membrane at 45ºC, c) Fouled membrane at 55ºC and d) Fouled membrane at 65ºC

Table 4.4. EDS analysis of the virgin and fouled membranes

Elements	**Element Mass Fraction of Different Membrane Samples (Wt.%)**			
	Virgin	**MDBR at 45°C**	**MDBR at 55°C**	**MDBR at 65°C**
Carbon	22.73	25.71	14.13	32.63
Fluorine	77.27	70.99	4.28	11.28
Oxygen	0.00	0.00	38.83	28.42
Sodium	0.00	0.96	4.57	5.15
Magnesium	0.00	0.00	1.51	1.13
Aluminium	0.00	0.00	0.13	0.52
Silicon	0.00	1.19	5.77	3.56
Chloride	0.00	0.00	2.06	1.38
Potassium	0.00	0.88	1.99	3.20
Calcium	0.00	0.27	26.73	10.27
Iron	0.00	0.00	0.00	0.82
Total	100.00	100.00	100.00	100.00

4.5.2 Contact angle measurement

The measurement of the contact angle proved the change in hydrophobicity of the membrane surface with an increase in MDBR operating temperature. Figure 4.8 displays the drop shape images of the virgin membrane and the fouled membranes at each of the MDBR operating temperatures of 45ºC, 55ºC and 65ºC. In Figure 4.8 a), the contact angle for the virgin membrane was determined as 129.8º due to the well-rounded shape of the water droplet. For the membrane used at a temperature of 45ºC, the contact angle decreased to 87.3º and this can be observed from the change in roundness of the water droplet in Figure 4.8 b). Further increases in the MDBR temperatures decreased the contact angle of the membranes used at the temperatures of 55ºC and 65ºC to 57.2º and 44.1º respectively. The decrease in contact angle at these temperatures is visible from the drastic change in the shape of the water droplets, as seen in Figures 4.8 c) and d). The significant loss of hydrophobicity of the membrane is a result of membrane fouling effects, as identified by the SEM imaging and EDS analysis in Section 4.5.1, which may have caused partial wetting of the membrane (Yao et al., 2019).

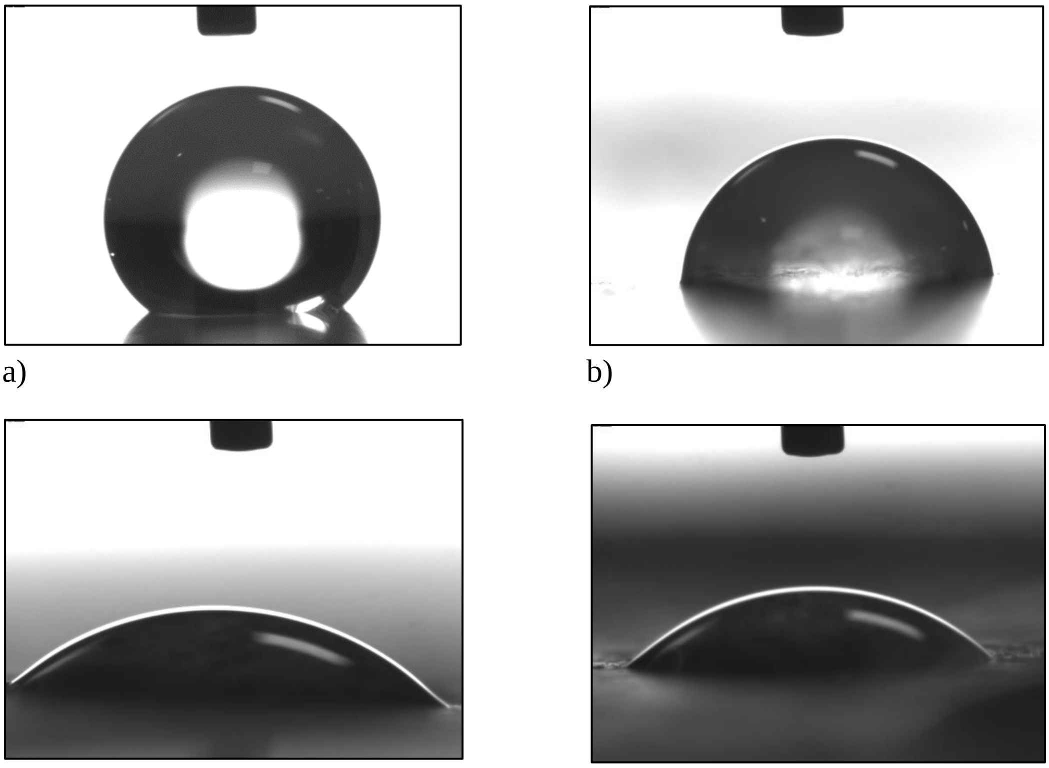

a) b) c) d)

Figure 4.8. Drop shape images used for the determination of the contact angles: a) Virgin membrane, b) Fouled membrane at 45ºC, c) Fouled membrane at 55ºC and d) Fouled membrane at 65ºC

4.6 Comparison of the MDBR results with the National Water Act standards

The comparison between the permeate results produced in this study and the permissible discharge limits of wastewater into a water resource according to the National Water Act No. 36 of 1998 is presented in Table 4.5. The MDBR product range at each of the MDBR operating temperatures provides the lowest (lower limit) and the highest (upper limit) result obtained for the duration of each experimental run over the twenty-one days. Ranges that exceeded the general discharge limit are highlighted in red font.

Table 4.5. Typical quality of MDBR product at operating temperatures of 45°C, 55°C and 65°C and the National Water Act (Department of Water Affairs and Forestry, 2004)

Parameter	**Unit**	**General Limit**	**MDBR Product at 45ºC**	**MDBR Product at 55ºC**	**MDBR Product at 65ºC**
pH	-	5.5-9.5	5.29-7.26	5.42-6.37	6.25-7.26
Conductivity	µS/cm	700-1 500	329-1 123	57.04-966	68.23-1 113
Total suspended solids (TSS)	mg/L	25	689-770	700-771	455-754
Chemical oxygen demand (COD)	mg/L	75	45.11-209	35.13-215	27.16-202
Nitrate	mg/L	15	0.41–1.13	0.05–2.80	0.11–1.60
Chloride	mg/L	0.25	6.58 – 23.34	1.29 – 7.12	0.81 – 9.69
Cadmium (II)	mg/L	0.005	0.00 – 1.07	0.00 – 0.87	0.00 – 0.60
Chromium (II)	mg/L	0.05	0.00 – 0.01	0.00	0.00 – 0.01
Copper (II)	mg/L	0.01	0.00 – 0.03	0.00	0.00
Iron (II)	mg/L	0.3	0.00 – 0.73	0.00 – 0.38	0.00 – 0.06
Manganese (II)	mg/L	0.1	0.00 – 0.26	0.00 – 0.52	0.00 – 0.40
Lead (II)	mg/L	0.01	0.00 – 0.06	0.00	0.00 – 0.08
Zinc (II)	mg/L	0.1	0.00 – 1.12	0.00 – 0.14	0.00 – 0.17

From the above results, it is noticeable that the MDBR in this study was effective at remediating the mill wastewater, however, the product water quality was unacceptable for discharge to the environment in terms of the general discharge limits of the National Water Act. Wastewater characteristics such as the pH, conductivity, and the concentration of NO_3 and Cr were well within the discharge limits whereas the concentration of Cu, Fe, Pb and Zn exceeded the limits, although the concentrations were still low. The concentration of Cl (>> 0.25 mg/L), Cd (>> 0.005 mg/L) and Mn (> 0.1 mg/L) was found to overshoot the general discharge limits of wastewater into a water resource by a significant amount. However, the TSS (>>> 25 mg/L) and the COD (>>> 75 mg/L) of the MDBR product at the operating temperatures of 45ºC, 55ºC and 65ºC exceeded the discharge limits by orders of magnitude. Due to the significant quantities of TSS and COD present in the MDBR product, the permeate will require further treatment before it can be discharged into a water resource or used at the mill for non-potable reuse applications such as irrigation and process water.

5 CONCLUSIONS AND FUTURE RESEARCH

This study reports the first attempt to design and investigate the feasibility of a laboratory-scale MDBR for the treatment and reuse of wastewater originating from the pulp and paper industry. The findings from this study are summarized in this chapter and related to the research objectives discussed in Section 1.1.

The first objective was to characterize the feed wastewater. The principal goal of this task was to identify the most significant components of pulp and paper mill effluent. The results are summarized below:

- Sulphate and chloride were identified as the main contributing non-metallic compounds of the feed wastewater on the basis of concentration. It was found that the maximum sulphate concentration was approximately 391 mg/L while the maximum chloride concentration was around 160 mg/L.
- Sodium and calcium were found to be the dominant metallic species with maximum concentrations of 300 mg/L and 157 mg/L respectively.
- The pH of the feed wastewater was approximately 6.25, making it slightly acidic.
- A high TDS (1 394–1 566 mg/L) and COD (398-496 mg/L) were found for the feed wastewater indicating the presence of a substantial amount of inorganic salts and organic matter. The large concentration of TDS also explained the elevated conductivity (1 885-1 993 µS/cm) in the feed.
- The TSS was found to be beyond the normal limit for pulp and paper mill effluent. This may be due to the presence of lignin fibers in the wastewater.

The second objective was to design, develop and construct a laboratory-scale MDBR capable of treating pulp and paper mill effluent. This was achieved by studying literature and considering the properties of the pulp and paper mill effluent (feed wastewater), the characteristics of the membrane being used, the chosen type of bioreactor configuration, and the system’s layout and process operating conditions. Design drawings were submitted to the School of Chemical and Metallurgical Engineering’s Workshop to assist with construction. The MDBR with the membrane module was then commissioned and tested.

The third objective of this study was to assess the use of a MDBR system for wastewater treatment through experimental work. The effect of temperature on process performance was also investigated. The results from this experiment provided substantial data and some insight into the operation and performance of the MDBR. Specifically, the following was found:

- The MDBR was effective at remediating mill wastewater as the system achieved a high removal efficiency of all compounds at all operating temperatures (45ºC-65ºC). The average removal rates for sulphate, chloride, sodium and calcium in particular were 99.2%, 98.1%, 99.5% and 99.6%.
- An increasing trend in pH at higher operating temperatures was observed. The pH shifted towards more neutral conditions.
- A high salt rejection rate of 86.3% was attained by the MDBR in this study regardless of the tested MDBR temperature (45ºC-65ºC), while the TSS rejection was not as high. Satisfactory organic removal rates in terms of COD (85.0%) and TOC (71.0%) were realized.
- The permeate flux decreased by an average of 88.1% over time at relatively low temperatures (45ºC-65ºC) as compact fouling layers formed of inorganics, organics and protein were observed on the membrane surface. Calcium was identified as the main foulant.
- A loss in membrane hydrophobicity was detected with an increase in operating temperature. The contact angle was found to decrease from 129.8º (virgin membrane) to 44.1º (at a MDBR operating temperature of 65ºC) due to the partial wetting of the membrane.
- Based on the results obtained, a MDBR operating temperature of 65ºC was determined as the optimal temperature for the MDBR system due to better process performance and overall treatment efficiency.
- The MDBR in this study was not able to treat pulp and paper mill effluent to meet the general discharge limits as stated in the National Water Act. Water quality parameters such as the TSS, COD and the concentration of chloride, cadmium and manganese were found to have exceeded the discharge limits.

In conclusion, the MDBR was shown to be a promising process for the treatment of pulp and paper mill effluent. To realize the full potential of the MDBR system, further studies still need to be undertaken with regards to design optimization, membrane fouling control, the effects of other process variables on the process performance and the improvement in water quality for water reuse applications. The role of microorganisms and their potential for bioremediation in MDBRs should also be determined. Additional tests could also be conducted to understand the potential usage of the MDBR for other types of effluent. Notwithstanding the limitations of this study, any technology that has the potential to reduce the impact of industrial activities on the environment can contribute towards creating more environmentally friendly industries. This study has shown that the MDBR technology can assist towards this.

REFERENCES

Abdel-Karim, A., Leaper, S., Skuse, C., Zaragoza, G., Gryta, M., & Gorgojo, P. (2021). Membrane cleaning and pretreatments in membrane distillation – a review. *Chemical Engineering Journal, 422*. doi:10.1016/j.cej.2021.129696

Abu-Zeid, M. A. E.-R., Zhang, Y., Dong, H., Zhang, L., Chen, H.-L., & Hou, L. (2015). A comprehensive review of vacuum membrane distillation technique. *Desalination, 356*, 1-14. doi:10.1016/j.desal.2014.10.033

Alkhudhiri, A., Darwish, N., & Hilal, N. (2012). Membrane distillation: A comprehensive review. *Desalination, 287*, 2-18. doi:10.1016/j.desal.2011.08.027

Ashrafi, O., Yerushalmi, L., & Haghighat, F. (2015). Wastewater treatment in the pulp-and-paper industry: A review of treatment processes and the associated greenhouse gas emission. *J Environ Manage, 158*, 146-157. doi:10.1016/j.jenvman.2015.05.010

Brink, A., Sheridan, C., & Harding, K. (2018). Combined biological and advance oxidation processes for paper and pulp effluent treatment. *South African Journal of Chemical Engineering, 25*, 116-122. doi:10.1016/j.sajce.2018.04.002

Chamani, H., Woloszyn, J., Matsuura, T., Rana, D., & Lan, C. Q. (2021). Pore wetting in membrane distillation: A comprehensive review. *Progress in Materials Science, 122*. doi:10.1016/j.pmatsci.2021.100843

Choudhury, M. R., Anwar, N., Jassby, D., & Rahaman, M. S. (2019). Fouling and wetting in the membrane distillation driven wastewater reclamation process - A review. *Adv Colloid Interface Sci, 269*, 370-399. doi:10.1016/j.cis.2019.04.008

Curcio, E., & Drioli, E. (2005). Membrane Distillation and Related Operations—A Review. *Separation & Purification Reviews, 34*(1), 35-86. doi:10.1081/spm-200054951

Damtie, M. M., Kim, B., Woo, Y. C., & Choi, J. S. (2018). Membrane distillation for industrial wastewater treatment: Studying the effects of membrane parameters on the wetting performance. *Chemosphere, 206*, 793-801. doi:10.1016/j.chemosphere.2018.05.070

Department of Water Affairs and Forestry. (2004). Revision of General Authorisations in terms of Section 39 of the National Water Act, 1998 (Act No. 36 of 1998). Gazette 26187.

Drioli, E., Ali, A., & Macedonio, F. (2015). Membrane distillation: Recent developments and perspectives. *Desalination, 356*, 56-84. doi:10.1016/j.desal.2014.10.028

El-Bourawi, M. S., Ding, Z., Ma, R., & Khayet, M. (2006). A framework for better understanding membrane distillation separation process. *Journal of Membrane Science, 285*(1-2), 4-29. doi:10.1016/j.memsci.2006.08.002

Eskelinen, K., Särkkä, H., Kurniawan, T. A., & Sillanpää, M. E. T. (2010). Removal of recalcitrant contaminants from bleaching effluents in pulp and paper mills using ultrasonic irradiation and Fenton-like oxidation, electrochemical treatment, and/or chemical precipitation: A comparative study. *Desalination, 255*(1-3), 179-187. doi:10.1016/j.desal.2009.12.024

Eykens, L., De Sitter, K., Dotremont, C., Pinoy, L., & Van der Bruggen, B. (2017). Membrane synthesis for membrane distillation: A review. *Separation and Purification Technology, 182*, 36-51. doi:10.1016/j.seppur.2017.03.035

Fortunato, L., Elcik, H., Blankert, B., Ghaffour, N., & Vrouwenvelder, J. (2021). Textile dye wastewater treatment by direct contact membrane distillation: Membrane performance and detailed fouling analysis. *Journal of Membrane Science, 636*. doi:10.1016/j.memsci.2021.119552

Fraga, F. A., García, H. A., Hooijmans, C. M., Míguez, D., & Brdjanovic, D. (2017). Evaluation of a membrane bioreactor on dairy wastewater treatment and reuse in Uruguay. *International Biodeterioration & Biodegradation, 119*, 552-564. doi:10.1016/j.ibiod.2016.11.025

Gebreyohannes, A. Y., Mazzei, R., & Giorno, L. (2016). Trends and current practices of olive mill wastewater treatment: Application of integrated membrane process and its future perspective. *Separation and Purification Technology, 162*, 45-60. doi:10.1016/j.seppur.2016.02.001

Goh, S., Zhang, J., Liu, Y., & Fane, A. G. (2013). Fouling and wetting in membrane distillation (MD) and MD-bioreactor (MDBR) for wastewater reclamation. *Desalination, 323*, 39-47. doi:10.1016/j.desal.2012.12.001

Goh, S., Zhang, J., Liu, Y., & Fane, A. G. (2015). Membrane Distillation Bioreactor (MDBR) - A lower Green-House-Gas (GHG) option for industrial wastewater reclamation. *Chemosphere, 140*, 129-142. doi:10.1016/j.chemosphere.2014.09.003

Goh, S., Zhang, Q., Zhang, J., McDougald, D., Krantz, W. B., Liu, Y., & Fane, A. G. (2013). Impact of a biofouling layer on the vapor pressure driving force and performance of a membrane distillation process. *Journal of Membrane Science, 438*, 140-152. doi:10.1016/j.memsci.2013.03.023

González, D., Amigo, J., & Suárez, F. (2017). Membrane distillation: Perspectives for sustainable and improved desalination. *Renewable and Sustainable Energy Reviews, 80*, 238-259. doi:10.1016/j.rser.2017.05.078

Huang, X., Xiao, K., & Shen, Y. (2010). Recent advances in membrane bioreactor technology for wastewater treatment in China. *Frontiers of Environmental Science & Engineering in China, 4*(3), 245-271. doi:10.1007/s11783-010-0240-z

Jacob, P., Phungsai, P., Fukushi, K., & Visvanathan, C. (2015). Direct contact membrane distillation for anaerobic effluent treatment. *Journal of Membrane Science, 475*, 330-339. doi:10.1016/j.memsci.2014.10.021

Jia, F., Li, J., Wang, J., & Sun, Y. (2017). Removal of strontium ions from simulated radioactive wastewater by vacuum membrane distillation. *Annals of Nuclear Energy, 103*, 363-368. doi:10.1016/j.anucene.2017.02.003

Jiao, B., Cassano, A., & Drioli, E. (2004). Recent advances on membrane processes for the concentration of fruit juices: a review. *Journal of Food Engineering, 63*(3), 303-324. doi:10.1016/j.jfoodeng.2003.08.003

Kamali, M., & Khodaparast, Z. (2015). Review on recent developments on pulp and paper mill wastewater treatment. *Ecotoxicol Environ Saf, 114*, 326-342. doi:10.1016/j.ecoenv.2014.05.005

Kaya, Y., Ersan, G., Vergili, I., Gönder, Z. B., Yilmaz, G., Dizge, N., & Aydiner, C. (2013). The treatment of pharmaceutical wastewater using in a submerged membrane bioreactor under different sludge retention times. *Journal of Membrane Science, 442*, 72-82. doi:10.1016/j.memsci.2013.03.059

Kesieme, U. K., & Aral, H. (2015). Application of membrane distillation and solvent extraction for water and acid recovery from acidic mining waste and process solutions. *Journal of Environmental Chemical Engineering, 3*(3), 2050-2056. doi:10.1016/j.jece.2015.07.008

Khaing, T.-H., Li, J., Li, Y., Wai, N., & Wong, F.-s. (2010). Feasibility study on petrochemical wastewater treatment and reuse using a novel submerged membrane distillation bioreactor. *Separation and Purification Technology, 74*(1), 138-143. doi:10.1016/j.seppur.2010.05.016

Kharraz, J. A., Khanzada, N. K., Farid, M. U., Kim, J., Jeong, S., & An, A. K. (2022). Membrane distillation bioreactor (MDBR) for wastewater treatment, water reuse, and resource recovery: A review. *Journal of Water Process Engineering, 47*. doi:10.1016/j.jwpe.2022.102687

Kim, S., Lee, D. W., & Cho, J. (2016). Application of direct contact membrane distillation process to treat anaerobic digestate. *Journal of Membrane Science, 511*, 20-28. doi:10.1016/j.memsci.2016.03.038

Li, J., Wu, J., Sun, H., Cheng, F., & Liu, Y. (2016). Advanced treatment of biologically treated coking wastewater by membrane distillation coupled with pre-coagulation. *Desalination, 380*, 43-51. doi:10.1016/j.desal.2015.11.020

Liang, S., Zhao, Y., Liu, C., & Song, L. (2008). Effect of solution chemistry on the fouling potential of dissolved organic matter in membrane bioreactor systems. *Journal of Membrane Science, 310*(1-2), 503-511. doi:10.1016/j.memsci.2007.11.026

Liu, H., & Wang, J. (2013). Treatment of radioactive wastewater using direct contact membrane distillation. *J Hazard Mater, 261*, 307-315. doi:10.1016/j.jhazmat.2013.07.045

Luo, W., Phan, H. V., Hai, F. I., Price, W. E., Guo, W., Ngo, H. H., . . . Nghiem, L. D. (2016). Effects of salinity build-up on the performance and bacterial community structure of a membrane bioreactor. *Bioresour Technol, 200*, 305-310. doi:10.1016/j.biortech.2015.10.043

Mannina, G., Gulhan, H., & Ni, B. J. (2022). Water reuse from wastewater treatment: The transition towards circular economy in the water sector. *Bioresour Technol, 363*, 127951. doi:10.1016/j.biortech.2022.127951

Mazhar, S., Ditta, A., Bulgariu, L., Ahmad, I., Ahmed, M., & Nadiri, A. A. (2019). Sequential treatment of paper and pulp industrial wastewater: Prediction of water quality parameters by Mamdani Fuzzy Logic model and phytotoxicity assessment. *Chemosphere, 227*, 256-268. doi:10.1016/j.chemosphere.2019.04.022

Melin, T., Jefferson, B., Bixio, D., Thoeye, C., De Wilde, W., De Koning, J., . . . Wintgens, T. (2006). Membrane bioreactor technology for wastewater treatment and reuse. *Desalination, 187*(1-3), 271-282. doi:10.1016/j.desal.2005.04.086

Meng, S., Hsu, Y.-C., Ye, Y., & Chen, V. (2015). Submerged membrane distillation for inland desalination applications. *Desalination, 361*, 72-80. doi:10.1016/j.desal.2015.01.038

Mokhtar, N. M., Lau, W. J., Ismail, A. F., & Veerasamy, D. (2015). Membrane Distillation Technology for Treatment of Wastewater from Rubber Industry in Malaysia. *Procedia CIRP, 26*, 792-796. doi:10.1016/j.procir.2014.07.161

Naidu, G., Tijing, L., Johir, M. A. H., Shon, H., & Vigneswaran, S. (2020). Hybrid membrane distillation: Resource, nutrient and energy recovery. *Journal of Membrane Science, 599*. doi:10.1016/j.memsci.2020.117832

Nguyen, N. C., Nguyen, H. T., Chen, S. S., Ngo, H. H., Guo, W., Chan, W. H., . . . Hsu, H. T. (2016). A novel osmosis membrane bioreactor-membrane distillation hybrid system for wastewater treatment and reuse. *Bioresour Technol, 209*, 8-15. doi:10.1016/j.biortech.2016.02.102

Onsekizoglu, P. (2012). Membrane Distillation: Principle, Advances, Limitations and Future Prospects in Food Industry. In *Distillation - Advances from Modeling to Applications*.

Phattaranawik, J., Fane, A. G., Pasquier, A. C. S., & Bing, W. (2008). A novel membrane bioreactor based on membrane distillation. *Desalination, 223*(1-3), 386-395. doi:10.1016/j.desal.2007.02.075

Pokhrel, D., & Viraraghavan, T. (2004). Treatment of pulp and paper mill wastewater--a review. *Sci Total Environ, 333*(1-3), 37-58. doi:10.1016/j.scitotenv.2004.05.017

Qasim, M., Samad, I. U., Darwish, N. A., & Hilal, N. (2021). Comprehensive review of membrane design and synthesis for membrane distillation. *Desalination, 518*. doi:10.1016/j.desal.2021.115168

Rezaei, M., Warsinger, D. M., Lienhard, V. J., Duke, M. C., Matsuura, T., & Samhaber, W. M. (2018). Wetting phenomena in membrane distillation: Mechanisms, reversal, and prevention. *Water Res, 139*, 329-352. doi:10.1016/j.watres.2018.03.058

Rusydi, A. (2018). Correlation between conductivity and total dissolved solid in various type of water: A review. *Earth and Environmental Science*.

Sert, G., Bunani, S., Yörükoğlu, E., Kabay, N., Egemen, Ö., Arda, M., & Yüksel, M. (2017). Performances of some NF and RO membranes for desalination of MBR treated wastewater. *Journal of Water Process Engineering, 16*, 193-198. doi:10.1016/j.jwpe.2016.11.009

Singh, A. K., & Chandra, R. (2019). Pollutants released from the pulp paper industry: Aquatic toxicity and their health hazards. *Aquat Toxicol, 211*, 202-216. doi:10.1016/j.aquatox.2019.04.007

Sundararaman, S., and Sathiyapriya, A., . (2016). Acclimatization of an Industrial Pharmaceutical Wastewater in an Aerobic Batch Mode of Operation. *International Journal of Environmental Research and Development, Voume 6*, pp. 1-10.

Thomas, N., Mavukkandy, M. O., Loutatidou, S., & Arafat, H. A. (2017). Membrane distillation research & implementation: Lessons from the past five decades. *Separation and Purification Technology, 189*, 108-127. doi:10.1016/j.seppur.2017.07.069

Tijing, L. D., Woo, Y. C., Choi, J.-S., Lee, S., Kim, S.-H., & Shon, H. K. (2015). Fouling and its control in membrane distillation—A review. *Journal of Membrane Science, 475*, 215-244. doi:10.1016/j.memsci.2014.09.042

Toczyłowska-Mamińska, R. (2017). Limits and perspectives of pulp and paper industry wastewater treatment – A review. *Renewable and Sustainable Energy Reviews, 78*, 764-772. doi:10.1016/j.rser.2017.05.021

Tripathi, C., & Allen, D. (1999). Comparison of mesophilic and thermophilic aerobic biological treatment in sequencing batch reactors treating bleached kraft pulp mill effluent. *Water Research*, 236-246.

Vijay, A., Ling, K. V., & Fane, A. G. (2013). Reserve management and real time optimization for a solar powered Membrane Distillation Bio-Reactor water recycling plant via convex optimization. *Renewable Energy, 60*, 489-497. doi:10.1016/j.renene.2013.05.035

Wang, L. K., & Menon, R. (2011). Treatment of Industrial Effluents, Municipal Wastes, and Potable Water by Membrane Bioreactors. In *Membrane and Desalination Technologies* (pp. 201-236).

Wang, P., & Chung, T.-S. (2015). Recent advances in membrane distillation processes: Membrane development, configuration design and application exploring. *Journal of Membrane Science, 474*, 39-56. doi:10.1016/j.memsci.2014.09.016

Warsinger, D. M., Swaminathan, J., Guillen-Burrieza, E., Arafat, H. A., & Lienhard V, J. H. (2015). Scaling and fouling in membrane distillation for desalination applications: A review. *Desalination, 356*, 294-313. doi:10.1016/j.desal.2014.06.031

Wijekoon, K. C., Hai, F. I., Kang, J., Price, W. E., Guo, W., Ngo, H. H., . . . Nghiem, L. D. (2014). A novel membrane distillation-thermophilic bioreactor system: biological stability and trace organic compound removal. *Bioresour Technol, 159*, 334-341. doi:10.1016/j.biortech.2014.02.088

Wu, Y., Kang, Y., Zhang, L., Qu, D., Cheng, X., & Feng, L. (2018). Performance and fouling mechanism of direct contact membrane distillation (DCMD) treating fermentation wastewater with high organic concentrations. *J Environ Sci (China), 65*, 253-261. doi:10.1016/j.jes.2017.01.015

Yang, X., Fane, A. G., & Wang, R. (2014). Membrane Distillation: Now and Future. In *Desalination* (pp. 373-424).

Yao, M., Woo, Y. C., Ren, J., Tijing, L. D., Choi, J. S., Kim, S. H., & Shon, H. K. (2019). Volatile fatty acids and biogas recovery using thermophilic anaerobic membrane distillation bioreactor for wastewater reclamation. *J Environ Manage, 231*, 833-842. doi:10.1016/j.jenvman.2018.11.009

APPENDICES

Appendix A: Feed wastewater composition over a 3-day period

Table A1: Feed wastewater ionic composition

Ions (mg/L)	**10 May Concentration 12:00**	**11 May Concentration 12:00**	**12 May Concentration 12:00**
Nitrate	0.16	0.70	0.34
Sulphate	307.70	390.50	341.90
Chloride	150.00	157.90	159.90
Calcium	139.40	155.10	156.90
Potassium	16.05	16.08	16.45
Magnesium	12.84	13.88	13.06
Sodium	300.20	299.70	277.00
Aluminium	0.20	0.25	0.28
Barium	0.12	0.12	0.11
Beryllium	< 0.05	<0.05	<0.05
Cadmium	< 0.09	<0.09	<0.09
Cobalt	< 0.21	0.01	<0.21
Chromium	0.01	0.01	0.01
Copper	< 0.07	<0.07	0.01
Iron	0.15	0.32	0.75
Manganese	0.38	0.40	0.40
Nickel	< 0.15	<0.15	<0.15
Lead	< 0.07	0.06	<0.07
Silicon	21.5	21.7	21.27
Strontium	0.16	0.18	0.17
Zinc	< 8.20	< 8.20	< 8.20

Table A2: Additional feed wastewater characteristics

Parameter	Unit	10 May 12:00	11 May 12:00	12 May 12:00
pH	-	6.31	6.19	6.27
Conductivity	µS/cm	1 885.00	1 993.00	1 924.00
Total Suspended Solids (TSS)	mg/L	876.00	606.00	496.00
Total Dissolved Solids (TDS)	mg/L	1 394.00	1 566.00	1 500.00
Chemical Oxygen Demand (COD)	mg/L	496.00	397.80	440.60
Total Organic Carbon (TOC)	mg/L	50.77	38.65	56.47

Appendix B: Acclimatization data

Table B1: TSS data for a temperature of 45°C

Date	**Day**	**Initial Weight (g)**	**Final Weight (g)**	**Sample Volume (mL)**	**TSS (mg/L)**
01 June 2022	0	0.0954	0.1172	50	436.00
03 June 2022	2	0.0946	0.1193	50	494.00
05 June 2022	4	0.0954	0.1217	50	526.00
07 June 2022	6	0.0964	0.1339	50	750.00
09 June 2022	8	0.0953	0.1324	50	742.00
11 June 2022	10	0.0953	0.1381	50	856.00
13 June 2022	12	0.0948	0.1398	50	900.00
15 June 2022	14	0.0959	0.1458	50	998.00
17 June 2022	16	0.0965	0.1497	50	1 064.00
19 June 2022	18	0.0951	0.1305	50	708.00
21 June 2022	20	0.0959	0.1566	50	1 214.00
23 June 2022	22	0.0955	0.1640	50	1 370.00
25 June 2022	24	0.0951	0.1743	50	1 584.00
27 June 2022	26	0.0970	0.1771	50	1 602.00
29 June 2022	28	0.0967	0.1624	50	1 314.00
01 July 2022	30	0.0962	0.1734	50	1 544.00

Table B2: TSS data for a temperature of 55°C

Date	Day	Initial Weight (g)	Final Weight (g)	Sample Volume (mL)	TSS (mg/L)
01 June 2022	0	0.0974	0.1242	50	536.00
03 June 2022	2	0.0972	0.1546	50	1 148.00
05 June 2022	4	0.0956	0.1662	50	1 412.00
07 June 2022	6	0.0938	0.1524	50	1 172.00
09 June 2022	8	0.0947	0.1709	50	1 524.00
11 June 2022	10	0.0947	0.1702	50	1 510.00
13 June 2022	12	0.1094	0.1751	50	1 314.00
15 June 2022	14	0.1144	0.1776	50	1 264.00
17 June 2022	16	0.1183	0.1783	50	1 200.00
19 June 2022	18	0.0939	0.1620	50	1 362.00
21 June 2022	20	0.0943	0.1708	50	1 530.00
23 June 2022	22	0.0937	0.1615	50	1 356.00
25 June 2022	24	0.0945	0.1785	50	1 680.00
27 June 2022	26	0.0951	0.1829	50	1 756.00
29 June 2022	28	0.0948	0.1833	50	1 770.00
01 July 2022	30	0.0928	0.1552	50	1 248.00

Table B3: TSS data for a temperature of 65°C

Date	Day	Initial Weight (g)	Final Weight (g)	Sample Volume (mL)	TSS (mg/L)
01 June 2022	0	0.093	0.1179	50	498.00
03 June 2022	2	0.0955	0.1438	50	966.00
05 June 2022	4	0.0944	0.1790	50	1 692.00
07 June 2022	6	0.0973	0.1909	50	1 872.00
09 June 2022	8	0.0954	0.1874	50	1 840.00
11 June 2022	10	0.1085	0.2161	50	2 152.00
13 June 2022	12	0.1188	0.2148	50	1 920.00
15 June 2022	14	0.1182	0.1995	50	1 626.00
17 June 2022	16	0.0957	0.1744	50	1 574.00
19 June 2022	18	0.0944	0.1996	50	2 104.00
21 June 2022	20	0.0945	0.1963	50	2 036.00
23 June 2022	22	0.0947	0.1932	50	1 970.00
25 June 2022	24	0.0955	0.2176	50	2 442.00
27 June 2022	26	0.0941	0.2006	50	2 130.00
29 June 2022	28	0.0943	0.1805	50	1 724.00
01 July 2022	30	0.0931	0.1870	50	1 878.00

Appendix C: Permeate ionic composition data

Table C1: Permeate ionic composition for a MDBR temperature of 45°C

Date	Day	Ions (mg/L)																				
		NO_3	SO_4	Cl	Ca	K	Mg	Na	Al	Ba	Be	Cd	Co	Cr	Cu	Fe	Mn	Ni	Pb	Si	Sr	Zn
24-Jul 22	0	0.68	36.41	23.34	10.78	16.81	4.39	21.51	0.18	0.01	0.00	1.07	0.14	0.01	0.03	0.73	0.26	0.00	0.06	8.78	0.02	1.12
26-Jul 22	2	0.55	25.54	19.60	10.23	16.63	1.62	19.62	0.04	0.00	0.00	0.09	0.02	0.00	0.01	0.22	0.13	0.00	0.05	6.94	0.00	0.17
28-Jul 22	4	0.51	22.35	14.85	8.36	16.45	0.36	13.24	0.00	0.00	0.00	0.09	0.00	0.00	0.01	0.08	0.13	0.00	0.06	6.85	0.00	0.14
30-Jul 22	6	0.49	18.70	10.34	6.93	16.21	0.79	13.05	0.00	0.00	0.00	0.33	0.00	0.00	0.00	0.01	0.01	0.00	0.02	6.85	0.00	0.00
1-Aug 22	8	0.41	13.44	7.82	2.44	16.09	0.04	3.67	0.01	0.00	0.00	0.04	0.00	0.00	0.00	0.00	0.00	0.00	0.00	6.77	0.00	0.00
3-Aug 22	10	0.62	7.97	7.02	0.58	16.02	0.03	3.33	0.00	0.00	0.00	0.04	0.00	0.00	0.00	0.00	0.00	0.00	0.00	6.74	0.00	0.00
5-Aug 22	12	0.59	6.83	6.74	0.52	14.56	0.07	5.23	0.00	0.00	0.00	0.00	0.00	0.00	0.00	0.00	0.00	0.00	0.00	6.53	0.00	0.00
7-Aug 22	14	0.67	7.11	6.58	0.53	14.15	1.04	4.12	0.00	0.00	0.00	0.00	0.00	0.00	0.00	0.00	0.00	0.00	0.00	6.07	0.00	0.12
9-Aug 22	16	0.78	7.52	8.25	3.18	15.37	1.22	3.57	0.00	0.00	0.00	0.00	0.00	0.00	0.00	0.00	0.01	0.00	0.00	6.16	0.00	0.00
11-Aug 22	18	1.13	7.61	7.82	2.46	16.05	1.47	4.63	0.00	0.00	0.00	0.00	0.00	0.00	0.00	0.00	0.00	0.00	0.00	6.29	0.00	0.17
13-Aug 22	20	0.71	8.03	7.63	2.18	16.08	1.39	4.68	0.00	0.00	0.00	0.00	0.00	0.00	0.00	0.00	0.00	0.00	0.00	6.25	0.00	0.00

Table C2: Permeate ionic composition for a MDBR temperature of 55°C

Date	Day	Ions (mg/L)																				
		NO_3	SO_4	Cl	Ca	K	Mg	Na	Al	Ba	Be	Cd	Co	Cr	Cu	Fe	Mn	Ni	Pb	Si	Sr	Zn
5-Sep 22	0	2.80	6.27	7.12	14.88	13.23	2.39	7.41	0.10	0.00	0.00	0.87	0.00	0.00	0.00	0.38	0.52	0.00	0.00	6.94	0.00	0.14
7-Sep 22	2	1.37	3.19	4.29	8.00	9.08	0.18	4.85	0.00	0.00	0.00	0.86	0.00	0.00	0.00	0.00	0.27	0.00	0.00	5.76	0.00	0.13
9-Sep 22	4	0.64	2.66	3.81	5.55	4.13	0.15	2.56	0.00	0.00	0.00	0.02	0.00	0.00	0.00	0.00	0.19	0.00	0.00	5.32	0.00	0.07
11-Sep 22	6	0.24	1.12	3.15	3.26	2.09	0.09	2.24	0.00	0.00	0.00	0.01	0.00	0.00	0.00	0.00	0.00	0.00	0.00	4.92	0.00	0.03
13-Sep 22	8	0.16	1.09	3.03	0.57	2.01	0.05	1.06	0.00	0.00	0.00	0.00	0.00	0.00	0.00	0.00	0.07	0.00	0.00	3.24	0.00	0.00
15-Sep 22	10	0.11	1.47	1.50	1.13	2.03	0.04	1.13	0.00	0.00	0.00	0.00	0.00	0.00	0.00	0.00	0.00	0.00	0.00	2.15	0.00	0.00
17-Sep 22	12	0.12	2.21	1.29	0.43	2.21	0.05	1.02	0.00	0.00	0.00	0.00	0.00	0.00	0.00	0.00	0.00	0.00	0.00	1.97	0.00	0.00
19-Sep 22	14	0.05	2.69	1.34	1.24	2.16	0.07	1.11	0.00	0.00	0.00	0.00	0.00	0.00	0.00	0.00	0.00	0.00	0.00	2.05	0.00	0.00
21-Sep 22	16	0.14	3.36	2.25	1.45	2.27	0.12	1.18	0.00	0.00	0.00	0.00	0.00	0.00	0.00	0.00	0.00	0.00	0.00	2.12	0.00	0.00
23-Sep 22	18	0.13	2.53	2.17	1.96	2.29	0.05	1.12	0.00	0.00	0.00	0.00	0.00	0.00	0.00	0.00	0.00	0.00	0.00	2.08	0.00	0.00
25-Sep 22	20	0.12	2.08	2.64	1.72	2.07	0.15	1.14	0.00	0.00	0.00	0.00	0.00	0.00	0.00	0.00	0.00	0.00	0.00	2.00	0.00	0.00

Table C3: Permeate ionic composition for a MDBR temperature of 65°C

Date	Day	Ions (mg/L)																				
		NO_3	SO_4	Cl	Ca	K	Mg	Na	Al	Ba	Be	Cd	Co	Cr	Cu	Fe	Mn	Ni	Pb	Si	Sr	Zn
27-Sep 22	0	1.60	8.40	9.69	4.13	15.55	0.08	12.60	0.00	0.00	0.00	0.60	0.00	0.00	0.00	0.06	0.40	0.00	0.08	8.83	0.00	0.17
29-Sep 22	2	1.34	8.18	9.21	2.09	9.19	0.03	11.25	0.00	0.00	0.00	0.35	0.01	0.00	0.00	0.03	0.21	0.00	0.05	7.84	0.00	0.08
1-Oct 22	4	1.01	3.69	3.86	1.94	3.87	0.03	7.66	0.00	0.00	0.00	0.31	0.00	0.00	0.00	0.02	0.02	0.00	0.00	5.38	0.00	0.06
3-Oct 22	6	0.58	2.91	2.56	1.82	3.65	0.01	4.51	0.00	0.07	0.00	0.27	0.00	0.00	0.00	0.01	0.00	0.00	0.00	5.26	0.00	0.05
5-Oct 22	8	0.36	2.79	2.49	1.57	2.67	0.03	4.51	0.00	0.00	0.00	0.12	0.00	0.00	0.00	0.00	0.00	0.00	0.00	5.12	0.00	0.04
7-Oct 22	10	0.17	1.02	1.74	0.87	0.29	0.01	3.54	0.00	0.00	0.00	0.02	0.00	0.00	0.00	0.00	0.00	0.00	0.00	4.70	0.00	0.02
9-Oct 22	12	0.11	1.06	0.81	0.89	0.36	0.00	0.00	0.00	0.00	0.00	0.00	0.00	0.00	0.00	0.00	0.00	0.00	0.00	2.52	0.00	0.00
11-Oct 22	14	0.14	1.29	0.87	0.85	0.41	0.00	0.00	0.00	0.00	0.00	0.00	0.00	0.00	0.00	0.01	0.00	0.00	0.00	2.04	0.00	0.00
13-Oct 22	16	0.22	1.34	0.91	0.94	0.38	0.03	2.21	0.13	0.06	0.00	0.00	0.01	0.01	0.00	0.00	0.05	0.00	0.00	2.33	0.00	0.00
15-Oct 22	18	0.20	1.28	0.92	1.03	0.44	0.04	1.45	0.00	0.07	0.00	0.00	0.01	0.01	0.00	0.00	0.07	0.00	0.00	2.19	0.00	0.00
17-Oct 22	20	0.18	1.07	0.94	0.98	0.45	0.01	0.00	0.09	0.00	0.00	0.00	0.00	0.01	0.00	0.00	0.07	0.00	0.00	2.24	0.00	0.02

Appendix D: Permeate water quality data

Table D1: Permeate water quality for a MDBR temperature of 45°C

Date	**Day**	**pH**	**EC (µS/cm)**	**TSS (mg/L)**	**TDS (mg/L)**	**COD (mg/L)**	**TOC (mg/L)**
24 July 2022	0	6.21	1 123.15	752.00	1120.00	209.33	52.70
26 July 2022	2	6.23	742.22	713.00	642.00	157.89	41.15
28 July 2022	4	7.26	413.40	689.00	222.00	32.03	34.70
30 July 2022	6	6.72	329.50	716.00	173.00	37.56	32.20
1 August 2022	8	6.54	327.55	743.00	111.00	45.11	27.89
3 August 2022	10	6.31	333.46	758.00	63.00	52.43	20.78
5 August 2022	12	5.29	337.20	770.00	55.00	218.2	25.35
7 August 2022	14	6.19	342.00	752.00	59.00	189.56	23.66
9 August 2022	16	6.28	335.64	768.00	47.00	157.80	20.49
11 August 2022	18	6.66	332.52	731.00	50.00	135.99	18.52
13 August 2022	20	6.85	328.60	724.00	48.00	100.70	17.30

Table D2: Permeate water quality for a MDBR temperature of 55°C

Date	Day	pH	EC (μS/cm)	TSS (mg/L)	TDS (mg/L)	COD (mg/L)	TOC (mg/L)
5 September 2022	0	6.23	966.03	771.00	1023.00	215.46	43.50
7 September 2022	2	6.06	324.77	765.00	543.00	79.52	22.78
9 September 2022	4	5.42	205.21	752.00	164.00	60.30	19.32
11 September 2022	6	5.89	128.30	747.00	33.00	78.45	10.60
13 September 2022	8	6.29	123.47	740.00	42.00	96.47	11.25
15 September 2022	10	6.32	119.11	736.00	58.00	100.6	11.59
17 September 2022	12	6.37	116.23	738.00	54.00	88.28	11.87
19 September 2022	14	6.30	114.10	725.00	82.00	77.98	10.74
21 September 2022	16	6.24	103.42	732.00	102.00	47.30	10.53
23 September 2022	18	6.21	77.59	706.00	110.00	42.58	10.31
25 September 2022	20	6.23	57.04	700.00	112.00	35.13	10.20

Table D3: Permeate water quality for a MDBR temperature of 65°C

Date	Day	pH	EC (µS/cm)	TSS (mg/L)	TDS (mg/L)	COD (mg/L)	TOC (mg/L)
27 September 2022	0	6.25	1 112.57	743.00	953.00	202.14	44.4
29 September 2022	2	6.31	435.18	674.00	415.00	97.7	40.29
1 October 2022	4	6.38	142.80	628.00	105.00	92.38	18.39
3 October 2022	6	6.45	96.20	688.00	8.00	42.15	17.50
5 October 2022	8	6.56	73.88	704.00	4.00	27.79	16.84
7 October 2022	10	6.55	70.02	713.00	11.00	34.55	16.63
9 October 2022	12	6.51	68.23	744.00	13.00	59.61	15.84
11 October 2022	14	6.78	71.15	754.00	19.00	66.52	15.03
13 October 2022	16	6.92	73.35	738.00	12.00	73.03	14.58
15 October 2022	18	7.04	191.30	612.00	86.00	27.16	14.01
17 October 2022	20	7.26	145.80	455.00	103.00	29.39	13.60

Appendix E: Permeate flux calculations

Table E1: Permeate flux for a MDBR temperature of 45°C

Date	Day	W_2 (kg)	W_1 (kg)	Density (g/m^3)	Area (m^2)	t (h)	J (L/m^2h)
24 July 2022	0	1.24	0.8248	997.00	0.007854	48	0.001092372
26 July 2022	2	1.04	0.8248	997.00	0.007854	48	0.000567524
28 July 2022	4	1.02	0.8248	997.00	0.007854	48	0.000532271
30 July 2022	6	1.03	0.8248	997.00	0.007854	48	0.000557254
1 August 2022	8	0.99	0.8248	997.00	0.007854	48	0.000450965
3 August 2022	10	0.99	0.8248	997.00	0.007854	48	0.000447133
5 August 2022	12	0.95	0.8248	997.00	0.007854	48	0.000325785
7 August 2022	14	0.91	0.8248	997.00	0.007854	48	0.000230112
9 August 2022	16	0.90	0.8248	997.00	0.007854	48	0.000209173
11 August 2022	18	0.88	0.8248	997.00	0.007854	48	0.000151466
13 August 2022	20	0.87	0.8248	997.00	0.007854	48	0.000125153

Table E2: Permeate flux for a MDBR temperature of 55°C

Date	Day	W_2 (kg)	W_1 (kg)	Density (g/m^3)	Area (m^2)	t (h)	J (L/m^2h)
5 September 2022	0	1.58	0.8248	997.00	0.007854	48	0.00200324
7 September 2022	2	1.37	0.8248	997.00	0.007854	48	0.001449312
9 September 2022	4	1.26	0.8248	997.00	0.007854	48	0.001166229
11 September 2022	6	1.16	0.8248	997.00	0.007854	48	0.000886578
13 September 2022	8	1.13	0.8248	997.00	0.007854	48	0.000808916
15 September 2022	10	1.01	0.8248	997.00	0.007854	48	0.0004963
17 September 2022	12	1.01	0.8248	997.00	0.007854	48	0.000489303
19 September 2022	14	0.98	0.8248	997.00	0.007854	48	0.000414515
21 September 2022	16	0.96	0.8248	997.00	0.007854	48	0.000351007
23 September 2022	18	0.94	0.8248	997.00	0.007854	48	0.000307534
25 September 2022	20	0.91	0.8248	997.00	0.007854	48	0.0002208

Table E3: Permeate flux for a MDBR temperature of 65°C

Date	Day	W_2 (kg)	W_1 (kg)	Density (g/m^3)	Area (m^2)	t (h)	J (L/m^2h)
27 September 2022	0	1.28	0.8248	997.00	0.007854	48	0.00120776
29 September 2022	2	1.24	0.8248	997.00	0.007854	48	0.001112273
1 October 2022	4	1.22	0.8248	997.00	0.007854	48	0.001044562
3 October 2022	6	1.20	0.8248	997.00	0.007854	48	0.001000636
5 October 2022	8	1.18	0.8248	997.00	0.007854	48	0.000938831
7 October 2022	10	1.10	0.8248	997.00	0.007854	48	0.000742721
9 October 2022	12	0.99	0.8248	997.00	0.007854	48	0.000427126
11 October 2022	14	0.97	0.8248	997.00	0.007854	48	0.000385488
13 October 2022	16	0.94	0.8248	997.00	0.007854	48	0.000303117
15 October 2022	18	0.94	0.8248	997.00	0.007854	48	0.0002933
17 October 2022	20	0.91	0.8248	997.00	0.007854	48	0.000231868

Appendix F: Bioreactor data

Table F1: Bioreactor data for a temperature of 45°C

Date	Day	pH	EC (µS/cm)	TSS (mg/L)	TDS (mg/L)
24 July 2022	0	8.11	6 258.00	1 087.00	4 256.00
26 July 2022	2	8.17	6 305.00	1 151.00	4 284.00
28 July 2022	4	8.25	6 324.00	1 174.00	4 322.00
30 July 2022	6	8.29	6 372.00	1 183.00	4 449.00
1 August 2022	8	8.21	6 363.00	935.00	4 595.00
3 August 2022	10	8.31	6 378.00	1 031.00	4 355.00
5 August 2022	12	8.27	6 393.00	1 213.00	4 337.00
7 August 2022	14	8.17	6 455.00	1 269.00	4 322.00
9 August 2022	16	8.34	5 349.00	1 156.00	3 712.00
11 August 2022	18	8.42	5 215.00	1 024.00	3 677.00
13 August 2022	20	8.49	5 192.00	804.00	3 430.00

Table F2: Bioreactor data for a temperature of 55°C

Date	Day	pH	EC (µS/cm)	TSS (mg/L)	TDS (mg/L)
5 September 2022	0	6.49	2 416.00	1 142.00	1 444.00
7 September 2022	2	7.13	2 262.00	1 220.00	1 344.00
9 September 2022	4	7.30	2 010.00	1 112.00	1 024.00
11 September 2022	6	7.35	2 174.00	1 389.00	1 407.00
13 September 2022	8	7.13	2 017.00	1 508.00	1 140.00
15 September 2022	10	7.65	2 647.00	2 536.00	1 780.00
17 September 2022	12	8.18	2 759.00	2 170.00	1 140.00
19 September 2022	14	8.47	2 624.00	1 488.00	1 715.00
21 September 2022	16	8.32	2 758.00	1 479.00	1 922.00
23 September 2022	18	8.17	2 967.00	1 436.00	2 104.00
25 September 2022	20	8.16	3 003.00	1 455.00	1 963.00

Table F3: Bioreactor data for a temperature of 65°C

Date	Day	pH	EC (µS/cm)	TSS (mg/L)	TDS (mg/L)
27 September 2022	0	8.03	4 431.00	1 285.00	2 819.00
29 September 2022	2	8.40	4 049.00	2 144.00	344.00
1 October 2022	4	8.63	3 728.00	1 744.00	752.00
3 October 2022	6	8.29	3 652.00	1 800.00	1 535.00
5 October 2022	8	8.33	3 428.00	884.00	2 128.00
7 October 2022	10	8.40	3 336.00	2 364.00	2 052.00
9 October 2022	12	8.51	3 249.00	1 400.00	1 600.00
11 October 2022	14	8.57	3 248.00	2 025.00	2 120.00
13 October 2022	16	8.76	3 250.00	1 553.00	1 891.00
15 October 2022	18	8.99	3 218.00	1 785.00	1 615.00
17 October 2022	20	8.88	3 146.00	1 688.00	1 920.00

Appendix G: Recorded Arduino data for a MDBR temperature of 45˚C

Minimum temperature for the day: 7˚C

Maximum temperature for the day: 17˚C

Table G1: Arduino data for 24 July 2022

Time	pH	EC (mS/cm)	DO (mg/L)
00:00	14.55	14.59	1.25
01:00	14.32	13.88	1.32
02:00	14.30	13.23	1.32
03:00	14.23	13.94	1.41
04:00	14.28	14.26	1.43
05:00	14.25	13.91	1.49
06:00	14.48	12.75	1.50
07:00	14.46	11.88	1.51
08:00	14.47	12.36	1.57
09:00	14.47	12.56	1.54
10:00	14.48	11.62	1.53
11:00	14.48	11.37	1.71
12:00	14.47	11.33	1.77
13:00	14.46	11.33	1.92
14:00	14.46	11.14	2.03
15:00	14.46	11.56	2.05
16:00	14.46	12.14	2.21
17:00	14.45	12.43	2.22
18:00	14.46	12.53	2.22
19:00	14.46	12.69	2.27
20:00	14.44	12.65	2.28
21:00	14.45	12.53	2.35
22:00	14.44	12.56	2.34
23:00	14.45	13.36	2.33

Minimum temperature for the day: 3˚C

Maximum temperature for the day: 18˚C

Table G2: Arduino data for 25 July 2022

Time	pH	EC (mS/cm)	DO (mg/L)
00:00	14.13	14.75	2.09
01:00	14.10	14.23	2.09
02:00	14.08	14.36	2.13
03:00	14.11	14.23	2.15
04:00	14.13	13.75	2.14
05:00	14.12	13.81	2.14
06:00	14.15	13.62	1.97
07:00	14.12	13.56	1.99
08:00	14.12	13.72	2.13
09:00	14.12	14.01	2.14
10:00	14.18	14.07	2.18
11:00	14.12	14.04	2.19
12:00	14.12	14.14	2.19
13:00	14.11	14.17	2.19
14:00	14.10	13.94	2.25
15:00	14.18	13.97	2.18
16:00	14.14	14.01	2.23
17:00	14.09	14.01	2.26
18:00	14.11	14.04	2.27
19:00	14.13	14.04	2.26
20:00	14.12	14.04	2.26
21:00	14.12	14.01	2.23
22:00	14.15	13.88	2.24
23:00	14.14	13.81	2.22

Minimum temperature for the day: 7˚C

Maximum temperature for the day: 19˚C

Table G3: Arduino data for 26 July 2022

Time	pH	EC (mS/cm)	DO (mg/L)
00:00	14.41	13.59	2.18
01:00	14.41	13.56	2.23
02:00	14.42	13.46	2.23
03:00	14.43	12.88	2.24
04:00	14.43	13.14	2.19
05:00	14.42	13.30	2.17
06:00	14.43	13.36	2.17
07:00	14.43	13.36	2.20
08:00	14.44	13.20	2.24
09:00	14.43	13.23	2.31
10:00	14.43	13.40	2.33
11:00	14.44	13.59	2.43
12:00	14.44	13.43	2.45
13:00	14.43	13.11	2.52
14:00	14.43	13.33	2.52
15:00	14.43	13.23	2.57
16:00	14.43	13.40	2.64
17:00	14.43	13.43	2.77
18:00	14.44	12.14	2.61
19:00	14.43	13.07	2.79
20:00	14.43	13.17	2.79
21:00	14.43	13.33	2.51
22:00	14.44	13.36	2.53
23:00	14.44	13.40	2.53

Minimum temperature for the day: 7˚C

Maximum temperature for the day: 20˚C

Table G4: Arduino data for 27 July 2022

Time	pH	EC (mS/cm)	DO (mg/L)
00:00	14.27	11.79	1.03
01:00	14.27	12.01	1.02
02:00	14.29	12.04	1.15
03:00	14.30	11.98	1.22
04:00	14.30	11.79	1.13
05:00	14.30	11.66	1.17
06:00	14.32	11.66	1.19
07:00	14.31	11.53	1.22
08:00	14.33	11.27	1.22
09:00	14.33	11.40	1.22
10:00	14.34	11.17	1.21
11:00	14.34	11.59	1.26
12:00	14.34	8.50	1.27
13:00	14.38	9.37	1.28
14:00	14.38	11.85	1.31
15:00	14.43	11.79	1.31
16:00	14.43	12.11	1.33
17:00	14.42	12.04	1.32
18:00	14.42	12.11	1.31
19:00	14.45	12.04	1.29
20:00	14.46	12.04	1.33
21:00	14.46	12.04	1.34
22:00	14.47	12.04	1.33
23:00	14.47	12.08	1.33

Minimum temperature for the day: 9˚C

Maximum temperature for the day: 19˚C

Table G5: Arduino data for 28 July 2022

Time	pH	EC (mS/cm)	DO (mg/L)
00:00	14.30	10.05	1.54
01:00	14.31	10.85	1.57
02:00	14.32	11.33	1.56
03:00	14.34	11.40	1.56
04:00	14.35	11.33	1.72
05:00	14.36	11.01	1.73
06:00	14.36	10.95	1.71
07:00	14.36	10.98	1.69
08:00	14.36	11.11	1.69
09:00	14.36	11.46	1.62
10:00	14.36	11.46	1.63
11:00	14.36	11.30	1.63
12:00	14.36	11.17	1.62
13:00	14.36	11.14	1.73
14:00	14.35	11.30	1.77
15:00	14.35	11.27	1.82
16:00	14.34	11.24	1.77
17:00	14.34	11.56	1.79
18:00	14.34	11.72	1.81
19:00	14.32	9.79	1.81
20:00	14.33	9.53	1.84
21:00	14.29	11.72	1.83
22:00	14.33	11.82	1.84
23:00	14.34	11.91	1.84

Minimum temperature for the day: 7˚C

Maximum temperature for the day: 19˚C

Table G6: Arduino data for 29 July 2022

Time	pH	EC (mS/cm)	DO (mg/L)
00:00	14.46	12.04	1.71
01:00	14.44	12.24	1.71
02:00	14.44	12.24	1.71
03:00	14.44	12.24	1.71
04:00	14.44	12.20	1.71
05:00	14.44	12.24	1.71
06:00	14.43	12.20	1.71
07:00	14.44	12.24	1.72
08:00	14.44	12.24	1.74
09:00	14.44	12.27	1.82
10:00	14.43	12.20	1.83
11:00	14.43	12.27	1.81
12:00	14.42	12.27	1.81
13:00	14.42	12.27	1.85
14:00	14.42	12.27	1.87
15:00	14.42	12.36	1.88
16:00	14.41	12.33	1.92
17:00	14.41	12.36	1.96
18:00	14.41	11.79	2.02
19:00	14.41	11.91	2.03
20:00	14.41	11.98	2.04
21:00	14.41	12.01	2.02
22:00	14.42	12.04	2.07
23:00	14.42	12.01	2.09

Minimum temperature for the day: 8˚C

Maximum temperature for the day: 20˚C

Table G7: Arduino data for 30 July 2022

Time	pH	EC (mS/cm)	DO (mg/L)
00:00	14.34	11.95	1.92
01:00	14.13	12.62	2.10
02:00	14.55	12.20	2.08
03:00	14.53	11.95	2.10
04:00	14.53	11.98	2.25
05:00	14.51	11.91	2.25
06:00	14.52	12.14	2.21
07:00	14.51	12.11	2.22
08:00	14.51	12.08	2.21
09:00	14.50	11.85	2.21
10:00	14.67	11.01	2.19
11:00	14.67	11.04	2.27
12:00	14.67	11.08	2.33
13:00	14.67	11.17	2.40
14:00	14.68	11.17	2.41
15:00	14.67	11.17	2.41
16:00	14.68	11.11	2.45
17:00	14.69	11.04	2.47
18:00	14.69	11.14	2.48
19:00	14.69	11.14	2.47
20:00	14.69	11.14	2.47
21:00	14.69	10.95	2.52
22:00	14.69	10.98	2.54
23:00	14.68	11.01	2.54

Minimum temperature for the day: 8˚C

Maximum temperature for the day: 21˚C

Table G8: Arduino data for 31 July 2022

Time	pH	EC (mS/cm)	DO (mg/L)
00:00	14.51	11.04	2.87
01:00	14.53	11.01	2.87
02:00	14.55	11.04	2.67
03:00	14.55	11.04	2.68
04:00	14.42	10.79	2.62
05:00	14.42	10.82	2.63
06:00	14.40	10.85	2.67
07:00	14.39	10.88	2.72
08:00	14.39	10.92	2.72
09:00	14.40	10.82	2.71
10:00	14.39	10.72	2.67
11:00	14.39	10.98	2.67
12:00	14.25	26.37	2.67
13:00	13.92	25.76	2.77
14:00	13.95	25.82	2.67
15:00	13.96	25.92	2.65
16:00	14.01	25.92	2.64
17:00	13.65	25.92	2.65
18:00	13.80	25.89	2.67
19:00	13.77	26.60	2.67
20:00	13.84	9.76	2.68
21:00	14..07	9.92	2.67
22:00	14.01	10.01	2.72
23:00	13.98	10.01	2.72

Minimum temperature for the day: 7˚C

Maximum temperature for the day: 19˚C

Table G9: Arduino data for 01 August 2022

Time	pH	EC (mS/cm)	DO (mg/L)
00:00	13.49	10.47	2.11
01:00	13.23	10.59	1.91
02:00	13.26	10.56	1.93
03:00	13.34	10.59	1.97
04:00	13.67	10.63	1.99
05:00	13.50	10.66	2.03
06:00	13.39	10.63	2.04
07:00	13.40	10.66	2.07
08:00	13.28	10.72	2.13
09:00	13.40	10.34	2.16
10:00	13.34	10.34	2.17
11:00	13.33	10.34	2.20
12:00	13.24	10.43	2.21
13:00	13.28	10.47	2.21
14:00	13.17	10.50	2.19
15:00	13.38	10.50	2.27
16:00	13.55	10.53	2.32
17:00	13.39	10.50	2.27
18:00	13.28	10.50	2.32
19:00	13.21	10.47	2.33
20:00	13.47	10.43	2.33
21:00	13.50	10.43	2.33
22:00	13.38	10.37	2.33
23:00	13.40	10.30	2.33

Minimum temperature for the day: 8˚C

Maximum temperature for the day: 17˚C

Table G10: Arduino data for 02 August 2022

Time	pH	EC (mS/cm)	DO (mg/L)
00:00	13.28	10.21	1.44
01:00	13.26	10.21	1.42
02:00	13.34	10.18	1.43
03:00	13.33	10.18	1.45
04:00	13.26	10.24	1.44
05:00	13.22	10.24	1.45
06:00	13.35	10.21	1.43
07:00	13.23	10.21	1.51
08:00	13.26	10.24	1.47
09:00	13.38	10.24	1.58
10:00	13.46	10.21	1.46
11:00	13.44	10.24	1.47
12:00	13.54	10.24	1.52
13:00	13.43	10.24	1.52
14:00	13.42	10.24	1.57
15:00	13.37	10.21	1.58
16:00	13.33	10.18	1.55
17:00	13.42	10.21	1.58
18:00	13.43	10.21	1.59
19:00	13.37	10.24	1.63
20:00	13.43	10.21	1.57
21:00	13.42	10.24	1.55
22:00	13.43	10.24	1.58
23:00	13.42	10.18	1.57

Minimum temperature for the day: 8˚C

Maximum temperature for the day: 17˚C

Table G11: Arduino data for 03 August 2022

Time	pH	EC (mS/cm)	DO (mg/L)
00:00	14.41	10.50	1.34
01:00	14.41	10.53	1.42
02:00	14.41	10.50	1.37
03:00	13.71	10.47	1.34
04:00	13.74	10.53	1.33
05:00	13.69	10.47	1.29
06:00	13.29	10.47	1.34
07:00	12.82	10.47	1.35
08:00	12.66	10.27	1.38
09:00	14.03	10.27	1.34
10:00	14.03	10.30	1.38
11:00	13.85	10.34	1.43
12:00	13.85	10.37	1.44
13:00	14.14	10.37	1.51
14:00	14.13	10.37	1.44
15:00	14.12	10.37	1.52
16:00	14.09	10.37	1.54
17:00	14.12	10.34	1.55
18:00	14.18	10.37	1.52
19:00	14.19	10.34	1.55
20:00	14.19	10.34	1.57
21:00	14.19	10.30	1.55
22:00	14.19	10.30	1.55
23:00	14.19	10.34	1.57

Minimum temperature for the day: 7˚C

Maximum temperature for the day: 19˚C

Table G12: Arduino data for 04 August 2022

Time	pH	EC (mS/cm)	DO (mg/L)
00:00	14.39	10.50	1.59
01:00	14.39	10.47	1.62
02:00	14.39	10.47	1.71
03:00	14.39	10.50	1.79
04:00	14.39	10.47	1.82
05:00	14.39	10.47	1.83
06:00	14.40	10.47	1.92
07:00	14.40	10.50	1.95
08:00	14.40	10.50	1.99
09:00	14.40	10.47	1.83
10:00	14.40	10.47	1.87
11:00	14.40	10.47	1.95
12:00	14.40	10.47	2.02
13:00	14.40	10.47	1.87
14:00	14.40	10.47	1.78
15:00	14.40	10.37	1.87
16:00	14.40	10.27	1.86
17:00	14.41	10.24	1.87
18:00	14.41	10.24	1.87
19:00	14.41	10.27	1.79
20:00	14.40	10.27	1.87
21:00	14.40	10.27	1.77
22:00	14.41	10.34	1.76
23:00	14.40	10.34	1.87

Minimum temperature for the day: 5˚C

Maximum temperature for the day: 22˚C

Table G13: Arduino data for 05 August 2022

Time	pH	EC (mS/cm)	DO (mg/L)
00:00	14.30	9.72	2.33
01:00	14.24	9.72	2.39
02:00	14.22	9.69	2.49
03:00	14.17	9.85	2.51
04:00	14.18	9.69	2.49
05:00	14.39	8.08	2.55
06:00	14.36	8.11	2.63
07:00	14.34	8.05	2.55
08:00	14.18	8.69	2.51
09:00	14.53	8.69	2.53
10:00	14.55	8.63	2.53
11:00	14.55	8.60	2.53
12:00	14.56	8.63	2.51
13:00	14.56	8.47	2.67
14:00	14.51	9.11	2.76
15:00	14.52	9.08	2.67
16:00	14.52	9.11	2.84
17:00	14.52	9.08	2.92
18:00	14.52	9.08	2.93
19:00	14.51	9.08	2.83
20:00	14.51	9.08	2.76
21:00	14.51	9.08	2.83
22:00	14.51	9.05	2.76
23:00	14.50	9.05	2.76

Minimum temperature for the day: 6˚C

Maximum temperature for the day: 22˚C

Table G14: Arduino data for 06 August 2022

Time	pH	EC (mS/cm)	DO (mg/L)
00:00	14.60	6.50	1.23
01:00	14.60	6.76	1.25
02:00	14.60	6.92	1.31
03:00	14.61	7.12	1.25
04:00	14.61	8.17	1.21
05:00	14.62	7.99	1.26
06:00	14.63	7.95	1.35
07:00	14.63	7.92	1.42
08:00	14.62	7.89	1.35
09:00	14.62	7.86	1.35
10:00	14.63	7.87	1.35
11:00	14.63	7.58	1.43
12:00	14.62	7.59	1.47
13:00	14.63	7.53	1.52
14:00	14.62	6.45	1.55
15:00	14.62	6.43	1.52
16:00	14.62	6.41	1.47
17:00	14.62	6.34	1.47
18:00	14.61	2.99	1.43
19:00	14.61	2.99	1.47
20:00	14.61	4.03	1.46
21:00	14.61	4.89	1.47
22:00	14.61	4.96	1.47
23:00	14.61	4.99	1.46

Minimum temperature for the day: 11˚C

Maximum temperature for the day: 23˚C

Table G15: Arduino data for 07 August 2022

Time	pH	EC (mS/cm)	DO (mg/L)
00:00	14.46	11.56	0.97
01:00	14.46	11.62	1.02
02:00	14.49	11.66	0.99
03:00	14.50	11.59	1.00
04:00	14.51	11.37	1.12
05:00	14.52	11.37	1.13
06:00	14.53	11.43	1.17
07:00	14.53	11.43	1.21
08:00	14.54	11.43	1.17
09:00	14.54	11.46	1.22
10:00	14.55	11.40	1.27
11:00	14.25	11.01	1.32
12:00	14.24	11.08	1.35
13:00	14.22	11.17	1.37
14:00	14.21	11.17	1.37
15:00	14.22	11.14	1.37
16:00	14.24	11.17	1.49
17:00	14.25	11.14	1.53
18:00	14.24	11.11	1.66
19:00	14.23	11.08	1.62
20:00	14.22	11.08	1.62
21:00	14.13	10.21	1.66
22:00	14.67	10.88	1.58
23:00	14.68	10.85	1.59

Minimum temperature for the day: 7˚C

Maximum temperature for the day: 19˚C

Table G16: Arduino data for 08 August 2022

Time	pH	EC (mS/cm)	DO (mg/L)
00:00	14.65	9.89	1.27
01:00	14.65	9.82	1.33
02:00	14.67	9.56	1.45
03:00	14.66	9.53	1.63
04:00	14.66	9.08	1.65
05:00	14.66	9.18	1.73
06:00	14.66	9.31	1.81
07:00	14.67	9.31	1.82
08:00	14.65	9.31	2.03
09:00	14.65	9.27	1.94
10:00	14.46	9.21	1.97
11:00	14.46	9.24	2.04
12:00	14.45	9.24	2.05
13:00	14.47	8.92	2.04
14:00	14..72	8.95	2.12
15:00	14.72	9.08	2.13
16:00	14.74	8.98	2.04
17:00	14.74	9.05	2.13
18:00	14.75	8.98	2.21
19:00	14.75	8.89	2.17
20:00	14.75	8.89	2.13
21:00	14.75	9.02	2.17
22:00	14.75	9.05	2.17
23:00	14.75	8.79	2.13

Minimum temperature for the day: 5˚C

Maximum temperature for the day: 20˚C

Table G17: Arduino data for 09 August 2022

Time	pH	EC (mS/cm)	DO (mg/L)
00:00	14.66	8.86	2.34
01:00	14.67	8.57	2.34
02:00	14.68	8.40	2.34
03:00	14.68	8.44	2.31
04:00	14.68	8.53	2.31
05:00	14.68	8.50	2.34
06:00	14.69	8.53	2.34
07:00	14.69	8.57	2.34
08:00	14.68	8.60	2.37
09:00	14.61	8.34	2.41
10:00	14.67	8.44	2.37
11:00	14.77	8.37	2.37
12:00	14.78	8.37	2.41
13:00	14.79	8.37	2.41
14:00	14.80	8.37	2.41
15:00	14.79	8.44	2.41
16:00	14.79	8.40	2.52
17:00	14.80	8.44	2.41
18:00	14.77	8.66	2.41
19:00	14.61	8.60	2.42
20:00	14.60	8.63	2.42
21:00	14.59	8.63	2.41
22:00	14.59	8.66	2.42
23:00	14.61	8.66	2.41

Minimum temperature for the day: 7˚C

Maximum temperature for the day: 21˚C

Table G18: Arduino data for 10 August 2022

Time	pH	EC (mS/cm)	DO (mg/L)
00:00	14.61	8.18	2.09
01:00	14.65	8.15	2.19
02:00	14.67	8.11	2.14
03:00	14.66	8.15	2.19
04:00	14.67	8.15	2.23
05:00	14.67	8.11	2.27
06:00	14.71	7.89	2.29
07:00	14.72	7.86	2.33
08:00	14.72	7.86	2.34
09:00	14.72	7.86	2.37
10:00	14.73	7.92	2.34
11:00	14.72	7.92	2.37
12:00	14.73	7.92	2.37
13:00	14.73	7.95	2.37
14:00	14.71	7.92	2.32
15:00	14.71	7.89	2.30
16:00	14.71	7.66	2.19
17:00	14.66	8.05	2.21
18:00	14.68	8.02	2.23
19:00	14.68	8.02	2.23
20:00	14.68	8.08	2.27
21:00	14.69	8.15	2.23
22:00	14.69	7.70	2.23
23:00	14.69	7.73	2.23

Minimum temperature for the day: 9˚C

Maximum temperature for the day: 22˚C

Table G19: Arduino data for 11 August 2022

Time	pH	EC (mS/cm)	DO (mg/L)
00:00	14.66	7.86	1.67
01:00	14.67	7.82	1.71
02:00	14.68	7.82	1.73
03:00	14.69	7.82	1.72
04:00	14.69	7.86	1.67
05:00	14.69	7.82	1.69
06:00	14.69	7.86	1.63
07:00	14.69	7.86	1.62
08:00	14.69	7.89	1.60
09:00	14.69	7.82	1.62
10:00	14.63	7.82	1.63
11:00	14.63	7.66	1.67
12:00	14.65	7.63	1.69
13:00	14.64	7.66	1.74
14:00	14.65	7.70	1.69
15:00	14.65	7.73	1.69
16:00	14.65	7.73	1.77
17:00	14.65	7.73	1.69
18:00	14.65	7.70	1.78
19:00	14.65	7.70	1.73
20:00	14.65	7.73	1.74
21:00	14.65	7.73	1.78
22:00	14.66	7.76	1.74
23:00	14.66	7.73	1.78

Minimum temperature for the day: 11˚C

Maximum temperature for the day: 21˚C

Table G20: Arduino data for 12 August 2022

Time	pH	EC (mS/cm)	DO (mg/L)
00:00	14.66	7.50	2.03
01:00	14.67	7.50	2.05
02:00	14.67	7.50	2.11
03:00	14.67	7.50	2.15
04:00	14.67	7.50	2.19
05:00	14.67	7.47	2.17
06:00	14.67	7.47	2.17
07:00	14.64	7.50	2.19
08:00	14.65	7.50	2.22
09:00	14.66	7.50	2.32
10:00	14.67	7.53	2.22
11:00	14.67	7.50	2.35
12:00	14.68	7.53	2.31
13:00	14.68	7.50	2.32
14:00	14.68	7.57	2.32
15:00	14.68	7.53	2.31
16:00	14.68	7.53	2.35
17:00	14.68	7.57	2.36
18:00	14.68	7.53	2.31
19:00	14.68	7.57	2.31
20:00	14.68	7.53	2.31
21:00	14.64	7.15	2.27
22:00	14.65	7.15	2.31
23:00	14.65	7.18	2.31

Minimum temperature for the day: 14˚C

Maximum temperature for the day: 24˚C

Table G21: Arduino data for 13 August 2022

Time	pH	EC (mS/cm)	DO (mg/L)
00:00	14.57	7.25	1.66
01:00	14.57	7.08	1.66
02:00	14.58	7.12	1.66
03:00	14.57	7.12	1.65
04:00	14.58	7.15	1.66
05:00	14.59	7.15	1.67
06:00	14.49	7.12	1.67
07:00	14.58	7.12	1.67
08:00	14.59	7.12	1.69
09:00	14.59	7.12	1.67
10:00	14.59	7.15	1.71
11:00	14.59	7.08	1.69
12:00	14.59	7.08	1.69
13:00	14.59	7.08	1.69
14:00	14.59	7.08	1.72
15:00	14.59	7.05	1.73
16:00	14.56	7.05	1.75
17:00	14.50	7.02	1.69
18:00	14.50	7.02	1.73
19:00	14.50	7.02	1.72
20:00	14.58	6.99	1.73
21:00	14.59	6.99	1.73
22:00	14.60	6.96	1.72
23:00	14.61	6.99	1.72

Minimum temperature for the day: 2˚C

Maximum temperature for the day: 16˚C

Table G22: Arduino data for 14 August 2022

Time	pH	EC (mS/cm)	DO (mg/L)
00:00	14.60	6.86	2.34
01:00	14.61	6.86	2.35
02:00	14.62	6.86	2.35
03:00	14.62	6.79	2.35
04:00	14.62	6.83	2.36
05:00	14.62	6.86	2.37
06:00	14.62	6.83	2.39
07:00	14.63	6.83	2.40
08:00	14.63	6.79	2.39
09:00	14.63	6.79	2.43
10:00	14.63	6.79	2.43
11:00	14.62	6.79	2.39
12:00	14.63	6.79	2.45
13:00	14.63	6.79	4.48
14:00	14.63	6.79	2.56
15:00	14.43	6.86	2.48
16:00	14.50	6.83	2.48
17:00	14.52	6.83	2.48
18:00	14.53	6.83	2.50
19:00	14.52	6.83	2.57
20:00	14.52	6.79	2.60
21:00	14.53	6.79	2.62
22:00	14.52	6.86	2.57
23:00	14.51	6.89	2.64

Appendix H: Recorded Arduino data for a MDBR temperature of 55˚C

Minimum temperature for the day: 13˚C

Maximum temperature for the day: 27˚C

Table H1: Arduino data for 05 September 2022

Time	pH	EC (mS/cm)	DO (mg/L)
00:00	14.37	3.64	1.84
01:00	14.34	3.64	1.85
02:00	14.35	3.67	1.87
03:00	14.34	3.64	1.85
04:00	14.34	3.67	1.87
05:00	14.32	3.67	1.87
06:00	14.32	3.74	1.92
07:00	14.32	3.70	1.87
08:00	14.32	3.70	1.93
09:00	14.30	3.70	1.93
10:00	14.30	3.74	2.02
11:00	13.54	3.67	1.97
12:00	13.59	3.64	1.99
13:00	13.53	3.64	2.02
14:00	13.54	3.61	2.02
15:00	14.12	3.67	2.02
16:00	14.14	3.64	2.05
17:00	14.15	3.67	2.07
18:00	14.17	3.70	2.08
19:00	14.17	3.74	2.04
20:00	14.17	3.77	2.03
21:00	14.17	3.77	2.07
22:00	14.17	3.77	2.04
23:00	14.16	3.74	2.07

Minimum temperature for the day: 9˚C

Maximum temperature for the day: 27˚C

Table H2: Arduino data for 06 September 2022

Time	pH	EC (mS/cm)	DO (mg/L)
00:00	14.54	3.83	0.84
01:00	14.54	3.86	0.89
02:00	14.55	3.83	0.87
03:00	14.55	3.83	0.93
04:00	14.56	3.86	0.97
05:00	14.55	3.86	0.97
06:00	14.56	3.93	0.97
07:00	14.55	3.86	1.10
08:00	14.56	3.86	1.16
09:00	14.56	3.96	1.13
10:00	14.56	4.09	1.13
11:00	14.56	4.15	1.17
12:00	14.56	4.22	1.21
13:00	14.56	4.19	1.17
14:00	14.56	4.48	1.17
15:00	14.58	26.82	1.17
16:00	14.58	26.89	1.16
17:00	14.53	10.72	1.17
18:00	14.53	11.82	1.24
19:00	14.47	14.68	1.21
20:00	14.49	3.96	1.24
21:00	14.49	3.99	1.24
22:00	14.50	3.99	1.24
23:00	14.53	3.93	1.24

Minimum temperature for the day: 7˚C

Maximum temperature for the day: 22˚C

Table H3: Arduino data for 07 September 2022

Time	pH	EC (mS/cm)	DO (mg/L)
00:00	14.49	5.89	1.56
01:00	14.49	5.73	1.57
02:00	14.71	5.86	1.64
03:00	13.85	2.32	1.66
04:00	15.50	2.09	1.69
05:00	15.51	3.41	1.73
06:00	14.85	3.41	1.79
07:00	14.85	5.79	1.85
08:00	14.85	5.85	1.79
09:00	14.86	5.92	1.86
10:00	14.86	6.03	1.75
11:00	14.85	6.18	1.73
12:00	14.84	7.85	1.80
13:00	14.85	6.25	1.91
14:00	14.86	8.09	1.92
15:00	14.87	8.05	1.91
16:00	14.86	8.85	1.80
17:00	14.86	8.93	1.82
18:00	14.86	10.45	1.83
19:00	14.87	10.37	1.85
20:00	14.87	11.17	1.82
21:00	14.88	10.75	1.82
22:00	14.88	10.88	1.79
23:00	14.88	10.79	1.79

Minimum temperature for the day: 11˚C

Maximum temperature for the day: 24˚C

Table H4: Arduino data for 08 September 2022

Time	pH	EC (mS/cm)	DO (mg/L)
00:00	14.81	3.28	2.43
01:00	14.80	3.32	2.47
02:00	14.82	3.28	2.56
03:00	14.82	3.25	2.58
04:00	14.82	3.25	2.65
05:00	14.82	3.32	2.69
06:00	14.82	3.28	2.70
07:00	14.82	3.32	2.73
08:00	14.83	3.25	2.74
09:00	14.83	3.25	2.69
10:00	14..84	3.28	2.69
11:00	14.84	3.28	2.72
12:00	14.85	3.28	2.76
13:00	14.85	3.25	2.69
14:00	14.85	3.28	2.76
15:00	14.85	3.28	2.77
16:00	14.85	3.28	2.77
17:00	14.85	3.28	2.76
18:00	14.85	3.28	2.78
19:00	14.85	3.28	2.77
20:00	14.85	3.28	2.77
21:00	14.85	3.28	2.87
22:00	14.82	3.38	2.77
23:00	14.83	3.38	2.76

Minimum temperature for the day: 15˚C

Maximum temperature for the day: 27˚C

Table H5: Arduino data for 09 September 2022

Time	pH	EC (mS/cm)	DO (mg/L)
00:00	14.81	3.22	2.41
01:00	14.80	3.22	2.43
02:00	14.80	3.22	2.47
03:00	14.81	3.22	2.52
04:00	14.82	3.22	2.47
05:00	14.82	3.22	2.47
06:00	14.82	3.28	2.48
07:00	14.82	3.22	2.54
08:00	14.82	3.25	2.53
09:00	14.83	3.19	2.58
10:00	14.83	3.19	2.62
11:00	14.83	3.25	2.58
12:00	14.83	3.28	2.63
13:00	14.83	3.28	2.63
14:00	14.82	3.32	2.63
15:00	14.83	3.32	2.64
16:00	14.83	3.28	2.63
17:00	14.83	3.28	2.64
18:00	14.83	3.28	2.64
19:00	14.83	3.28	2.67
20:00	14.83	3.28	2.64
21:00	14.83	3.28	2.67
22:00	14.83	3.28	2.71
23:00	14.83	3.25	2.70

Minimum temperature for the day: 15˚C

Maximum temperature for the day: 29˚C

Table H6: Arduino data for 10 September 2022

Time	pH	EC (mS/cm)	DO (mg/L)
00:00	14.73	3.19	1.17
01:00	14.75	3.19	1.21
02:00	14.75	3.19	1.23
03:00	14.83	14.20	1.27
04:00	14.84	14.78	1.31
05:00	14.85	14.62	1.32
06:00	14.85	14.14	1.35
07:00	14.85	16.26	1.31
08:00	14.66	3.19	1.31
09:00	14.66	3.19	1.32
10:00	14.66	3.19	1.36
11:00	14.68	3.19	1.32
12:00	14.68	3.19	1.32
13:00	14.69	3.12	1.33
14:00	14.69	3.16	1.42
15:00	14.69	3.19	1.45
16:00	14.69	3.22	1.33
17:00	14.69	3.22	1.37
18:00	14.69	3.22	1.39
19:00	14.69	3.22	1.37
20:00	14.68	3.22	1.33
21:00	14.69	3.22	1.34
22:00	14.69	3.19	1.33
23:00	14.69	3.16	1.33

Minimum temperature for the day: 16˚C

Maximum temperature for the day: 28˚C

Table H7: Arduino data for 11 September 2022

Time	pH	EC (mS/cm)	DO (mg/L)
00:00	14.76	0.46	2.23
01:00	14.77	0.43	2.26
02:00	14.77	0.43	2.29
03:00	14.77	0.39	2.32
04:00	14.77	0.43	2.33
05:00	14.77	0.39	2.35
06:00	14.78	0.39	2.37
07:00	14.78	0.36	2.42
08:00	14.78	0.36	2.46
09:00	14.78	0.39	2.42
10:00	14.78	0.36	2.46
11:00	14.78	3.9	2.49
12:00	14.78	3.9	2.52
13:00	14.78	3.6	2.54
14:00	14.78	0.39	2.59
15:00	14.83	3.12	2.54
16:00	14.83	3.06	2.55
17:00	14.86	19.29	2.54
18:00	14.86	15.04	2.56
19:00	14.86	19.42	2.56
20:00	14.85	17.48	2.57
21:00	14.86	20.48	2.56
22:00	14.86	20.06	2.57
23:00	14.87	16.33	2.54

Minimum temperature for the day: 10˚C

Maximum temperature for the day: 27˚C

Table H8: Arduino data for 12 September 2022

Time	pH	EC (mS/cm)	DO (mg/L)
00:00	14.85	18.93	1.46
01:00	14.85	22.31	1.49
02:00	14.85	22.06	1.53
03:00	14.85	20.87	1.56
04:00	14.85	14.04	1.56
05:00	14.86	15.07	1.63
06:00	14.86	12.98	1.63
07:00	14.85	15.26	1.63
08:00	14.85	16.71	1.67
09:00	14.86	22.06	1.72
10:00	14.86	19.45	1.72
11:00	14.81	4.77	1.72
12:00	14.82	5.22	1.73
13:00	14.83	4.73	1.72
14:00	14.83	4.96	1.82
15:00	14.83	4.80	1.82
16:00	14.83	4.86	1.90
17:00	14.83	5.28	1.93
18:00	14.83	6.02	1.82
19:00	14.83	5.83	1.82
20:00	14.83	5.62	1.92
21:00	14.83	5.41	1.94
22:00	14.83	5.99	1.95
23:00	14.83	6.21	1.82

Minimum temperature for the day: 8˚C

Maximum temperature for the day: 20˚C

Table H9: Arduino data for 13 September 2022

Time	pH	EC (mS/cm)	DO (mg/L)
00:00	14.69	3.03	2.67
01:00	14.70	3.06	2.70
02:00	14.71	3.06	2.74
03:00	14.72	3.06	2.77
04:00	14.72	3.09	2.74
05:00	14.71	3.06	2.81
06:00	14.71	3.09	2.74
07:00	14.72	3.06	2.75
08:00	14.64	2.99	2.74
09:00	14.65	2.93	2.75
10:00	14.65	2.93	2.75
11:00	14.65	2.93	2.75
12:00	14.65	2.93	2.75
13:00	14.65	2.93	2.75
14:00	14.66	2.93	2.75
15:00	14.66	2.93	2.77
16:00	14.66	2.96	2.75
17:00	14.66	3.03	2.78
18:00	14.61	3.12	2.75
19:00	14.59	3.09	2.74
20:00	14.58	3.12	2.74
21:00	14.58	3.09	2.74
22:00	14.58	3.09	2.74
23:00	14.58	3.09	2.74

Minimum temperature for the day: 9˚C

Maximum temperature for the day: 20˚C

Table H10: Arduino data for 14 September 2022

Time	pH	EC (mS/cm)	DO (mg/L)
00:00	14.69	2.99	2.84
01:00	14.70	2.96	2.81
02:00	14.71	2.96	2.81
03:00	14.71	2.96	2.81
04:00	14.71	2.93	2.84
05:00	14.71	2.96	2.84
06:00	14.71	2.93	2.85
07:00	14.71	2.99	2.85
08:00	14.71	3.03	2.85
09:00	14.65	2.51	2.84
10:00	14.65	2.67	2.89
11:00	14.66	3.09	2.84
12:00	14.66	3.16	2.89
13:00	14.66	3.22	2.91
14:00	14.66	3.25	2.92
15:00	14.65	3.25	2.89
16:00	14.65	3.22	2.92
17:00	14.65	3.22	2.92
18:00	14.65	3.22	2.93
19:00	14.66	3.19	2.92
20:00	14.65	3.16	2.92
21:00	14.65	3.19	2.92
22:00	14.67	2.99	2.89
23:00	14.68	2.99	2.92

Minimum temperature for the day: 9˚C

Maximum temperature for the day: 25˚C

Table H11: Arduino data for 15 September 2022

Time	pH	EC (mS/cm)	DO (mg/L)
00:00	14.63	3.96	1.47
01:00	14.63	4.06	1.49
02:00	14.65	3.99	1.47
03:00	14.65	3.86	1.47
04:00	14.63	3.86	1.47
05:00	14.63	3.86	1.52
06:00	14.65	3.93	1.55
07:00	14.65	3.99	1.55
08:00	14.64	4.06	1.59
09:00	14.64	4.06	1.63
10:00	14.65	4.03	1.47
11:00	14.65	4.03	1.63
12:00	14.64	3.99	1.63
13:00	14.63	3.96	1.63
14:00	14.63	3.96	1.64
15:00	14.63	3.99	1.64
16:00	14.56	3.90	1.64
17:00	14.56	3.90	1.64
18:00	14.57	3.90	1.64
19:00	14.61	3.83	1.63
20:00	14.62	3.83	1.62
21:00	14.64	3.86	1.63
22:00	14.65	3.83	1.64
23:00	14.65	3.80	1.63

Minimum temperature for the day: 14˚C

Maximum temperature for the day: 27˚C

Table H12: Arduino data for 16 September 2022

Time	pH	EC (mS/cm)	DO (mg/L)
00:00	14.59	3.83	1.32
01:00	14.59	3.83	1.37
02:00	14.60	3.86	1.42
03:00	14.59	3.86	1.46
04:00	14.60	3.86	1.47
05:00	14.61	3.86	1.53
06:00	14.62	3.86	1.55
07:00	14.54	3.96	1.57
08:00	14.55	3.96	1.55
09:00	14.59	4.86	1.59
10:00	14.61	4.80	1.64
11:00	14.61	4.83	1.59
12:00	14.62	4.80	1.59
13:00	14.63	4.77	1.63
14:00	14.64	4.80	1.67
15:00	14.63	4.80	1.64
16:00	14.63	4.83	1.64
17:00	14.62	4.86	1.68
18:00	14.62	4.80	1.69
19:00	14.58	3.93	1.68
20:00	14.58	4.12	1.64
21:00	14.59	4.22	1.59
22:00	14.58	4.19	1.59
23:00	14.58	4.15	1.59

Minimum temperature for the day: 16˚C

Maximum temperature for the day: 27˚C

Table H13: Arduino data for 17 September 2022

Time	pH	EC (mS/cm)	DO (mg/L)
00:00	14.56	4.09	1.09
01:00	14.56	4.15	1.09
02:00	14.57	4.15	1.09
03:00	14.58	4.19	1.11
04:00	14.58	4.22	1.13
05:00	14.59	4.19	1.11
06:00	14.59	4.22	1.11
07:00	14.59	4.09	1.27
08:00	14.59	4.12	1.32
09:00	14.59	4.09	1.27
10:00	14.60	4.12	1.35
11:00	14.60	4.12	1.36
12:00	14.59	4.15	1.37
13:00	14.59	4.09	1.40
14:00	14.59	4.12	1.42
15:00	14.60	4.09	1.37
16:00	14.60	4.09	1.37
17:00	14.60	4.15	1.44
18:00	14.60	4.12	1.42
19:00	14.60	4.12	1.37
20:00	14.60	4.12	1.37
21:00	14.59	4.12	1.42
22:00	14.61	4.15	1.42
23:00	14.61	4.12	1.44

Minimum temperature for the day: 13˚C

Maximum temperature for the day: 27˚C

Table H14: Arduino data for 18 September 2022

Time	pH	EC (mS/cm)	DO (mg/L)
00:00	14.56	10.24	2.57
01:00	14.54	3.74	2.61
02:00	14.68	25.66	2.63
03:00	14.70	25.79	2.67
04:00	14.71	25.89	2.67
05:00	14.68	4.09	2.66
06:00	14.70	4.70	2.72
07:00	14.70	4.73	2.72
08:00	14.63	3.86	2.67
09:00	14.66	3.86	2.76
10:00	14.66	3.86	2.72
11:00	14.66	3.86	2.72
12:00	14.66	3.86	2.80
13:00	14.66	3.86	2.85
14:00	14.66	3.90	2.85
15:00	14.67	3.86	2.77
16:00	14.66	4.57	2.83
17:00	14.66	4.60	2.85
18:00	14.65	3.80	2.85
19:00	14.65	3.80	2.92
20:00	14.66	3.80	2.85
21:00	14.66	3.77	2.92
22:00	14.66	3.77	2.92
23:00	14.66	3.77	2.85

Minimum temperature for the day: 12˚C

Maximum temperature for the day: 28˚C

Table H15: Arduino data for 19 September 2022

Time	pH	EC (mS/cm)	DO (mg/L)
00:00	14.56	3.83	2.85
01:00	14.56	3.93	2.86
02:00	14.56	3.99	2.87
03:00	14.57	3.96	2.76
04:00	14.58	4.06	2.75
05:00	14.58	3.99	2.75
06:00	14.58	3.99	2.75
07:00	14.58	4.03	2.83
08:00	14.58	4.03	2.83
09:00	14.58	4.03	2.75
10:00	14.58	4.03	2.69
11:00	14.58	3.99	2.68
12:00	14.58	4.03	2.69
13:00	14.58	4.03	2.69
14:00	14.58	4.03	2.55
15:00	14.58	4.06	2.53
16:00	14.58	4.03	2.68
17:00	14.58	4.03	2.53
18:00	14.58	4.03	2.53
19:00	14.57	4.06	2.53
20:00	14.58	4.03	2.55
21:00	14.57	4.06	2.53
22:00	14.58	4.09	2.52
23:00	14.58	4.03	2.52

Minimum temperature for the day: 8˚C

Maximum temperature for the day: 24˚C

Table H16: Arduino data for 20 September 2022

Time	pH	EC (mS/cm)	DO (mg/L)
00:00	14.46	3.99	2.47
01:00	14.46	4.03	2.47
02:00	14.46	4.09	2.21
03:00	14.46	4.09	2.19
04:00	14.44	4.09	2.18
05:00	14.44	4.06	2.21
06:00	14.44	4.09	2.21
07:00	14.44	4.15	2.21
08:00	14.44	4.22	2.22
09:00	14.44	4.22	2.32
10:00	14.44	4.22	2.32
11:00	14.44	4.28	2.22
12:00	14.44	4.31	2.19
13:00	14.44	4.25	2.17
14:00	14.50	4.28	2.16
15:00	14.49	4.31	2.16
16:00	14.49	4.15	2.23
17:00	14.50	4.22	2.23
18:00	14.49	4.22	2.16
19:00	14.49	4.25	2.15
20:00	14.49	4.28	2.17
21:00	14.48	4.31	2.16
22:00	13.06	4.19	2.17
23:00	13.31	4.22	2.17

Minimum temperature for the day: 9˚C

Maximum temperature for the day: 20˚C

Table H17: Arduino data for 21 September 2022

Time	pH	EC (mS/cm)	DO (mg/L)
00:00	14.49	5.67	2.24
01:00	14.49	5.64	2.27
02:00	14.48	5.70	2.24
03:00	14.48	5.64	2.24
04:00	14.48	5.60	2.19
05:00	14.46	5.54	2.19
06:00	14.45	5.47	2.19
07:00	14.44	5.47	2.18
08:00	14.37	5.47	2.14
09:00	14.34	5.47	2.11
10:00	14.32	5.54	2.12
11:00	14.48	5.18	2.12
12:00	14.50	4.64	2.14
13:00	14.49	4.60	2.03
14:00	14.49	4.60	2.03
15:00	14.50	4.64	2.04
16:00	14.49	4.64	2.05
17:00	14.49	4.60	2.05
18:00	14.50	4.57	1.99
19:00	14.51	4.60	1.98
20:00	14.51	4.57	2.01
21:00	14.51	4.48	2.02
22:00	14.51	4.48	1.98
23:00	14.51	4.31	1.97

Minimum temperature for the day: 11˚C

Maximum temperature for the day: 22˚C

Table H18: Arduino data for 22 September 2022

Time	pH	EC (mS/cm)	DO (mg/L)
00:00	14.32	4.57	2.02
01:00	14.31	4.57	2.03
02:00	14.31	4.54	1.97
03:00	14.30	4.54	1.97
04:00	14.30	4.57	2.08
05:00	14.30	4.57	2.08
06:00	14.30	4.54	2.02
07:00	14.26	4.57	2.02
08:00	14.25	4.57	1.97
09:00	14.24	4.57	1.98
10:00	14.23	4.60	1.89
11:00	14.54	4.70	1.89
12:00	14.55	4.67	1.89
13:00	14.54	4.67	1.74
14:00	14.54	3.93	1.89
15:00	14.53	4.12	1.89
16:00	14.53	4.25	1.87
17:00	14.53	4.31	1.84
18:00	14.50	4.35	1.87
19:00	14.50	4.31	1.87
20:00	14.50	4.31	1.84
21:00	14.51	4.31	1.85
22:00	14.51	4.22	1.87
23:00	14.51	4.25	1.84

Minimum temperature for the day: 12˚C

Maximum temperature for the day: 27˚C

Table H19: Arduino data for 23 September 2022

Time	pH	EC (mS/cm)	DO (mg/L)
00:00	14.53	4.96	1.93
01:00	14.54	4.93	1.89
02:00	1454	5.12	1.87
03:00	14.54	4.73	1.93
04:00	14.55	4.73	1.94
05:00	14.55	4.83	1.94
06:00	14.55	4.86	1.93
07:00	14.55	4.54	1.96
08:00	14.55	4.77	1.96
09:00	14.56	4.86	1.96
10:00	14.56	4.99	2.03
11:00	14.56	4.99	2.05
12:00	14.56	5.12	2.12
13:00	14.56	5.06	2.20
14:00	14.44	5.57	2.21
15:00	14.43	5.57	2.21
16:00	14.44	5.60	2.17
17:00	14.44	5.67	2.17
18:00	14.43	5.70	2.12
19:00	14.44	5.67	2.15
20:00	14.44	5.73	2.21
21:00	14.44	5.73	2.23
22:00	14.44	5.80	2.21
23:00	14.42	6.09	2.21

Minimum temperature for the day: 13˚C

Maximum temperature for the day: 28˚C

Table H20: Arduino data for 24 September 2022

Time	pH	EC (mS/cm)	DO (mg/L)
00:00	14.56	9.40	2.31
01:00	14.57	9.34	2.27
02:00	14.50	9.27	2.35
03:00	14.42	7.92	2.31
04:00	14.41	8.47	2.27
05:00	14.41	8.47	2.27
06:00	14.42	8.53	2.21
07:00	14.41	8.76	2.09
08:00	14.40	8.57	2.08
09:00	14.28	8.02	2.01
10:00	14.25	7.82	1.99
11:00	14.36	7.25	1.98
12:00	14.36	5.80	2.01
13:00	14.35	6.54	1.97
14:00	12.62	6.63	1.87
15:00	12.77	6.76	1.83
16:00	12.87	6.79	1.83
17:00	12.89	6.70	1.87
18:00	13.98	15.81	1.83
19:00	14.57	7.08	1.79
20:00	14.59	7.15	1.76
21:00	14.61	7.15	1.76
22:00	14.63	7.50	1.79
23:00	14.63	7.63	1.73

Minimum temperature for the day: 15˚C

Maximum temperature for the day: 28˚C

Table H21: Arduino data for 25 September 2022

Time	pH	EC (mS/cm)	DO (mg/L)
00:00	14.50	10.98	1.79
01:00	14.50	9.69	1.67
02:00	14.56	14.97	1.64
03:00	14.56	9.18	1.63
04:00	14.56	8.60	1.67
05:00	14.56	8.60	1.67
06:00	14.56	8.60	1.67
07:00	14.56	8.63	1.63
08:00	14.56	8.60	1.59
09:00	14.56	8.60	1.59
10:00	14.57	8.57	1.59
11:00	14.54	5.76	1.58
12:00	14.55	5.96	1.57
13:00	14.55	6.05	1.57
14:00	14.55	6.09	1.57
15:00	14.54	6.09	1.57
16:00	14.54	6.05	1.55
17:00	14.54	6.05	1.53
18:00	14.53	6.09	1.55
19:00	14.53	6.05	1.54
20:00	14.52	6.05	1.55
21:00	14.51	6.02	1.57
22:00	14.51	5.96	1.57
23:00	14.36	6.31	1.57

Minimum temperature for the day: 15˚C

Maximum temperature for the day: 28˚C

Table H22: Arduino data for 26 September 2022

Time	pH	EC (mS/cm)	DO (mg/L)
00:00	14.41	5.89	1.62
01:00	14.42	5.86	1.63
02:00	14.56	5.76	1.63
03:00	14.57	5.54	1.68
04:00	14.57	5.57	1.69
05:00	14.58	5.64	1.69
06:00	14.58	5.64	1.70
07:00	14.58	5.64	1.69
08:00	14.58	5.70	1.70
09:00	14.58	5.70	1.63
10:00	14.58	5.64	1.57
11:00	14.58	5.67	1.51
12:00	14.51	5.86	1.51
13:00	14.53	5.83	1.42
14:00	14.53	5.89	1.41
15:00	14.54	5.89	1.34
16:00	14.54	5.86	1.33
17:00	14.55	5.83	1.34
18:00	14.55	5.80	1.29
19:00	14.54	5.86	1.33
20:00	14.55	5.83	1.28
21:00	14.55	5.83	1.23
22:00	14.55	5.89	1.23
23:00	14.54	5.92	1.22

Appendix I: Recorded Arduino data for a MDBR temperature of 65˚C

Minimum temperature for the day: 14˚C

Maximum temperature for the day: 30˚C

Table I1: Arduino data for 27 September 2022

Time	pH	EC (mS/cm)	DO (mg/L)
00:00	14.56	5.76	1.67
01:00	14.56	5.73	1.73
02:00	14.56	5.76	1.75
03:00	14.57	5.54	1.73
04:00	14.57	5.44	1.73
05:00	14.58	5.44	1.73
06:00	14.58	5.54	1.77
07:00	14.51	5.41	1.78
08:00	14.53	5.47	1.82
09:00	14.53	5.44	1.83
10:00	14.53	5.44	1.84
11:00	14.54	5.41	1.84
12:00	14.54	5.38	1.84
13:00	14.54	5.09	1.88
14:00	14.54	5.09	1.90
15:00	14.54	5.02	1.88
16:00	14.54	5.06	1.90
17:00	14.54	5.15	1.91
18:00	14.54	5.15	1.90
19:00	14.55	5.15	1.90
20:00	14.54	5.12	1.90
21:00	14.54	5.15	1.91
22:00	14.54	5.15	1.89
23:00	14.54	5.22	1.90

Minimum temperature for the day: 12˚C

Maximum temperature for the day: 27˚C

Table I2: Arduino data for 28 September 2022

Time	pH	EC (mS/cm)	DO (mg/L)
00:00	14.43	4.73	2.00
01:00	14.43	4.77	1.90
02:00	14.44	4.67	1.93
03:00	14.43	4.73	1.93
04:00	14.44	4.48	1.98
05:00	14.44	4.51	2.00
06:00	14.44	4.54	2.03
07:00	14.44	4.54	2.03
08:00	14.44	4.57	2.03
09:00	14.44	4.60	2.04
10:00	14.44	4.60	2.05
11:00	14.44	4.60	2.05
12:00	14.44	4.64	2.05
13:00	14.38	4.64	2.10
14:00	14.34	4.64	2.11
15:00	14.30	4.64	2.11
16:00	14.30	4.64	2.12
17:00	14.30	4.64	2.12
18:00	14.27	4.67	2.13
19:00	14.26	4.70	2.10
20:00	14.22	4.64	2.10
21:00	14.20	4.64	2.11
22:00	14.18	4.64	2.11
23:00	14.15	4.51	2.11

Minimum temperature for the day: 11˚C

Maximum temperature for the day: 26˚C

Table I3: Arduino data for 29 September 2022

Time	pH	EC (mS/cm)	DO (mg/L)
00:00	14.32	2.07	2.11
01:00	13.94	2.04	2.13
02:00	13.85	2.04	2.19
03:00	13.68	2.07	2.22
04:00	13.69	2.07	2.26
05:00	13.75	2.10	2.27
06:00	13.80	2.14	2.29
07:00	13.77	2.17	2.29
08:00	13.75	2.17	2.31
09:00	13.72	2.14	2.32
10:00	13.71	2.20	2.32
11:00	13.65	2.20	2.37
12:00	13.62	2.20	2.41
13:00	13.56	2.20	2.42
14:00	13.65	2.10	2.50
15:00	13.63	2.20	2.51
16:00	13.63	2.20	2.51
17:00	13.63	2.20	2.52
18:00	13.66	2.27	2.53
19:00	13.68	2.37	2.52
20:00	13.67	2.40	2.53
21:00	13.68	2.33	2.52
22:00	13.70	2.33	2.52
23:00	13.68	2.33	2.53

Minimum temperature for the day: 14˚C

Maximum temperature for the day: 28˚C

Table I4: Arduino data for 30 September 2022

Time	pH	EC (mS/cm)	DO (mg/L)
00:00	14.55	0.82	2.42
01:00	14.56	0.76	2.42
02:00	14.58	4.12	2.42
03:00	14.59	4.09	2.43
04:00	14.59	3.90	2.57
05:00	14.59	3.90	2.52
06:00	14.59	3.93	2.54
07:00	14.55	3.99	2.57
08:00	14.55	3.96	2.57
09:00	14.50	3.96	2.57
10:00	14.51	3.99	2.60
11:00	14.52	3.96	2.61
12:00	14.52	3.93	2.72
13:00	14.53	3.90	2.75
14:00	14.56	3.83	2.76
15:00	14.53	3.83	2.77
16:00	14.62	3.83	2.77
17:00	14.62	3.80	2.76
18:00	14.63	3.83	2.77
19:00	14.63	3.80	2.77
20:00	14.63	3.83	2.77
21:00	14.59	3.90	2.78
22:00	14.60	3.90	2.77
23:00	14.62	3.83	2.76

Minimum temperature for the day: 16˚C

Maximum temperature for the day: 30˚C

Table I5: Arduino data for 01 October 2022

Time	pH	EC (mS/cm)	DO (mg/L)
00:00	13.75	2.99	2.77
01:00	13.63	3.06	2.78
02:00	13.52	3.03	2.81
03:00	13.57	2.96	2.87
04:00	13.55	3.06	2.93
05:00	13.61	3.06	2.93
06:00	13.42	3.19	2.97
07:00	13.18	3.16	2.93
08:00	12.87	3.19	2.93
09:00	13.23	3.16	2.87
10:00	13.40	3.12	2.83
11:00	13.40	3.16	2.81
12:00	13.58	3.61	2.79
13:00	13.73	3.74	2.79
14:00	13.71	3.74	2.76
15:00	13.73	3.70	2.76
16:00	13.72	3.64	2.76
17:00	13.75	3.67	2.71
18:00	13.75	3.51	2.71
19:00	13.75	3.51	2.69
20:00	13.71	3.48	2.67
21:00	13.75	3.51	2.69
22:00	13.95	3.70	2.69
23:00	13.96	3.74	2.67

Minimum temperature for the day: 14˚C

Maximum temperature for the day: 31˚C

Table I6: Arduino data for 02 October 2022

Time	pH	EC (mS/cm)	DO (mg/L)
00:00	14.37	3.70	2.62
01:00	14.36	3.70	2.62
02:00	14.36	3.70	2.63
03:00	14.36	3.67	2.61
04:00	14.33	3.67	2.59
05:00	13.13	3.64	2.59
06:00	14.30	3.64	2.59
07:00	14.27	3.70	2.53
08:00	14.36	3.64	2.53
09:00	14.36	3.64	2.53
10:00	14.35	3.61	2.51
11:00	14.35	3.67	2.48
12:00	14.34	3.64	2.48
13:00	14.34	3.64	2.48
14:00	14.32	3.64	2.47
15:00	14.36	3.61	2.48
16:00	14.36	3.64	2.46
17:00	14.36	3.67	2.46
18:00	13.92	3.67	2.45
19:00	13.17	3.54	2.47
20:00	12.91	3.57	2.45
21:00	13.56	3.61	2.43
22:00	13.33	3.61	2.41
23:00	13.22	3.61	2.39

Minimum temperature for the day: 17˚C

Maximum temperature for the day: 32˚C

Table I7: Arduino data for 03 October 2022

Time	pH	EC (mS/cm)	DO (mg/L)
00:00	13.82	3.32	2.29
01:00	13.85	3.38	2.29
02:00	13.74	3.41	2.30
03:00	14.11	2.46	2.19
04:00	14.48	2.50	2.18
05:00	14.40	3.16	2.18
06:00	14.33	2.77	2.13
07:00	14.42	2.90	2.20
08:00	13.33	2.77	2.21
09:00	14.34	3.57	2.22
10:00	14.42	3.64	2.23
11:00	14.44	3.48	2.23
12:00	14.45	3.51	2.23
13:00	14.45	3.51	2.23
14:00	14.46	3.74	2.27
15:00	14.48	3.67	2.27
16:00	14.48	3.57	2.21
17:00	14.46	3.41	2.21
18:00	14.48	3.48	2.19
19:00	14.46	3.64	2.21
20:00	14.47	3.64	2.23
21:00	14.48	4.03	2.21
22:00	14.49	4.12	2.21
23:00	14.48	4.09	2.23

Minimum temperature for the day: 16˚C

Maximum temperature for the day: 32˚C

Table I8: Arduino data for 04 October 2022

Time	pH	EC (mS/cm)	DO (mg/L)
00:00	13.43	2.48	2.25
01:00	13.37	2.51	2.23
02:00	13.46	2.51	2.19
03:00	13.80	2.64	2.19
04:00	14.10	2.61	2.19
05:00	14.08	2.61	2.12
06:00	14.05	2.64	2.11
07:00	14.13	2.67	2.11
08:00	14.06	2.70	2.11
09:00	14.52	3.06	2.09
10:00	14.52	2.74	2.07
11:00	14.52	2.80	2.07
12:00	14.51	2.90	2.07
13:00	14.53	2.80	2.01
14:00	14.53	2.77	2.01
15:00	14.52	2.87	1.90
16:00	14.53	2.90	1.87
17:00	14.53	2.83	1.83
18:00	14.53	2.80	1.83
19:00	14.53	2.87	1.81
20:00	14.37	2.61	1.83
21:00	14.02	2.67	1.77
22:00	14.38	2.67	1.83
23:00	14.41	2.67	1.77

Minimum temperature for the day: 14˚C

Maximum temperature for the day: 28˚C

Table I9: Arduino data for 05 October 2022

Time	pH	EC (mS/cm)	DO (mg/L)
00:00	13.95	3.77	1.79
01:00	13.96	3.67	1.73
02:00	13.50	3.67	1.67
03:00	13.66	3.70	1.67
04:00	13.69	3.64	1.67
05:00	13.74	3.64	1.67
06:00	13.78	3.64	1.61
07:00	13.81	3.67	1.61
08:00	13.81	3.61	1.58
09:00	13.81	3.67	1.57
10:00	13.83	3.64	1.58
11:00	13.83	3.64	1.58
12:00	13.83	3.64	1.55
13:00	13.84	3.61	1.58
14:00	13.84	3.61	1.58
15:00	13.84	3.61	1.55
16:00	13.85	3.64	1.54
17:00	13.85	3.61	1.53
18:00	14.01	3.64	1.54
19:00	13.82	3.48	1.54
20:00	13.84	4.67	1.53
21:00	13.86	4.64	1.53
22:00	13.86	4.60	1.53
23:00	13.83	4.67	1.54

Minimum temperature for the day: 18˚C

Maximum temperature for the day: 32˚C

Table I10: Arduino data for 06 October 2022

Time	pH	EC (mS/cm)	DO (mg/L)
00:00	13.83	4.67	1.51
01:00	13.83	4.67	1.51
02:00	13.85	4.57	1.50
03:00	13.83	4.60	1.46
04:00	13.83	4.51	1.43
05:00	13.84	4.54	1.42
06:00	13.83	4.51	1.42
07:00	13.83	4.51	1.41
08:00	13.83	4.54	1.41
09:00	13.84	4.57	1.39
10:00	13.84	4.54	1.41
11:00	13.84	4.60	1.39
12:00	13.84	4.51	1.38
13:00	13.84	4.54	1.38
14:00	13.84	4.48	1.38
15:00	13.84	4.54	1.38
16:00	13.85	4.51	1.38
17:00	13.85	4.60	1.32
18:00	13.85	4.48	1.37
19:00	13.84	4.54	1.37
20:00	13.84	4.54	1.34
21:00	13.86	4.54	1.34
22:00	13.86	4.51	1.33
23:00	13.86	4.51	1.32

Minimum temperature for the day: 15˚C

Maximum temperature for the day: 31˚C

Table I11: Arduino data for 07 October 2022

Time	pH	EC (mS/cm)	DO (mg/L)
00:00	13.21	3.48	1.32
01:00	13.09	3.48	1.33
02:00	12.85	3.48	1.35
03:00	12.78	3.45	1.35
04:00	12.86	3.51	1.32
05:00	12.90	3.48	1.31
06:00	12.93	3.67	1.29
07:00	12.89	3.51	1.27
08:00	12.98	3.54	1.27
09:00	13.02	3.57	1.27
10:00	12.98	3.61	1.27
11:00	12.90	3.54	1.17
12:00	12.83	3.54	1.15
13:00	12.82	3.32	1.19
14:00	12.82	3.35	1.22
15:00	12.74	3.32	1.23
16:00	12.72	3.38	1.23
17:00	12.78	3.38	1.23
18:00	12.75	3.41	1.22
19:00	12.75	3.42	1.22
20:00	12.75	3.41	1.23
21:00	12.76	3.45	1.23
22:00	12.80	3.51	1.24
23:00	12.76	3.54	1.24

Minimum temperature for the day: 11˚C

Maximum temperature for the day: 27˚C

Table I12: Arduino data for 08 October 2022

Time	pH	EC (mS/cm)	DO (mg/L)
00:00	13.07	2.74	1.27
01:00	13.32	2.77	1.27
02:00	13.35	2.83	1.27
03:00	13.33	2.80	1.29
04:00	13.35	2.80	1.31
05:00	14.50	2.43	1.33
06:00	14.51	2.46	1.33
07:00	14.50	2.46	1.33
08:00	14.51	4.45	1.34
09:00	14.51	2.42	1.33
10:00	14.51	2.45	1.29
11:00	14.51	2.45	1.29
12:00	14.51	2.48	1.29
13:00	14.51	2.54	1.27
14:00	14.51	2.58	1.29
15:00	14.51	2.61	1.28
16:00	14.51	2.54	1.27
17:00	14.51	2.58	1.27
18:00	14.51	2.54	1.26
19:00	14.51	2.54	1.26
20:00	14.51	2.58	1.27
21:00	14.51	2.61	1.26
22:00	14.51	2.67	1.26
23:00	14.51	2.67	1.27

Minimum temperature for the day: 17˚C

Maximum temperature for the day: 29˚C

Table I13: Arduino data for 09 October 2022

Time	pH	EC (mS/cm)	DO (mg/L)
00:00	14.48	3.99	1.17
01:00	14.48	4.09	1.13
02:00	14.48	4.09	1.12
03:00	14.48	4.12	1.12
04:00	14.48	4.09	1.09
05:00	14.49	4.12	1.11
06:00	14.49	4.06	1.11
07:00	14.49	4.09	1.11
08:00	14.49	4.12	1.21
09:00	14.49	4.09	1.24
10:00	14.44	4.12	1.32
11:00	14.44	4.25	1.33
12:00	14.44	4.19	1.33
13:00	14.44	4.19	1.34
14:00	14.43	4.25	1.36
15:00	14.43	4.15.	1.38
16:00	14.44	4.28	1.38
17:00	14.44	4.22	1.37
18:00	14.44	4.19	1.38
19:00	14.43	4.22	1.39
20:00	14.44	4.22	1.39
21:00	14.43	4.22	1.39
22:00	14.43	4.25	1.40
23:00	14.43	4.25	1.40

Minimum temperature for the day: 16˚C

Maximum temperature for the day: 30˚C

Table I14: Arduino data for 10 October 2022

Time	pH	EC (mS/cm)	DO (mg/L)
00:00	14.36	3.90	2.13
01:00	14.31	3.90	2.13
02:00	13.65	3.90	2.14
03:00	13.72	3.93	2.15
04:00	13.65	3.96	2.15
05:00	14.41	3.93	2.15
06:00	14.41	3.93	2.17
07:00	14.40	3.96	2.27
08:00	14.40	3.86	2.23
09:00	14.40	3.86	2.23
10:00	14.40	3.90	2.23
11:00	14.41	3.86	2.23
12:00	14.40	3.86	2.27
13:00	14.39	3.83	2.28
14:00	14.36	3.83	2.29
15:00	14.39	3.86	2.29
16:00	13.42	3.83	2.29
17:00	14.34	3.93	2.31
18:00	14.36	3.96	2.31
19:00	14.41	3.96	2.31
20:00	14.41	4.03	2.32
21:00	14.42	3.90	2.33
22:00	14.42	3.90	2.32
23:00	14.42	3.90	2.31

Minimum temperature for the day: 13˚C

Maximum temperature for the day: 29˚C

Table I15: Arduino data for 11 October 2022

Time	pH	EC (mS/cm)	DO (mg/L)
00:00	14.46	3.86	2.41
01:00	14.46	3.90	2.45
02:00	14.46	3.90	2.47
03:00	14.46	3.93	2.47
04:00	14.46	3.96	2.48
05:00	14.46	3.99	2.47
06:00	14.46	4.03	2.48
07:00	14.46	3.96	2.48
08:00	14.46	4.03	2.52
09:00	14.46	3.96	2.53
10:00	14.45	3.96	2.54
11:00	14.46	3.99	2.55
12:00	14.46	3.99	2.57
13:00	14.46	3.96	2.57
14:00	14.44	4.09	2.61
15:00	14.42	4.06	2.62
16:00	14.42	4.03	2.62
17:00	14.42	4.06	2.63
18:00	14.40	4.03	2.63
19:00	12.88	3.99	2.64
20:00	12.48	4.03	2.63
21:00	12.64	4.03	2.63
22:00	14.37	4.03	2.64
23:00	14.39	4.06	2.64

Minimum temperature for the day: 16˚C

Maximum temperature for the day: 31˚C

Table I16: Arduino data for 12 October 2022

Time	pH	EC (mS/cm)	DO (mg/L)
00:00	13.99	4.31	2.65
01:00	13.97	4.31	2.66
02:00	14.04	4.31	2.64
03:00	14.03	4.38	2.65
04:00	14.05	4.35	2.65
05:00	14.04	4.38	2.67
06:00	14.05	4.38	2.67
07:00	14.47	3.77	2.67
08:00	14.49	4.09	2.66
09:00	14.49	4.06	2.66
10:00	14.51	4.12	2.67
11:00	14.51	4.12	2.67
12:00	14.52	4.09	2.67
13:00	14.52	4.09	2.65
14:00	14.52	4.09	2.65
15:00	14.52	4.19	2.63
16:00	14.52	4.09	2.67
17:00	14.52	4.06	2.67
18:00	14.52	3.90	2.67
19:00	14.52	3.96	2.72
20:00	14.52	3.93	2.67
21:00	14.52	3.96	2.72
22:00	14.53	3.99	2.72
23:00	14.51	3.93	2.67

Minimum temperature for the day: 14˚C

Maximum temperature for the day: 30˚C

Table I17: Arduino data for 13 October 2022

Time	pH	EC (mS/cm)	DO (mg/L)
00:00	14.46	4.09	2.55
01:00	14.48	4.12	2.53
02:00	14.48	3.86	2.57
03:00	14.46	3.86	2.55
04:00	14.46	3.86	2.53
05:00	14.32	3.86	2.49
06:00	14.27	3.93	2.48
07:00	14.26	4.06	2.49
08:00	14.20	4.06	2.49
09:00	13.05	4.03	2.43
10:00	13.04	3.86	2.43
11:00	12.89	3.90	2.41
12:00	13.06	3.93	2.41
13:00	13.16	3.93	2.41
14:00	13.34	3.99	2.41
15:00	13.36	3.96	2.31
16:00	13.16	3.99	2.33
17:00	13.30	4.03	2.33
18:00	13.21	3.99	2.29
19:00	13.28	4.03	2.29
20:00	13.29	4.03	2.27
21:00	13.14	4.03	2.25
22:00	13.28	3.99	2.27
23:00	13.29	3.96	2.29

Minimum temperature for the day: 14˚C

Maximum temperature for the day: 31˚C

Table I18: Arduino data for 14 October 2022

Time	pH	EC (mS/cm)	DO (mg/L)
00:00	13.86	4.31	2.19
01:00	13.88	4.38	2.14
02:00	13.88	4.35	2.08
03:00	13.63	4.38	2.05
04:00	13.63	4.35	2.05
05:00	13.62	4.35	2.08
06:00	13.62	4.38	2.03
07:00	12.58	4.31	2.03
08:00	12.26	4.35	2.01
09:00	11.99	4.35	1.90
10:00	12.42	4.35	1.97
11:00	11.76	4.35	1.97
12:00	14.36	4.35	1.90
13:00	14.37	4.51	1.89
14:00	14.37	4.51	1.79
15:00	14.38	4.51	1.79
16:00	14.38	4.57	1.83
17:00	14.38	4.54	1.83
18:00	14.38	4.64	1.79
19:00	14.38	4.60	1.79
20:00	14.38	4.67	1.79
21:00	14.38	4.67	1.80
22:00	14.43	3.93	1.80
23:00	14.43	3.61	1.79

Minimum temperature for the day: 15˚C

Maximum temperature for the day: 30˚C

Table I19: Arduino data for 15 October 2022

Time	pH	EC (mS/cm)	DO (mg/L)
00:00	14.37	3.57	1.66
01:00	14.37	3.61	1.67
02:00	14.36	3.70	1.69
03:00	14.32	3.70	1.66
04:00	14.29	3.77	1.63
05:00	14.25	3.16	1.62
06:00	14.22	3.70	1.67
07:00	14.19	3.70	1.55
08:00	14.16	3.74	1.53
09:00	13.46	3.70	1.52
10:00	13.86	3.77	1.50
11:00	13.86	3.70	1.49
12:00	13.83	3.77	1.47
13:00	13.80	3.74	1.47
14:00	13.74	3.70	1.49
15:00	13.49	3.74	1.55
16:00	13.37	3.67	1.55
17:00	13.75	3.70	1.52
18:00	13.67	3.74	1.47
19:00	13.71	3.70	1.52
20:00	13.65	3.70	1.52
21:00	13.64	3.61	1.52
22:00	13.34	3.70	1.47
23:00	13.01	3.70	1.47

Minimum temperature for the day: 13˚C

Maximum temperature for the day: 25˚C

Table I20: Arduino data for 16 October 2022

Time	pH	EC (mS/cm)	DO (mg/L)
00:00	14.36	3.38	1.47
01:00	14.29	3.83	1.49
02:00	12.89	3.93	1.41
03:00	13.33	3.90	1.39
04:00	13.09	3.96	1.39
05:00	12.98	3.93	1.37
06:00	12.87	3.77	1.36
07:00	12.85	3.74	1.30
08:00	13.37	3.90	1.31
09:00	12.97	3.90	1.30
10:00	12.79	3.93	1.30
11:00	12.86	3.96	1.40
12:00	12.83	3.96	1.43
13:00	12.81	3.99	1.43
14:00	12.70	3.99	1.47
15:00	12.64	4.03	1.56
16:00	12.63	3.99	1.56
17:00	12.64	3.99	1.73
18:00	12.60	3.96	1.75
19:00	13.71	3.99	1.73
20:00	13.81	4.03	1.75
21:00	13.79	3.83	1.69
22:00	13.70	3.83	1.69
23:00	13.64	3.83	1.69

Minimum temperature for the day: 13˚C

Maximum temperature for the day: 23˚C

Table I21: Arduino data for 17 October 2022

Time	pH	EC (mS/cm)	DO (mg/L)
00:00	13.97	5.99	1.69
01:00	13.97	6.05	1.77
02:00	14.07	4.35	1.80
03:00	14.31	4.31	1.81
04:00	14.30	4.41	1.87
05:00	14.32	4.44	1.90
06:00	14.32	4.38	1.93
07:00	14.32	4.41	1.98
08:00	14.32	4.41	1.98
09:00	14.33	4.44	2.09
10:00	14.32	4.41	2.17
11:00	14.32	4.44	2.17
12:00	14.32	4.41	2.16
13:00	14.32	4.38	2.09
14:00	14.32	4.35	2.11
15:00	14.30	4.38	2.16
16:00	14.31	4.25	2.15
17:00	14.32	4.38	2.17
18:00	14.32	4.35	2.18
19:00	14.32	4.38	2.17
20:00	14.32	4.41	2.19
21:00	14.32	4.35	2.19
22:00	14.32	4.35	2.17
23:00	14.32	4.38	2.15

Minimum temperature for the day: 14˚C

Maximum temperature for the day: 24˚C

Table I22: Arduino data for 18 October 2022

Time	pH	EC (mS/cm)	DO (mg/L)
00:00	14.40	3.83	2.20
01:00	14.42	3.83	2.22
02:00	14.42	3.83	2.28
03:00	14.42	3.86	2.30
04:00	14.42	3.90	2.28
05:00	14.42	3.83	2.27
06:00	14.41	3.74	2.27
07:00	14.41	3.93	2.28
08:00	14.40	3.99	2.30
09:00	14.29	3.99	2.34
10:00	14.26	4.03	2.30
11:00	14.18	3.99	2.37
12:00	13.52	3.99	2.34
13:00	13.84	4.03	2.34
14:00	13.53	5.28	2.37
15:00	13.59	5.02	2.41
16:00	12.96	5.12	2.41
17:00	13.66	3.96	2.41
18:00	13.94	3.96	2.41
19:00	13.98	3.96	2.37
20:00	14.01	3.93	2.38
21:00	13.99	3.93	2.38
22:00	14.00	4.86	2.38
23:00	13.99	5.06	2.38